

PHOTOSYNTHETIC REACTIONS  
AT LOW TEMPERATURES

J. W. M. VISSER

**BIBLIOTHEEK  
CORLAEUS LABORATORIA**

Postbus 9502  
2300 RA LEIDEN

Universiteit Leiden



2 056 453 5

Bibliotheek  
Gorlaeus Laboratoria  
Universiteit Leiden  
Postbus 9502  
NL-2300 RA LEIDEN

8D6

# PHOTOSYNTHETIC REACTIONS AT LOW TEMPERATURES

PROEFSCHRIFT

TER VERKRIJGING VAN DE GRAAD VAN DOCTOR IN  
DE WISKUNDE EN NATUURWETENSCHAPPEN AAN  
DE RIJKSUNIVERSITEIT TE LEIDEN, OP GEZAG VAN  
DE RECTOR MAGNIFICUS DR. A. E. COHEN,  
HOGLERAAR IN DE FACULTEIT DER LETTEREN,  
VOLGENS BESLUIT VAN HET COLLEGE VAN  
DEKANEN TE VERDEDIGEN OP WOENSDAG  
22 OKTOBER 1975 TE KLOKKE 16.15 UUR

door

JOHANNES WILHELMUS MARIA VISSER  
geboren te Bennebroek in 1948

Krips Repro B.V. — Meppel

Promotor: Dr. J. Amez

Co-referent: Prof. Dr. L.N.M. Duyens

## STELLINGEN

### I

Gegevens omtrent fotosynthetische reacties onder fysiologische omstandigheden kunnen niet zonder meer verkregen worden uit extrapolatie van meetresultaten verkregen bij temperaturen beneden 200 K.

Dit proefschrift, hoofdstuk III en IV.

### II

Zowel de reactiecentra van fotosysteem 1 als die van fotosysteem 2 zijn heterogeen.

Dit proefschrift, hoofdstuk III en IV.

### III

De metingen van Ben-Hayyim en Malkin en van Takahama e.a. zijn niet uitgevoerd onder omstandigheden, die het mogelijk maken de kinetiek van licht-geïnduceerde absorptieveranderingen te vergelijken met die van veranderingen in fluorescentierendement.

Ben-Hayyim, G. en Malkin, S. (1971) in: Proc. 2nd Int. Congr. Photosynth. Res., Stresa (Forti, G., e.a. eds.) Vol. I, pp. 61-72, Den Haag.

Takahama, U., e.a. (1974) Plant Cell Physiol. 15, 979-986.

Dit proefschrift, hoofdstuk II.

### IV

Het meten van actiespectra met een bij iedere golflengte gelijke intensiteit van actinisch licht kan tot onnodig moeilijk interpreteerbare resultaten leiden.

Heath, R.L. (1972) Biochim. Biophys. Acta 256, 645-655.

Clark, J.B. en Lister, G.R. (1975) Plant Physiol. 55, 401-406.

### V

Het door Zabirova e.a. gemeten verband tussen fotofosforylatiesnelheid en de grootte van een EPR-signaal bij  $g = 2.002$  in chloroplasten van spinazie is veel eenvoudiger te verklaren dan de auteurs vermoeden.

Zabirova, I.G., e.a. (1973) Studia Biophysica, Berlin 39, 237-241.

## VI

Bij de metingen van Murata e.a. en die van Malkin e.a. betreffende het effect van kalium-ferricyanide op de fluorescentieopbrengst van spinazie-chloroplasten is ten onrechte geen rekening gehouden met lichtabsorptie door de toegevoegde stof.

Murata, N., e.a. (1973) *Biochim. Biophys. Acta* 325, 463-471.

Malkin, R., e.a. (1974) *FEBS Letters* 47, 140-142.

## VII

De hooggespannen verwachtingen van de puls-cytofotometrie voor medische toepassingen zijn niet bewaarheid.

Proc. 2nd Int. Symp. Pulse-cytophotometry, in druk, Antwerpen.

## VIII

Wanneer men in de toekomst overweegt by patienten die intermitterend hemodialyse ondergaan een substitutietherapie met erythropoietine ter bestrijding van de anemie in te stellen, dient men er rekening mee te houden dat de effectiviteit van erythropoietine omgekeerd evenredig is met de graad van uremie.

Erslev, A.J. (1970) *Arch. Intern. Med.* 126, 774-780.

Wagemaker, G., e.a. (1974) *Neth. J. Med.* 17, 27.

## IX

Bij het construeren van een sociale stratificatie van het platteland in het verleden, op basis van beroep, inkomen of vermogen, vormt het vinden van consistente criteria toepasbaar op zowel boeren als op niet-boeren een zeer groot probleem.

Slicher van Bath, B.H. (1957) in: *Een samenleving onder spanning; geschiedenis van het platteland in Overijssel*, pp. 183-191, 250-300 en 442-481, Assen.

## X

Het is niet zinvol de capaciteit van een psychiatrisch ziekenhuis in aantal bedden uit te drukken.

J.W.M. Visser, 22 oktober 1975

CONTENTS

1	Introduction	1
2	1.1. The general situation in the world	2
3	1.2. The general situation in the United States	3
4	1.3. The general situation in the Soviet Union	4
5	1.4. The general situation in the Western Europe	5
6	1.5. The general situation in the Eastern Europe	6
7	1.6. The general situation in the Middle East	7
8	1.7. The general situation in the Latin America	8
9	1.8. The general situation in the Africa	9
10	1.9. The general situation in the Asia	10
11	1.10. The general situation in the Oceania	11
12	1.11. The general situation in the Antarctica	12
13	1.12. The general situation in the Arctic	13
14	1.13. The general situation in the Southern Ocean	14
15	1.14. The general situation in the Indian Ocean	15
16	1.15. The general situation in the Pacific Ocean	16
17	1.16. The general situation in the Atlantic Ocean	17
18	1.17. The general situation in the Mediterranean Sea	18
19	1.18. The general situation in the Black Sea	19
20	1.19. The general situation in the Red Sea	20
21	1.20. The general situation in the Persian Gulf	21
22	1.21. The general situation in the Arabian Sea	22
23	1.22. The general situation in the Bay of Bengal	23
24	1.23. The general situation in the Andaman Sea	24
25	1.24. The general situation in the South China Sea	25
26	1.25. The general situation in the East China Sea	26
27	1.26. The general situation in the Yellow Sea	27
28	1.27. The general situation in the Bohai Sea	28
29	1.28. The general situation in the Korean Peninsula	29
30	1.29. The general situation in the Japanese Archipelago	30
31	1.30. The general situation in the Philippines	31
32	1.31. The general situation in the Indonesian Archipelago	32
33	1.32. The general situation in the Malay Peninsula	33
34	1.33. The general situation in the Sumatra	34
35	1.34. The general situation in the Java	35
36	1.35. The general situation in the Bali	36
37	1.36. The general situation in the Lombok	37
38	1.37. The general situation in the Sunda Islands	38
39	1.38. The general situation in the Moluccas	39
40	1.39. The general situation in the Irian Jaya	40
41	1.40. The general situation in the New Guinea	41
42	1.41. The general situation in the Papua New Guinea	42
43	1.42. The general situation in the Solomon Islands	43
44	1.43. The general situation in the Vanuatu	44
45	1.44. The general situation in the Fiji	45
46	1.45. The general situation in the Tonga	46
47	1.46. The general situation in the Samoa	47
48	1.47. The general situation in the Tokelau	48
49	1.48. The general situation in the Cook Islands	49
50	1.49. The general situation in the Niue	50
51	1.50. The general situation in the Wallis and Futuna	51
52	1.51. The general situation in the French Polynesia	52
53	1.52. The general situation in the New Caledonia	53
54	1.53. The general situation in the French Southern Territories	54
55	1.54. The general situation in the Antarctic	55
56	1.55. The general situation in the Arctic	56
57	1.56. The general situation in the Southern Ocean	57
58	1.57. The general situation in the Indian Ocean	58
59	1.58. The general situation in the Pacific Ocean	59
60	1.59. The general situation in the Atlantic Ocean	60
61	1.60. The general situation in the Mediterranean Sea	61
62	1.61. The general situation in the Black Sea	62
63	1.62. The general situation in the Red Sea	63
64	1.63. The general situation in the Persian Gulf	64
65	1.64. The general situation in the Arabian Sea	65
66	1.65. The general situation in the Bay of Bengal	66
67	1.66. The general situation in the Andaman Sea	67
68	1.67. The general situation in the South China Sea	68
69	1.68. The general situation in the East China Sea	69
70	1.69. The general situation in the Yellow Sea	70
71	1.70. The general situation in the Bohai Sea	71
72	1.71. The general situation in the Korean Peninsula	72
73	1.72. The general situation in the Japanese Archipelago	73
74	1.73. The general situation in the Philippines	74
75	1.74. The general situation in the Indonesian Archipelago	75
76	1.75. The general situation in the Malay Peninsula	76
77	1.76. The general situation in the Sumatra	77
78	1.77. The general situation in the Java	78
79	1.78. The general situation in the Bali	79
80	1.79. The general situation in the Lombok	80
81	1.80. The general situation in the Sunda Islands	81
82	1.81. The general situation in the Moluccas	82
83	1.82. The general situation in the Irian Jaya	83
84	1.83. The general situation in the New Guinea	84
85	1.84. The general situation in the Papua New Guinea	85
86	1.85. The general situation in the Solomon Islands	86
87	1.86. The general situation in the Vanuatu	87
88	1.87. The general situation in the Fiji	88
89	1.88. The general situation in the Tonga	89
90	1.89. The general situation in the Samoa	90
91	1.90. The general situation in the Tokelau	91
92	1.91. The general situation in the Cook Islands	92
93	1.92. The general situation in the Niue	93
94	1.93. The general situation in the Wallis and Futuna	94
95	1.94. The general situation in the French Polynesia	95
96	1.95. The general situation in the New Caledonia	96
97	1.96. The general situation in the French Southern Territories	97
98	1.97. The general situation in the Antarctic	98
99	1.98. The general situation in the Arctic	99
100	1.99. The general situation in the Southern Ocean	100
101	1.100. The general situation in the Indian Ocean	101

Aan Agnes

## CONTENTS

		page
Chapter I	GENERAL INTRODUCTION	
	1.1. The electron transport scheme of photosynthesis	7
	1.2. Primary and associated reactions	8
	1.3. Purpose of the experiments	10
	References	11
Chapter II	MATERIALS AND METHODS	
	2.1. Photosynthetic organisms	14
	2.2. Apparatus for measurements of changes in absorbance, fluorescence and electron paramagnetic resonance	
	2.2.1. Single beam spectrophotometer	15
	2.2.2. Split-beam spectrophotometer	17
	2.2.3. EPR spectrometers	22
	2.3. Experimental methods	
	2.3.1. Measurements of absorbance changes	23
	2.3.2. Fluorescence measurements	25
	2.3.3. Low temperatures	25
	2.3.4. Oxidation-reduction potential measurements	26
	2.4. Theoretical	
	2.4.1. Precision of measurements as function of absorbance	27
	2.4.2. Kinetic parameters of photoreactions	29
	2.4.3. Time course of fluorescence yield changes	33
	References	35
Chapter III	PHOTOSYSTEM 1 AT LOW TEMPERATURES	
	3.1. Introduction	38
	3.2. Materials and methods	39
	3.3. Results	
	3.3.1. Absorbance difference spectra	39
	3.3.2. EPR spectra of P700 and ferredoxin	44
	3.3.3. Temperature dependence	46
	3.3.4. Rate constants of the back reaction	48
	3.3.5. Quantum yield	48



	page
3.3.6. Plastocyanin oxidation	51
3.4. Discussion	
3.4.1. The back reaction	55
3.4.2. The primary acceptor	57
3.4.3. The absorbance difference spectrum of P700	60
References	62
 Chapter IV	
PHOTOSYSTEM 2 AT LOW TEMPERATURES	
4.1. Introduction	66
4.2. Materials and methods	66
4.3. Results	
4.3.1. C550, cytochrome $b_{559}$ and fluorescence yield changes at 90 K	67
4.3.2. Secondary electron donors at 170 K	76
4.3.3. A slow recovery of photosystem-2 reactions at 90 K	79
4.3.4. Quantum efficiencies	81
4.3.5. The back reaction	85
4.3.6. Photooxidation of chlorophyll at 110 K	91
4.3.7. Transient light-induced EPR signals near $g = 2$ at 10 - 50 K	97
4.4. Discussion	
4.4.1. Two different types of reaction centers in photosystem 2 at low temperatures	100
4.4.2. Intermediate reactions at low temperatures	101
4.4.3. Summary: a model of the photosystem-2 reaction center	103
References	106
 SUMMARY	111
 SAMENVATTING	113
 ABBREVIATIONS AND SYMBOLS	115
 CURRICULUM VITAE	116

CONTENTS

100	1.0. Introduction	100
Chapter I	1.1. The structure of the atom	101
101	1.1.1. The Rutherford model	101
102	1.1.2. The Bohr model	102
103	1.1.3. The quantum model	103
104	1.1.4. The wave nature of matter	104
105	1.1.5. The uncertainty principle	105
Chapter II	2.0. The periodic table of elements	106
106	2.1. Classification of elements	106
107	2.2. Properties of elements	107
108	2.3. Periodic trends	108
109	2.4. The periodic table	109
110	2.5. The periodic table	110
111	2.6. The periodic table	111
112	2.7. The periodic table	112
113	2.8. The periodic table	113
114	2.9. The periodic table	114
115	2.10. The periodic table	115
116	2.11. The periodic table	116
117	2.12. The periodic table	117
118	2.13. The periodic table	118
119	2.14. The periodic table	119
120	2.15. The periodic table	120
121	2.16. The periodic table	121
122	2.17. The periodic table	122
123	2.18. The periodic table	123
124	2.19. The periodic table	124
125	2.20. The periodic table	125
126	2.21. The periodic table	126
127	2.22. The periodic table	127
128	2.23. The periodic table	128
129	2.24. The periodic table	129
130	2.25. The periodic table	130
131	2.26. The periodic table	131
132	2.27. The periodic table	132
133	2.28. The periodic table	133
134	2.29. The periodic table	134
135	2.30. The periodic table	135
136	2.31. The periodic table	136
137	2.32. The periodic table	137
138	2.33. The periodic table	138
139	2.34. The periodic table	139
140	2.35. The periodic table	140
141	2.36. The periodic table	141
142	2.37. The periodic table	142
143	2.38. The periodic table	143
144	2.39. The periodic table	144
145	2.40. The periodic table	145
146	2.41. The periodic table	146
147	2.42. The periodic table	147
148	2.43. The periodic table	148
149	2.44. The periodic table	149
150	2.45. The periodic table	150
151	2.46. The periodic table	151
152	2.47. The periodic table	152
153	2.48. The periodic table	153
154	2.49. The periodic table	154
155	2.50. The periodic table	155
156	2.51. The periodic table	156
157	2.52. The periodic table	157
158	2.53. The periodic table	158
159	2.54. The periodic table	159
160	2.55. The periodic table	160
161	2.56. The periodic table	161
162	2.57. The periodic table	162
163	2.58. The periodic table	163
164	2.59. The periodic table	164
165	2.60. The periodic table	165
166	2.61. The periodic table	166
167	2.62. The periodic table	167
168	2.63. The periodic table	168
169	2.64. The periodic table	169
170	2.65. The periodic table	170
171	2.66. The periodic table	171
172	2.67. The periodic table	172
173	2.68. The periodic table	173
174	2.69. The periodic table	174
175	2.70. The periodic table	175
176	2.71. The periodic table	176
177	2.72. The periodic table	177
178	2.73. The periodic table	178
179	2.74. The periodic table	179
180	2.75. The periodic table	180
181	2.76. The periodic table	181
182	2.77. The periodic table	182
183	2.78. The periodic table	183
184	2.79. The periodic table	184
185	2.80. The periodic table	185
186	2.81. The periodic table	186
187	2.82. The periodic table	187
188	2.83. The periodic table	188
189	2.84. The periodic table	189
190	2.85. The periodic table	190
191	2.86. The periodic table	191
192	2.87. The periodic table	192
193	2.88. The periodic table	193
194	2.89. The periodic table	194
195	2.90. The periodic table	195
196	2.91. The periodic table	196
197	2.92. The periodic table	197
198	2.93. The periodic table	198
199	2.94. The periodic table	199
200	2.95. The periodic table	200

CHAPTER I  
GENERAL INTRODUCTION

1.1. *The electron transport scheme of photosynthesis.*

Green plants and other chlorophyll-containing organisms contain an efficient machinery for the conversion of solar energy into "chemical" free energy by means of the process of photosynthesis. The ultimate products of this process, oxygen and various cellular components (e.g. carbohydrates, fats and proteins) are essential for all life.

The photosynthetic process consists of many steps. Fig.1.1 shows the temporal sequence of events in four stages<sup>1</sup>. (1) Light is absorbed by pigment molecules and the energy of light is conveyed to photoreactive molecules, the so-called reaction center chlorophylls. (2) An electron is transferred rapidly from such an excited reaction center chlorophyll to a primary acceptor molecule. (3) The charge separation is stabilized by secondary electron transport towards the oxidized chlorophyll and from the reduced primary acceptor. (4) The ultimate electron acceptor of this chain of oxidation-reduction reactions, NADPH, diffuses into the Calvin-cycle for fixation of CO<sub>2</sub>; the oxygen diffuses out of the cells into the environment.

In green plants and algae there are two types of reaction centers belonging to photosystem 1 and photosystem 2, respectively. These systems

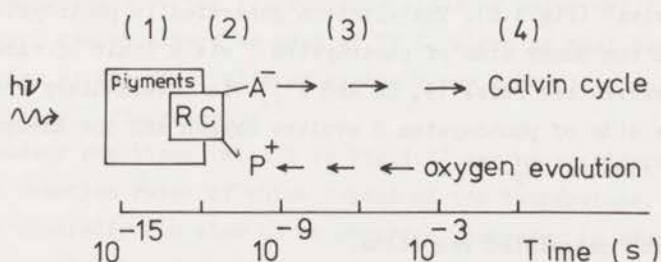


Fig.1.1. Schematic representation of photosynthesis. RC, reaction center complex; P, reaction center chlorophyll; A, primary electron acceptor. Numbers between parentheses denote different stages of the process, as described in the text. The time scale indicates the rates of transfer of energy and electrons at the different stages. Horizontal arrows indicate the direction of electron transport.

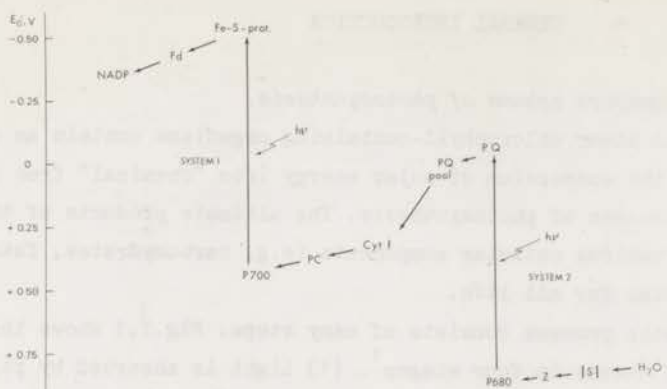


Fig.1.2. General scheme of photosynthetic electron transport in oxygen-evolving organisms. The arrows point out the direction of electron transport. Vertical arrows indicate photoreactions (primary reactions). The vertical scale indicates the midpoint potentials of the electron carriers at pH 7. Fd, (soluble) ferredoxin (refs. 3-5); PC, plastocyanin (refs. 6-8); Cyt f, cytochrome f (refs. 9-11); PQ, plastoquinone (refs. 12-14); Z and S are unknown intermediates (e.g. refs. 15, 16). According to some investigators (refs. 17, 18) the sequence of PC and Cyt f is opposite to that shown here.

operate in series<sup>2</sup> (Fig.1.2). The electron generated in photosystem 2 is transferred to the donor side of photosystem 1 via a chain of carrier molecules (for a review see refs. 19, 20 and 21). Via intermediary reactions the electron donor side of photosystem 2 evolves oxygen and the acceptor side of photosystem 1 reduces  $\text{CO}_2$ .

### 1.2. Primary and associated reactions.

This thesis deals mainly with primary reactions: the charge transfer between the reaction center chlorophyll and its acceptor molecule (step 2 in Fig.1.1). The reaction center chlorophylls of photosystems 1 and 2 are called P700 (or Chl  $a_I$ ) and P680 (or Chl  $a_{II}$ ), respectively<sup>22-25</sup>, the primary electron acceptors are denoted by X and Q, respectively<sup>26, 27</sup>.

The identity of X is not known with certainty (see reviews in refs. 21 and 28). Since P700 is photooxidized at 77 K (refs. 29-31), one of the features of X has to be its photoreduction at that temperature. Malkin and

Bearden<sup>32, 33</sup> recently discovered that in spinach chloroplasts a non-haem, iron-sulphur protein "bound ferredoxin" with electron paramagnetic resonance (EPR) lines at *g*-values of 2.05, 1.94 and 1.86 is photoreduced at 77 K. This suggests that X is a bound ferredoxin. However, the observation of photoreduction of ferredoxin at 77 K is not sufficient to prove its identity with X. In photosystem 2 the occurrence of secondary (dark) electron transport at 77 K has been demonstrated<sup>24, 34, 35</sup>. Similarly it may be speculated that ferredoxin is reduced in a dark reaction with X<sup>-</sup> at 77 K.

The primary electron acceptor of photosystem 2, Q, is probably bound plastoquinone which is reduced to plastosemiquinone in the primary reaction with P680 (refs. 36, 37 and 38). Until now, direct evidence for the photoreduction of plastoquinone at 77 K has not been reported; at that temperature, however, the oxidation-reduction state of Q may be assayed by absorbance difference measurements near 550 nm: upon reduction of Q at 77 K an absorption band peaking at 546 nm shifts to 544 nm (ref. 39). The identity of the component responsible for this band is not known yet. It has been proposed<sup>40, 41</sup> to be a  $\beta$ -carotene-protein complex and, more recently, to be pheophytin<sup>37</sup>. The substance, which is called C550 (refs. 42 and 43) is probably not an electron carrier, but an "indicator pigment" that shows a blue shift of its absorption band at 546 nm upon reduction of Q, perhaps due to a change in the local electrical field<sup>37, 44</sup>. Since Q is a quencher of chlorophyll fluorescence, whereas the reduced form, Q<sup>-</sup>, is not, reactions of Q may also be studied by measurements of the fluorescence yield of chlorophyll<sup>27</sup>. This method, however, cannot always be used at 77 K, since at that temperature an oxidized species at the donor side of system 2 may accumulate which also quenches chlorophyll fluorescence<sup>45</sup>.

The secondary reactions (step 3 in Fig.1.1) may be considered as chemical processes the reaction rates of which depend on the temperature. At 77 K these reactions are generally too slow to be observed. However, in addition to the primary processes mentioned above, the photooxidation of cytochrome  $b_{559}$  has also been observed at 77 K (refs. 24, 34, 46 and 47). Floyd et al.<sup>24</sup> reported that cytochrome  $b_{559}$  reduces P<sup>+</sup>680 with a half time of 4.2 ms at temperatures between 77 and 210 K. This indicates that the photooxidation of cytochrome  $b_{559}$  is a secondary reaction, and, therefore, that some secondary electron transport is still possible at these temperatures. Since photooxidation of cytochrome  $b_{559}$  has not been observed under physiological conditions at room temperature (refs. 48, 49), the results also indicate that reactions occurring

at low temperatures do not necessarily take place at room temperature too. Therefore a careful study of the temperature dependence of the reactions is necessary which may make possible a valid extrapolation from low temperatures to room temperature.

### 1.3. Purpose of the experiments.

The present study was undertaken to obtain information about electron transport in and near the reaction centers of photosystems 1 and 2 by measurements of the reactions of these systems at low temperatures. With respect to photosystem 1 the experiments were focussed on the roles of bound ferredoxin ( $g = 1.94$ ) and of plastocyanin. These experiments were performed in co-operation with Mr. C.P. Rijgersberg, and most of the results have also been published elsewhere<sup>50-52</sup>. Experiments on photosystem 2 dealt with the kinetics of the photoconversion of Q, P680 and cytochrome  $b_{559}$ . The measurements indicated that in addition to these three, other compounds may also take part in the reactions of system 2 at temperatures between 10 and 180 K. The properties of these compounds were also investigated. Some of the early experiments were done in collaboration with Prof. W.L. Butler, assisted by Mr. H.L. Simons; Mr. C.P. Rijgersberg and Mr. P. Gast participated at a later stage. Some of the results concerning system 2 have also been reported previously<sup>52-55</sup>.

I am indebted to many people for their contributions to the investigations reported in this thesis. I would like to thank Dr. J. Ames and Prof. Dr. L.N.M. Duysens for their stimulating discussions and valuable suggestions, as well as for a critical reading of the manuscript. Dr. B.F. van Gelder and Dr. R. Wever made me enjoy EPR measurements and placed their apparatus at my disposal. Prof. Dr. W.L. Butler introduced me to the special problems involved with photosynthetic reactions at low temperatures, and stimulated the early phases of the work. Discussions with Mr. P. Geldof, Mr. H.J. van Gorkom, Mr. M.P.J. Pulles, Mr. C.P. Rijgersberg and Mr. B.R. Velthuys have inspired me to many experiments. The technical and administrative staff of the Biophysical Laboratory have given invaluable assistance.

The work was supported in part by the Netherlands Foundation for Chemical Research (S.O.N.), and by the Netherlands Foundation for Biophysics, both financed by the Netherlands Organization for the Advancement of Pure Research (Z.W.O.).

REFERENCES.

1. Duysens, L.N.M. (1964) in: *Progress in Biophysics* Vol.14, pp. 1-104, Pergamon Press, Oxford
2. Duysens, L.N.M., Amesz, J. and Kamp, B.M. (1961) *Nature* 196, 510-511
3. Hill, R. and San Pietro, A. (1963) *Z. Naturforsch.* 18, 677-683
4. Tagawa, K. and Arnon, D.I. (1962) *Nature* 195, 537-543
5. Hall, D.O. and Evans, M.C.W. (1969) *Nature* 223, 1342-1346
6. Katoh, S. (1960) *Nature* 186, 533-534
7. Katoh, S., Suga, I., Shiratori, I. and Takamiya, A. (1961) *Arch. Biochem. Biophys.* 94, 136-141
8. Kimimura, M. and Katoh, S. (1972) *Biochim. Biophys. Acta* 283, 279-292
9. Hill, R. and Scarisbrick, R. (1951) *New Phytologist* 50, 98-111
10. Hill, R. and Bonner, W.D. (1961) in: *A Symposium on Light and Life* (McElroy, W.D. and Glass, B., eds.), pp. 424-435, Johns Hopkins Press, Baltimore
11. Elstner, E. (1969) in: *Proc. 3rd Int. Congr. Progr. Photobiol.* (Christensen, B.C. and Buchman, B., eds.) Vol.3, pp. 1035-1041, Elsevier, Amsterdam
12. Lester, R.L. and Crane, F.L. (1959) *J. Biol. Chem.* 234, 2169-2175
13. Crane, F.L. (1968) in: *Biological Oxidations* (Singer, T.P., ed.), pp. 533-580, Interscience, New York
14. Amesz, J. (1973) *Biochim. Biophys. Acta* 301, 35-51
15. Kok, B. and Cheniae, G.M. (1966) in: *Current Topics in Bioenergetics* (Sanadi, D.R., ed.) Vol.1, pp. 1-47, Academic Press, New York and London
16. Van Gorkom, H.J. and Donze, M. (1973) *Photochem. Photobiol.* 17, 333-342
17. Malkin, R., Knaff, D.B. and Bearden, A.J. (1973) *Biochim. Biophys. Acta* 305, 675-678
18. Murata, N. and Fork, D.C. (1971) *Carnegie Inst. Year Book Wash.* 70, 468-471
19. Boardman, N.K. (1968) *Adv. Enzymol.* 30, 1-79
20. Bishop, N.I. (1971) *Ann. Rev. Biochem.* 40, 197-226
21. Trebst, A. (1974) *Ann. Rev. Plant Physiol.* 25, 423-450
22. Kok, B. (1957) *Acta Botan. Neerl.* 6, 316-336
23. Witt, H.T., Müller, A. and Rumberg, B. (1961) *Nature* 192, 967-969
24. Floyd, R.A., Chance, B. and DeVault, D. (1971) *Biochim. Biophys. Acta* 226, 103-112

25. Döring, G., Renger, G., Vater, J. and Witt, H.T. (1969) *Z. Naturforsch.* 24b, 1139-1143
26. Hill, R. and Bendall, F. (1960) *Nature* 186, 136-137
27. Duysens, L.N.M. and Sweers, H.E. (1963) in: *Studies on Microalgae and Photosynthetic Bacteria*, pp. 353-372, Univ. of Tokyo Press, Tokyo
28. Ke, B. (1973) *Biochim. Biophys. Acta* 301, 1-33
29. Sogō, P., Jost, M. and Calvin, M. (1959) *Radiat. Res. Suppl.* 1, 511-518
30. Chance, B. and Bonner, W.D. (1963) in: *Photosynthetic Mechanisms of Green Plants* (Kok, B. and Jagendorf, A.T., eds.), pp. 66-81, Publ. 1145, Natl. Acad. Sci., Natl. Res. Council, Washington D.C.
31. Beinert, H. and Kok, B. (1964) *Biochim. Biophys. Acta* 88, 278-288
32. Malkin, R. and Bearden, A.J. (1971) *Proc. Natl. Acad. Sci. U.S.* 68, 16-19
33. Bearden, A.J. and Malkin, R. (1972) *Biochim. Biophys. Acta* 283, 456-468
34. Erixon, K. and Butler, W.L. (1971) *Photochem. Photobiol.* 14, 427-433
35. Erixon, K. and Butler, W.L. (1971) *Biochim. Biophys. Acta* 234, 381-389
36. Stiehl, H.H. and Witt, H.T. (1969) *Z. Naturforsch.* 24b, 1588-1598
37. Van Gorkom, H.J. (1974) *Biochim. Biophys. Acta* 347, 439-442
38. Pulles, M.P.J., Kerkhof, P.L.M. and Amesz, J. (1974) *FEBS Letters* 47, 143-145
39. Butler, W.L. and Okayama, S. (1971) *Biochim. Biophys. Acta* 245, 237-239
40. Okayama, S. and Butler, W.L. (1972) *Plant Physiol.* 49, 769-774
41. Cox, R.P. and Bendall, D.S. (1974) *Biochim. Biophys. Acta* 347, 49-59
42. Knaff, D.B. and Arnon, D.I. (1969) *Proc. Natl. Acad. Sci. U.S.* 63, 963-969
43. Butler, W.L. (1973) *Acc. Chem. Research* 6, 177-184
44. Clayton, R.K. and Straley, S.C. (1972) *Biophys. J.* 12, 1221-1234
45. Okayama, S. and Butler, W.L. (1972) *Biochim. Biophys. Acta* 267, 523-527
46. Knaff, D.B. and Arnon, D.I. (1969) *Proc. Natl. Acad. Sci. U.S.* 63, 956-962
47. Bendall, D.S. and Sofrova, D. (1971) *Biochim. Biophys. Acta* 234, 371-380
48. Amesz, J., Pulles, M.P.J., Visser, J.W.M. and Sibbing, F.A. (1972) *Biochim. Biophys. Acta* 275, 442-452
49. Cramer, W.A. and Boehme, H. (1972) *Biochim. Biophys. Acta* 256, 358-369
50. Visser, J.W.M., Rijgersberg, K.P. and Amesz, J. (1974) *Biochim. Biophys. Acta* 368, 235-246
51. Visser, J.W.M., Amesz, J. and Van Gelder, B.F. (1974) *Biochim. Biophys.*



Acta 333, 279-287

52. Visser, J.W.M. and Rijgersberg, C.P. (1974) in: *Proc. 3rd Int. Congr. Photosynthesis, Rehovot* (Avron, M., ed.) Vol.I, pp. 399-408, Elsevier, Amsterdam
53. Visser, J.W.M. and Butler, W.L. (1972) in: *Proc. Vith Int. Congr. Photo-ciology, Bochum* (Schenck, G.O., ed.), abstract 238, Max-Planck-Institut, Mülheim a.d. Ruhr
54. Butler, W.L., Visser, J.W.M. and Simons, H.L. (1973) *Biochim. Biophys. Acta* 292, 140-151
55. Butler, W.L., Visser, J.W.M. and Simons, H.L. (1973) *Biochim. Biophys. Acta* 325, 539-545

CHAPTER II  
MATERIALS AND METHODS

2.1. *Photosynthetic organisms.*

Algae were grown in liquid culture media as described elsewhere<sup>1</sup>. *Chlorella vulgaris*, *Euglena gracilis* var *bacillaris* and *Scenedesmus obliquus*, were grown in the media given by refs. 2 (M.C. medium), 3 and 4, respectively; the growth media for *Anacystis nidulans* and *Porphyridium aeruginosum* are given in ref. 1. The algae were harvested by centrifugation, usually at 3000 x g during 10 minutes. Subsequently, they were either stored in concentrated suspension at 0 °C in the dark until about 5 minutes before use, or they were diluted in fresh growth medium, gassed with air and 5 % CO<sub>2</sub>.

The concentration of the algal suspensions was determined from the absorbance at 680 nm in a 1-mm cuvette, measured with a Zeiss PMQ II absorbance spectrophotometer equipped with opal glass. The apparent absorbance at 740 nm was subtracted from the absorbance measured at 680 nm in order to correct for light scattering<sup>5</sup>. To determine absorbances of concentrated suspensions, aliquots were diluted such that accurate measurements could be performed.

Chloroplasts were obtained from market spinach. Leaves (60 g) were washed and ground in a blender (Braun MX 32) for 30-60 s in an ice-cold solution (80 ml) of pH 7.8 containing 50 mM tricine, 0.4 M sucrose, 10 mM KCl and 2 mM MgCl<sub>2</sub>. The homogenate was filtered during 3-4 minutes through 1 or 4 layers of nylon gauze (mesh width 20 µm x 20 µm or 20 µm x 80 µm, respectively) and the filtrate was centrifuged at up to 8000 x g (duration about 5 min) the rotor of the centrifuge being cooled at +2 °C. The chloroplast pellet was resuspended in 1 - 4 ml of the same cold, buffered solution, and stored at 0 °C in the dark.

The time elapsed between grinding of the spinach leaves and resuspension of the chloroplasts was 10 - 15 minutes. The concentration of chlorophyll was determined according to Arnon<sup>6</sup>. The stored suspension usually contained 3-7 mg chlorophyll per ml. The chloroplasts were resuspended shortly before use in a small volume of the buffered solution to the concentration of chlorophyll which was suitable for the measurement.

## 2.2. Apparatus for measurements of changes in absorbance, fluorescence and electron paramagnetic resonance.

### 2.2.1. Single beam spectrophotometer.

Photometric measurements of light-induced absorbance changes were performed with two different spectrophotometers. Firstly, a single-beam apparatus, designed by Dr.L.N.M. Duysens, was used in combination with a cuvette holder and dewar enabling optical measurements at temperatures between 77 and 280 K. Continuous (non-modulated) measuring light was provided by a Bausch and Lomb monochromator ( $f/4.4$ , 500 mm focal length, slit height 20 mm, 1200 lines/mm grating, dispersion 1.6 nm/mm) and a tungsten halogen lamp (Osram, 24 V, 250 W) powered with a current-stabilized d.c. power supply (Oltronix B32-10R). The wavelength indicator of the monochromator was calibrated regularly against the emission lines of a mercury arc. The measuring beam was focussed on the sample cuvette. The measuring light transmitted by the sample (1 or 2 mm optical pathway) was measured with a S-20 or S-20 modified photomultiplier (EMI 9558 or 9658) provided with suitable filters to minimize stray light from the monochromator and to block actinic illumination. The voltage signal developed across the 1 M $\Omega$  load resistor of the photomultiplier was taken directly to an oscilloscope which was connected to a 1 kHz strip-chart recorder (2-channel Siemens oscillomink) for data recording. With some experiments the oscilloscope was connected to a signal averager (Datalab DL 102.S.). Without averaging the sensitivity of the apparatus was found to be determined by the noise in the primary current of the photomultiplier. With samples having an apparent absorbance of 0.87 (see Section 2.4.1) the sensitivity was about  $5 \times 10^{-4}$  absorbance units between 420 and 700 nm, the time constant of the apparatus being 1 kHz. Limiting the frequency response by means of electrical filters the sensitivity could be improved; this was usually done with measurements of relatively slow signals. Care was taken not to affect the measurements of kinetics by the use of the filters.

Filtered actinic light provided by a tungsten halogen lamp (Osram, 24 V, 250 W) placed in a Leitz Pradolux, type 37852 condensor set or by a xenon flash lamp (FT 230, General Electric, C=10  $\mu$ F, V=2400 V) was incident on the front surface of the cuvette at a small angle ( $14^\circ$ ) to the measuring beam. The half width of the flash was typically 7  $\mu$ s. The flash light was filtered by a broad green filter combination consisting of a Balzers Filtraflex DT interference, a Schott OG 4 cut-off and a Balzers Calflex C heat reflecting filter, unless noted otherwise. This combination was chosen in order to have

a homogeneous distribution of saturating light through the depth of the cuvette without causing "double hits" of the reaction centers by one flash. With this combination of filters the energy of the flash at the cuvette surface was determined to be approx.  $100 \mu\text{J}\cdot\text{cm}^{-2}$ . The intensity of light provided by the tungsten lamp was calibrated with a Yellow Springs radiometer (model 65) and monitored continuously with a photodiode. The radiometer was calibrated against a standard Eppley thermopile.

Measurements at temperatures between 77 and 280 K were performed by means of a cuvette holder, which was cooled by liquid nitrogen, as is illustrated in Fig.2.1. A thermocouple (iron-constantan) attached to the cuvette was used to monitor the temperature. Temperatures above 90 K were obtained by cooling the sample at 77 K with liquid nitrogen and subsequently blowing a stream of dry nitrogen gas through the dewar. Temperatures between 77 and 90 K were obtained by cooling to 77 K and waiting for some minutes: the heating rate was about 2 degrees per minute with liquid nitrogen present at the bottom of the dewar. Measurements at a constant temperature of 77 K were made with the cuvette submerged completely in liquid nitrogen. Only fluorescence could be measured in this case and small, short disturbances appeared on the fluorescence trace, when bubbles of nitrogen gas passed the windows of the dewar.

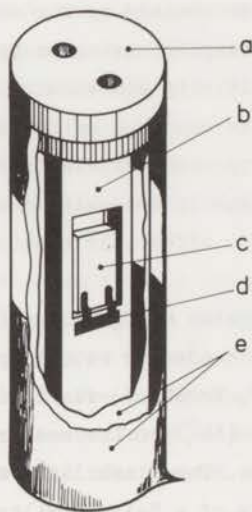


*Fig.2.1. Low-temperature cuvette holder. A teflon lid (a) provided with holes was attached to a metal bar (b), the end of which was submerged in liquid nitrogen. The sample cuvette (c) was fastened by use of springs (d) upon a gap in the bar. The bar was placed in a silvered cylindrical dewar (e) with windows at the sample position.*

### 2.2.2. Split-beam spectrophotometer.

The second spectrophotometer used to measure light-induced absorbance changes was also constructed in our laboratory according to the same principle as one described earlier<sup>7</sup>. The apparatus was of the "split-beam" type, equipped with two independent measuring beams by use of two monochromators, two choppers and two photomultipliers as is illustrated in Fig.2.2. We will refer to the two different beams as beam A and beam B. The optical geometry of both beams was the same, only one of these will be described (beam A).

Measuring light was provided by a monochromator, similar to the one specified above, and a tungsten ribbon filament lamp (6 V, 18 A) or a tungsten halogen lamp (Osram, 24 V, 250 W) operated on stabilized d.c. power supplies. Measurements in the ultra-violet wavelength region were performed using a high-pressure xenon arc (Osram 900 W). After passing the monochromator and lens  $L_1$  the light was split into two beams ( $A_1$  and  $A_2$ ) of about equal intensity by means of a beam splitter mirror. This consisted of a stack of thin horizontal glass plates, silvered on their edges and staggered alternately right and left, so as to reflect half the light one way and half the other. Each beam then was reflected by a concave mirror ( $M_1$  and  $M_2$ ) which focussed an image of the exit slit of the monochromator upon a rotating disk provided with five holes at equal distances. This light chopper (l.c.) was driven by a synchronous motor (Dunker 42 x 60-2) and rotating at a speed of 50 r.p.s. The chopper was positioned such that both beams were modulated with the same frequency (250 Hz); the phases of the beams, however, were different by  $\pi$  radians. Subsequently, the beams passed the lenses  $L_2$  and  $L_3$  and were deflected upwards by means of mirror  $M_A$  at an angle of  $53^\circ$  to the original direction. Each beam passed a different horizontally mounted cuvette ( $c_1$  and  $c_2$ ) filled with suspension, one or more filters  $F_A$  and finally reached the photocathode of a photomultiplier (EMI 9558 or 9658). The photomultiplier was positioned at the intersection of the two beams ( $A_1$  and  $A_2$ ) at a distance of about 7 cm from both cuvettes. The horizontal cross sections of the beams were about 20 mm x 10 mm at the sample positions, almost independently of the size of the exit slit of the monochromator (generally 20 mm high and 1 - 3 mm wide). Usually the inner thickness of the cuvettes was 1 or 2 mm. Due to the oblique incidence of the measuring beam the optical pathway through glass and plexiglass cuvettes filled with water was 12 % longer than the cuvette thickness.

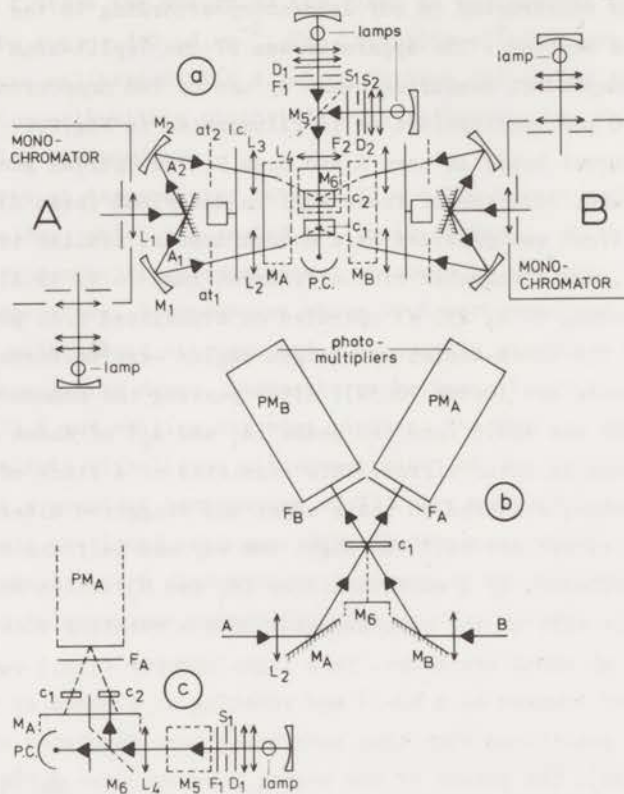


Fig.2.2 Schematic diagram of the double split-beam spectrophotometer. The apparatus consists of two completely independent split-beam spectrophotometers, which have only the two cuvettes in common. A and B are two independently modulated measuring beams; L, lenses; M, mirrors; F, optical filters; S, shutters; D, diaphragms; at, light attenuators; l.c., light choppers; P.C., photocell;  $c_1$  and  $c_2$ , sample cuvettes; PM, photomultipliers. Fig.a represents a top view of the total apparatus without the photomultipliers; Fig.b: a side view of the part where the photomultipliers are mounted; and Fig.c: a cross section perpendicular to Figs. a and b in the plane of the path of the actinic illumination. The light paths laying in the plane of the figures are given by solid lines.

The anode signal of the multiplier was fed to an a.c. amplifier (Brookdeal, type 450), which transmitted a band of 0.1 - 1 kHz. The a.c. signal was smoothed by a window amplifier eliminating peaks, which occurred during the change of the light beams ( $A_1$  and  $A_2$ ) causing the multiplier current. Subsequently the signal was rectified (Brookdeal, type 411) and recorded on a Clevite Brush strip-chart recorder (mark 220), or by a 4-channel signal averager (Nuclear Chicago, model 7100). The rectification was performed by use of an a.c. current in phase with the photo current effected by one of the two beams ( $A_1$  or  $A_2$ ) and provided by a photodiode and a phaseshifter, the photodiode being illuminated through the holes of the rotating chopper by a light emitting diode. The total current from the photomultiplier was measured by a  $\mu\text{A}$  meter. A block diagram of the electronics is shown in Fig.2.3. The independent beams (A and B) were measured by means of separate amplifiers, phase shifters and rectifiers. The recorder had two channels, one for each beam.

By means of light attenuators the intensity of each beam could be adjusted separately. The attenuators consisted of horizontal parallel wires (at<sub>1</sub>) or lamellae (at<sub>2</sub>), which were attached at equal distances in a rectangular frame, and the number of which crossing the light beam could be varied by turning the frame around a horizontal axis. To calibrate the extent of absorbance changes a slide of known absorbance was brought into one of the beams ( $A_1$ ),

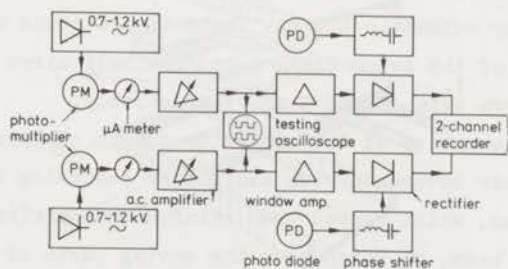


Fig.2.3. Block diagram of the electronics of the split-beam spectrophotometer.

causing a decrease of the intensity of that beam. The transmission of this slide was determined by use of a Zeiss PMQ II spectrophotometer. With samples of low absorbance the sensitivity of the apparatus was  $2 - 4 \times 10^{-5}$  absorbance units, with a response time of 300 ms. This sensitivity was rather independent of the intensity of the measuring light at wavelengths between 400 and 800 nm, where the intensity of light incident on the cuvettes was  $0.1 - 1 \mu\text{W}\cdot\text{cm}^{-2}$ .

Since, generally, scattering suspensions were used, the light of each beam was incident on both photomultipliers. Therefore, the light choppers of both beams (A and B) could be set such that the phase of the modulation of both beams differed by  $\pi/2$  radians. Thus the changes of the light intensity of each beam were only converted into deflections of the recorder traces belonging to that beam.

The actinic light was provided by tungsten halogen lamps placed in projector condenser sets (Leitz Pradolux, type 37852), or by a xenon flash tube, as shown in Fig.2.2. Lens  $L_4$  focussed images of diaphragms  $D_1$  and  $D_2$  (both 37 mm x 37 mm) upon the sample cuvette ( $c_2$ ). The size of the image was about 20 mm x 20 mm. After passing  $L_4$  part of the actinic light was reflected upwards by a partially reflecting mirror ( $M_6$ ). The light transmitted by that mirror was focussed (by  $L_4$ ) upon a calibrated vacuum photocell (p.c.) (RCA 925) serving to measure continuously the intensity of the radiation. The intensity of actinic light could be varied by use of neutral density filters ( $F_1$  and  $F_2$ ) or by changing the lamp voltage. Filters ( $F_1$  and  $F_2$ ) provided also the desired spectral composition of the actinic light. Two independent actinic light sources could be used simultaneously by use of a half reflecting mirror ( $M_5$ ). Close to each lamp a shutter (S) (Gitzo) was mounted, which was operated by electro-magnets (Robot, 3364 Sagib). The power for the magnets could be switched on and off by automatic timers. These timers could also be used to trigger the ignition of the xenon flash tube. The half times of opening and closing of the shutters were 10 and 7 ms, respectively.

Vibrations of the optics of the apparatus due to chopper motors, lamp ventilators and shutter movements were avoided by fastening the optics rigidly upon a heavy iron beam, which rested upon reinforcements ribs. These ribs were mounted upon another beam, on which also the moving parts of the apparatus were mounted.

For some purposes (e.g. fluorescence yield measurements, double beam absorbance difference measurements) the beam splitter could be replaced by a mirror, which reflected the measuring light from the monochromator towards the concave mirror,  $M_2$ . Thus only the sample cuvette,  $c_2$ , was illuminated by



modulated light.

The spectrophotometer could be connected with a PDP-9 computer via a 1-channel analogue-to-digital convertor (40 Hz, 12 bits). This computer could also be used to drive the wavelength of one of the monochromators at steps of 1 nm. Measurements were stored on a magnetic tape unit and treated conveniently in the desired manner.

#### *Low temperature attachment.*

With the split beam apparatus described above measurements at temperatures between 80 and 300 K could be performed by use of a cuvette holder which is illustrated in Fig.2.4. The suspension was contained between two plexiglass plates, pinched at a brass block. The two sample compartments were 1 mm x 10 mm x 25 mm, the optical pathway being 1 mm. By means of a controlled flow of liquid nitrogen through the block the suspension could be cooled to any desired temperature above 80 K. The flow rate was adjusted by a valve that was driven by an automatic temperature controller (Cryoson, TR). The temperature was measured with a thermocouple (copper-constantan) positioned in the sample. The sample holder was surrounded by a box of polystyrene foam with plexiglass or quartz windows at the sample positions. The windows were kept free of condensation by a stream of nitrogen gas. All plexiglass was selected for high transmission at 290 nm.

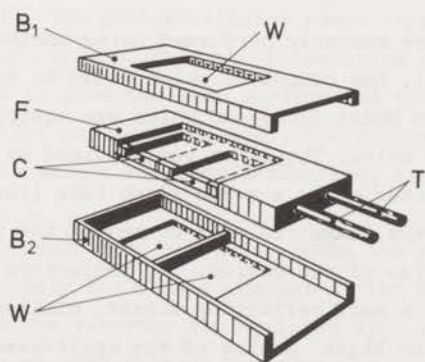


*Fig.2.4. Low-temperature cuvette holder used with the double split-beam spectrophotometer: B<sub>1</sub> and B<sub>2</sub>, top and bottom parts of a polystyrene foam box, respectively; W, window; F, brass frame; C, cuvette; T, cooling tubes. For further details see text.*

### 2.2.3. EPR spectrometers.

Electron paramagnetic resonance measurements were recorded at the B.C.P. Jansen Institute, Amsterdam, using a Varian E-3 or E-9 spectrometer, operating near 9 GHz. The microwave frequency was calibrated by use of a frequency counter (Hewlett-Packard 5246 L) with frequency convertor (5255 A). The field strength was calibrated using an AEG Magnetfield meter (GA 11-22.2). First derivative EPR spectra were obtained by 100 kHz modulation of the magnetic field. Samples in standard quartz tubes (3 mm inner diameter) were cooled to the desired temperature by a stream of nitrogen, provided by a variable temperature accessory (Varian, E-257), for measurements at  $90 < T < 200$  K and by a stream of helium, provided by a liquid transfer system (Air Product Inc., LTD-3-100) with automatic temperature controller (OC-20) for measurements at  $10 < T < 90$  K. These lower temperatures could also be obtained using a helium flow system as described in ref. 8. The temperature was measured with a carbon resistor, previously calibrated against a calibrated germanium resistor.

The sample was illuminated in the cavity by a slide projector (Aldis, 500 W). The beam passed through a cuvette (5-mm pathway) filled with water and through suitable lenses to illuminate the slotted front side of the cavity. The intensity in the cavity was determined by use of a calibrated Yellow Springs radiometer (model 65) to be about  $100 \text{ mW}\cdot\text{cm}^{-2}$ . Continuous illumination with this intensity generally caused an increase of the temperature, which amounted to  $2 - 4^\circ$  near 80 K using the nitrogen gas device and  $5 - 10^\circ$  near 10 K with the helium gas stream, depending on the flow rates of the gases.

Some experiments were recently performed using another Varian E-9 spectrometer (at our laboratory), the output of which could be fed into a signal averager (Nuclear Chicago Model 7100) and which was equipped with an illumination set-up as described below. The light was provided by a tungsten halogen lamp fitted into a projector or by a xenon flash tube (for details see Section 2.2.1). A lens focussed the image (20 mm x 20 mm) of the projector diaphragm upon the slotted front side of the cavity. Two projectors could be used simultaneously by means of a half reflecting mirror, similarly as can be seen in Fig.2.2 for the actinic light device of the split-beam apparatus. Each light beam could be filtered to obtain the desired spectral distribution. The intensity of each beam could be varied by use of neutral density filters or by changing the lamp voltage. Shutters provided with electro-magnets were used to turn the light on and off. The halftime of opening and closing was 4 and 15 ms, respectively. The electro-magnets were triggered by automatic

timers to enable averaging of the kinetics of light-induced signals. The intensity of illumination was measured with a calibrated Yellow Springs radiometer (model 65).

### 2.3. Experimental methods.

#### 2.3.1. Measurements of absorbance changes.

Since the time response of the split-beam spectrophotometer was much lower than the frequency of the light modulation (250 Hz), flash-induced absorbance changes were generally measured by means of the single beam apparatus, described in Section 2.2.1. Measurements were made by adjusting the photomultiplier power supply to give a 1-V signal. The sensitivity of the oscilloscope amplifier was then increased 100-fold and a d.c. voltage offset was used to position the trace. Absorbance changes were calculated from the measured transmission changes with  $\Delta A = -0.43 \Delta T/T$ . The intensity of the measuring light was kept less than  $1 \mu\text{W}\cdot\text{cm}^{-2}$ , which was too weak to activate significantly photosynthetic reactions. Measurements of absorbance changes induced by continuous irradiation could also be performed using the single beam apparatus, except at wavelengths between 640 and 780 nm due to fluorescence excited by the actinic light. With measurements of flash-induced changes in this spectral region the fluorescence excited by the actinic flash caused an overload of the apparatus during about 30 ms.

Absorbance changes between 640 and 780 nm induced by continuous irradiation were measured by means of the split-beam spectrophotometer described above (Section 2.2.2). The photomultiplier power supply was adjusted to give a 1 - 5  $\mu\text{A}$  multiplier current. Then the intensities of the measuring beams were attenuated so as to give the same current and the measurements were made. Since the actinic light was not modulated, the fluorescence excited by this illumination did not cause a recorder deflection, except for disturbances as described in ref. 7.

Due to the two independent measuring beams the apparatus could be used to measure simultaneously absorbance changes at two different wavelengths (e.g. ref. 9). Since the recorder was equipped with a differential input it was also possible to measure changes according to the dual wavelength method (refs. 10-12), an example of which is given in Fig.2.5. The figure also shows that the results of this frequently applied technique may be misleading if the difference between the absorbance changes at only two wavelengths is measured.

Measurements of absorbance changes near 680 nm with photosynthetic

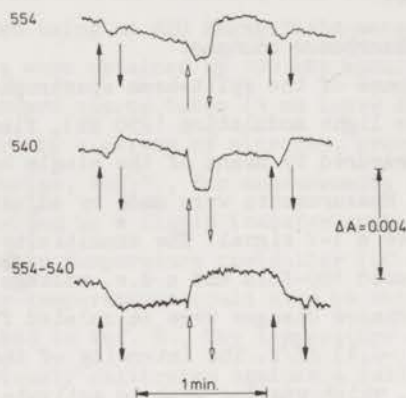


Fig. 2.5. Light-induced absorbance changes at 540 and 552 nm and the difference between these changes with spinach chloroplasts (0.4 mg chlorophyll/ml in 1-mm cuvette) at room temperature. Actinic light:  $(676 \pm 6)$  nm,  $10 \text{ mW}\cdot\text{cm}^{-2}$  and  $(715 \pm 6)$  nm,  $3.0 \text{ mW}\cdot\text{cm}^{-2}$ . Light on at upward, off at downward pointing arrows. Open arrows: 680 nm, and closed arrows: 715 nm light. The upper tracings were recorded simultaneously;  $\Delta A_{554} - \Delta A_{540}$  was registered by use of the differential input of the recorder of the split-beam apparatus. This figure may serve to illustrate that double beam recordings in this spectral region at room temperature may be caused by relatively small differences between large absolute absorbance changes at two different wavelengths.

organisms may be distorted significantly by changes in the yield of the fluorescence excited by the measuring beam (e.g. refs. 13, 14). In order to minimize this distortion narrow band pass interference filters were placed in front of the photomultiplier and (oxidized) dibromothymoquinone (DBMIB), a potent quencher of the fluorescence yield of pigment system 2 in spinach chloroplasts (refs. 15, 16), was added to the sample. Addition of DBMIB may also lower the quantum efficiency of photosystem-2 reactions. The proportional decrease of this efficiency, however, is relatively less than that of the fluorescence yield<sup>17</sup>.

### 2.3.2. Fluorescence measurements.

Measurements of fluorescence yield changes were generally performed with the single beam spectrophotometer described in Section 2.2.1. Flash-induced changes were measured using the steady light provided by tungsten halogen lamp and monochromator, to excite fluorescence. The intensity of this light was kept essentially non-actinic (less than  $1 \mu\text{W}\cdot\text{cm}^{-2}$ ): illumination with this light for two minutes at 77 K of spinach chloroplasts caused an increase of the fluorescence yield which was smaller than 3 % of the maximally obtainable yield. Xenon flashes were used to induce changes of the fluorescence yield. If samples were irradiated with actinic continuous light the power supply of the multiplier was switched off in order to protect the phototube, or the number of dynodes and the power supply were adjusted to measure the fluorescence excited by the irradiation.

Fluorescence yield changes could also be measured with the split-beam spectrophotometer described in Section 2.2.2. In that case only the sample cuvette was illuminated with modulated light (250 Hz) of low intensity (less than  $1 \mu\text{W}\cdot\text{cm}^{-2}$ ). The fluorescence excited by this illumination was detected by one of the photomultipliers supplied with appropriate filters. The multiplier current was converted via the demodulator into a recorder deflection as for measurements of absorbance changes. Changes of the fluorescence yield were induced by continuous light or by xenon flashes and were detected by the modulated beam (ref. 18). The fluorescence excited by the steady actinic illumination did not cause a recorder deflection, except for transient disturbances as described in ref. 7. With the split-beam apparatus the fluorescence yield changes could also be measured using the non-modulated actinic illumination as excitation light. For that purpose the tungsten halogen lamps providing the actinic light were powered with stabilized power supplies and the multiplier current was fed directly into the recorder (e.g. ref. 19).

Evidently it was also possible to measure simultaneously absorbance and fluorescence yield changes using the split-beam apparatus.

### 2.3.3. Low temperatures.

For optical measurements below  $0^\circ\text{C}$  the cuvette holders described in Section 2.2.1 and 2.2.2 were used. Shortly before lowering the temperature samples were suspended in glycerol or ethylene glycol (final concentrations: 50 - 55 % v/v) for measurements at temperatures below 200 K or between 200 and 270 K, respectively. EPR measurements were performed without these solvents,

unless stated otherwise. To minimize effects of the presence of glycerol or glycol (e.g. refs. 20 and 21) the suspensions were, generally, prepared in the dark within 5 minutes before the freezing was started. However, measurements of the fluorescence of pigment system 2 with samples of *Chlorella vulgaris* suspended in glycerol shortly before freezing indicated a decrease of the fluorescence yield similarly as described by Frackowiak<sup>20, 21</sup> with *Chlorella pyrenoidosa* suspended in glycol. With spinach chloroplasts the fluorescence yield was found to be the same with and without glycerol or glycol. These solvents were used - in spite of their possible effects on the phenomena studied - in order to obtain highly transparent samples upon freezing. Measurements of the transmission at 550 nm of a sample of spinach chloroplasts (1 mg chlorophyll/ml in a 1-mm cuvette) suspended in glycerol indicated that the scattering of the measuring light was the same at room temperature and at 80 K. Without glycerol or glycol the cuvette content crystallized when the temperature was lowered, giving an intensification of absorbance bands, as had also been observed by Keilin and Hartree<sup>22</sup>. The effect is due to an increase of the optical pathlength<sup>23</sup>. The extent of the intensification, however, was found to be dependent upon, firstly, the temperature of the sample, and, secondly, the rate of freezing the sample, probably since shape and size of the crystals are also dependent on these parameters. Therefore, only samples that remained transparent glasses, due to the presence of glycerol and glycol, were used for the measurements. The effect of crystals on measurements of absorbance changes at low temperatures will also be discussed in Chapter IV.

#### 2.3.4. Oxidation-reduction potential measurements.

Potentiometric titration curves for optical and ESR signals at temperatures near 110 K were determined as follows. Dark-adapted spinach chloroplasts (Section 2.1) were suspended in darkness in 2 ml isolation buffer, a mixture of potassium ferri- and ferrocyanide (2 ml) and glycerol (5 ml). The sum of the concentrations of ferri- and ferrocyanide was approximately the same in every sample (molar ratio:  $\text{Fe}(\text{CN})_6/\text{chlorophyll} = 300$ ). If desired, aliquots (<20  $\mu\text{l}$ ) of oxidant ( $0.5 \text{ M K}_3 [\text{Fe}(\text{CN})_6]$ ) or reductant ( $0.5 \text{ M K}_4 [\text{Fe}(\text{CN})_6]$ ) were added to adjust the potential slightly. The suspension was stirred in an open beaker at 25 °C in the dark. The redox potential of the medium was measured with a combination of a platinum flag and a calomel (saturated KCl) electrode (Radiometer type P 101 and K 401, respectively). The electrode was calibrated against a saturated quinhydrone electrode at 25 °C and the

potential was found to be  $225 \pm 10$  mV. This value was used to convert the potential measurement to the scale based on the hydrogen electrode. The potential was found to be stable after about two minutes. Then a sample of the suspension was taken and frozen in a cuvette to 77 K in darkness. A different suspension was used for each measurement. The rate of cooling was kept the same for each sample to avoid differences between samples caused by the temperature dependence of the potential of the ferri-ferrocyanide redox buffer<sup>25</sup>.

Care was taken to perform measurements involving the absorption of light at wavelengths where the contribution of the ferri- and ferrocyanide to the absorption was negligible.

With our electrode we determined the midpoint potential ( $E_m$ ) of the ferri-/ferrocyanide system in glycerol-water (55 - 45 % v/v, respectively) and in water to be 380 and 430 mV, respectively, at 20 °C, the ionic strength being 0.6 M. The latter value of  $E_m$  is, within the limits of the accuracy of our measurements ( $\pm 10$  mV), similar to values reported in the literature (e.g. refs. 25 and 26). The decrease of the potential by the addition of glycerol was also observed with chloroplasts present. The phenomenon may be due to a change of the solvation as has been reported for the  $K_4 [Fe(CN)_6] - K_3 [Fe(CN)_6]$  system in various organic solvent-water mixtures (ref. 27).

It will be clear that due to the presence of glycerol as well as due to the use of temperature changes the results of our measurements cannot be considered to give absolute values of the potential behavior of the phenomena studied. Since, however, the conditions were the same for each experiment, the results may be used to compare the effect of the redoxpotential on various phenomena occurring at low temperatures.

#### 2.4. Theoretical.

We will describe a mathematical procedure to calculate the kinetic parameters of photoreactions from measurements of absorbance changes using optically dense suspensions. Analogous procedures have been described previously<sup>28</sup>. Furthermore it will be shown, that, under certain conditions, this procedure may also be applied to measurements of fluorescence yield changes.

##### 2.4.1. Precision of measurements as function of absorbance.

The signal-to-noise ratio, S/N, of measurements of absorbance changes with suspensions which contain scattering particles depends on the absorbance of the sample in the following manner. For a photomultiplier S/N is linearly proportional to the square root of the cathode current. I is proportional to

the light intensity; the proportionality factor depends on the quantum yield of the light-sensitive layer.

$$S/N \sim I^{\frac{1}{2}} \quad (2.1)$$

A change of the signal,  $\Delta S$ , is due to a change of the measured intensity,  $\Delta I$ , or:

$$\Delta S/S = \Delta I/I \quad (2.2)$$

Hence from (2.1) and (2.2)

$$\frac{\Delta S}{N} \sim \frac{\Delta I}{I^{\frac{3}{2}}} \quad (2.3)$$

With light-induced absorbance changes,  $\Delta I/I$  is caused by a change of the concentration,  $\Delta c/c$ , of one or more of the compounds present in the sample. Furthermore, in photosynthetic organisms generally,

$$\Delta c \sim C \quad (2.4)$$

where  $C$  is the sum of the concentrations of all compounds absorbing the measuring light. With homogeneous suspensions of cubic, colored particles for not too concentrated suspensions the extinction is linearly proportional to the concentration<sup>29</sup>:  $\log [I_0/I(\alpha)] = E(\alpha) \sim p \sim C$  where  $I_0$  is the light intensity incident on the sample cuvette;  $I(\alpha)$  is the light intensity transmitted by the cuvette and detected by the photodetector, which catches only light with a deviation from the incident beam of less than the angle  $\alpha$ ;  $E(\alpha)$  is the absorbance measured with such a photodetector. For cubic particles  $p$  is equal to the total area of all particles in the light beam projected on a plane perpendicular to this beam, divided by the illuminated area of this beam. In samples of different concentration only  $p$  varies;  $p$  is linearly proportional to the concentration of the particles in the cuvette.

Then from (2.4):  $\Delta E(\alpha) \sim E(\alpha)$ . So that in first approximation

$$\Delta I(\alpha) \sim \frac{dI(\alpha)}{dE(\alpha)} \Delta E(\alpha) \sim E(\alpha) \frac{dI(\alpha)}{dE(\alpha)}$$

Thus from (2.3) we find:

$$\frac{\Delta S}{N} \sim \frac{E(\alpha)}{I^{\frac{3}{2}}(\alpha)} \frac{dI(\alpha)}{dE(\alpha)} \quad (2.5)$$

This function has a maximum if its derivative with respect to  $E(\alpha)$  equals zero. This yields  $E(\alpha) = 0.87$ . Borisov et al.<sup>30</sup> obtained the same value for the optimal precision of measurements of absorbance changes as a function of the concentration, although they did not account for the particle flattening.



The same result is obtained for measurements of absorbances if the absorbance-concentration dependence obeys Beer's law (e.g. ref. 31). Thus, for dilute scattering, as well as for non-scattering suspensions, the best concentration of the sample for measurements of absorbance changes is that causing 14 % of the light incident on the sample to be caught by the photodetector.

#### 2.4.2. Kinetic parameters of photoreactions.

With samples having an absorbance of 0.87 the intensity of the measuring light at the front side of the sample cuvette is 7.4 times higher than at the back side. Generally, the absorbance at the wavelength of measurement is different from that of actinic illumination. With samples having an absorbance of 0.87 at the wavelength of the measurement, the ratio of the intensities of actinic light at the front and back side of the sample cuvette may amount to factors of 100 or more if the absorbance is higher for actinic than for measuring light. Consequently, the rate of photoreactions occurring in the cuvette may depend strongly upon the position of the reacting compounds in the cuvette with respect to the actinic beam. Fig.2.6 shows an example of an irreversible light-induced absorbance change, reflecting the photoreduction of the primary electron acceptor of photosystem 2 at 90 K, brought about by actinic illumination of different wavelengths at various concentration of sample material. Fig.2.7 illustrates that the deviation of the measured absorbance change from the exponential behavior expected for suspensions with a small absorbance of actinic light, is more pronounced the higher the absorbance at the wavelength of the actinic light of the material in the sample.

The intensity of light in the cuvette decreases with increasing distance from the front layer according to the formula:

$$I_x = I_0 f(x) = I_0 [\exp (-qx)] \quad (2.6)$$

where  $x$  is the distance from the front layer and  $q$  is the extinction coefficient of the sample at the wavelength of illumination. In a thin layer of thickness  $dx$  at distance  $x$  to the front the number of absorbed quanta per unit thickness is equal to the product of the intensity at this layer and the extinction coefficient ( $q I_x$ ). If the quantum yield ( $\gamma$ ) for an absorbed photon does not depend on the amount of photoreactive centers ( $Y$ ), the rate of the reaction, which in photosynthesis is a charge transfer between two species in one reaction center, is expressed by:

$$\frac{dY}{dt} = - \gamma q I \frac{Y}{Y_0}$$

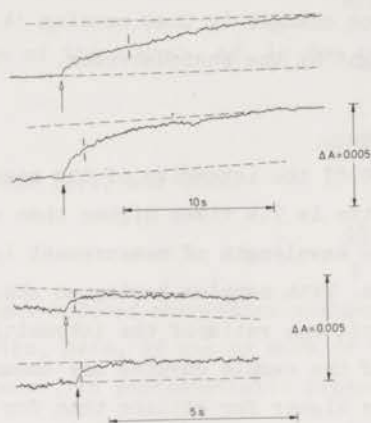


Fig.2.6. Time course of absorbance at 542 nm during irradiation of spinach chloroplasts in a 1-mm cuvette at 90 K. Actinic light on at upward arrows; open arrows:  $(676 \pm 6)$  nm,  $0.6 \text{ mW}\cdot\text{cm}^{-2}$ ; closed arrows:  $(630 \pm 6)$  nm,  $0.7 \text{ mW}\cdot\text{cm}^{-2}$ . Chlorophyll concentration: upper curves: 1.5 mg/ml; lower curves: 0.4 mg/ml. Vertical lines on curves indicate half times.

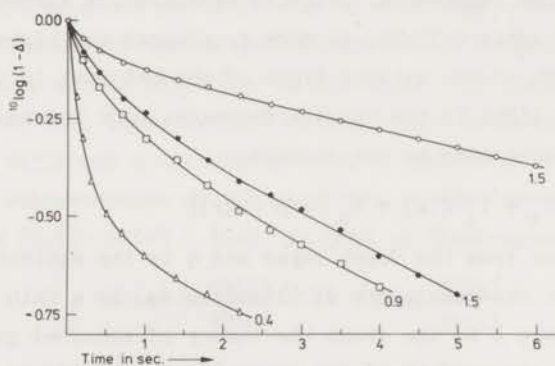


Fig.2.7. Semilogarithmic plots of data in Fig.2.6.  $\log(1-\Delta)$  vs time where  $\Delta$  is the fraction of maximal change. Open and closed symbols: 676 and 630 nm irradiation, respectively. Chlorophyll concentration in mg/ml; circles, 1.5; squares, 0.9 and triangles, 0.4.

or:

$$Y = Y_0 [\exp (- \gamma q I t / Y_0)]$$

where  $Y_0$  is the total number of reaction centers. In a small layer at distance  $x$  from the front layer:

$$Y = Y_0 [\exp (- \gamma q I_x t / Y_0)] \quad (2.7)$$

If the reaction causes absorbance changes ( $\Delta E$ ) then in a thin layer of thickness  $dx$ :

$$\Delta E_{dx} = \epsilon_y \Delta Y dx = \epsilon_y (Y_0 - Y) dx$$

where  $\epsilon_y$  is the specific differential extinction coefficient of one of the reactants  $Y$  at the wavelength of measurement. Thus, substituting (2.7) in this expression:

$$\Delta E_{dx} = \epsilon_y Y_0 [1 - \exp(- \gamma q I_x t / Y_0)] dx$$

and with (2.6) we find

$$\Delta E_{dx} = \epsilon_y Y_0 [1 - \exp(- \gamma q I_0 e^{-qx} t / Y_0)] dx$$

For  $t \rightarrow \infty$ :  $\Delta E = \epsilon_y Y_0 dx$ , which is independent on the distance  $x$ . This shows that each layer  $dx$  contributes to the same amount to the total extent of the absorbance change. In the course of the change, however, the contributions of the different layers is not the same. The time course of the absorbance change is expressed by an integration of exponential functions over the layers.

Integration over  $dx$  gives the absorbance change for the cuvette with optical pathway  $d$ .

$$\begin{aligned} \Delta E &= \epsilon_y Y_0 \int_0^d [1 - \exp(- \gamma q I_0 e^{-qx} t / Y_0)] dx \\ &= \epsilon_y Y_0 d - \epsilon_y Y_0 \int_0^d \exp(- \gamma q I_0 e^{-qx} t / Y_0) dx \end{aligned}$$

In first approximation  $q$  is independent of  $x$ . Substituting  $a = \gamma q I_0 e^{-qx} t / Y_0$ , (so  $a_0 = \gamma q I_0 t / Y_0$  and  $a_d = \gamma q I_0 e^{-qd} t / Y_0 = a_0 T_d$ , where  $T_d$  is the transmittancy of the cuvette at the wavelength of actinic illumination):

$$\Delta E = \epsilon_y Y_0 \{d - [\int_{a_d}^{a_0} a^{-1} e^{-a} da] / q\} \quad (2.8)$$

By splitting the integral term into two terms

$$\int_{a_d}^{a_0} a^{-1} e^{-a} da = \int_{a_d}^{\infty} a^{-1} e^{-a} da - \int_{a_0}^{\infty} a^{-1} e^{-a} da,$$

(2.8) may be written:

$$\Delta E = \epsilon_y Y_o \{d - [G(a_d) - G(a_o)]/q\} \quad (2.9)$$

with  $G(x) = \int_x^\infty a^{-1} e^{-a} da$ .

Values of  $G(x)$  can be found in tables (e.g. ref. 31).

From measurements of the time course of a light-induced absorbance change  $\Delta E$  is known as a function of the time. Furthermore by substituting  $x = d$  in equation (2.6),  $q$  can be calculated from measured values of  $I_d$ ,  $I_o$  and  $d$ , and also the ratio  $a_o/a_d$  is obtained from  $T_d (= I_d/I_o)$ . If  $\epsilon_y$  is known,  $Y_o$  can be found from the final value of the extent of  $\Delta E$  (at  $t \rightarrow \infty$ ), if the reaction is irreversible or if corrections can be made for back reactions.  $I_o$  can be measured by means of a calibrated photodetector. By means of the tables of  $G(x)$  it is then possible to calculate  $\gamma$ , the quantum efficiency of the photoreaction.

It is clear that  $\gamma$  may also be determined from measurements of the initial slope of the absorbance change. However, the method described above has the advantage of taking into account the full time course of the change. Table 2.1 presents the values of  $\gamma$  as determined with both methods from the measurements shown in Fig.2.6, and with  $\epsilon_y$  chosen to be  $7 \text{ mM}^{-1} \cdot \text{cm}^{-1}$ .

The values of the estimated error given in the table for  $\gamma_a$  are mainly due to inaccuracy of measurements of  $T_d$ . Generally, this error is smaller than that of measurements of the initial slope, which for the greater part determines the accuracy of values of  $\gamma_b$ .

Table 2.1. Values of the quantum efficiency (in electron equivalents per quantum) of the photoreduction at 90 K of the primary electron acceptor of photosystem 2 as determined from data in Fig.2.6 by use of methods described in Section 2.4.2,  $\gamma_a$ ; from measurements of the initial slope  $\gamma_b$  was calculated.  $\epsilon_y$  was taken to be  $7 \text{ mM}^{-1} \cdot \text{cm}^{-1}$ .

wavelength of actinic light	$\gamma_a$	$\gamma_b$
630 nm	$0.14 \pm 0.02$	$0.18 \pm 0.05$
676 nm	$0.10 \pm 0.01$	$0.15 \pm 0.04$

Eq. 2.9 may also be used to calculate the efficiency of photoreactions occurring in highly scattering suspensions, e.g. in samples containing a micro-crystalline mass due to freezing (see Section 2.3.3). It has to be emphasized that the value of  $d$  then has to be determined differently. With scattering suspensions the distribution of the actinic light does not obey eq. 2.6. According to refs. 33 and 34 reflections within the sample tend to increase the length of the optical path. Therefore with scattering suspensions eq. 2.6 has to be replaced by

$$I = I_0 [\exp (- \beta qx)] ,$$

where  $\beta$  is the ratio of the pathlength of a scattering suspension and of a clear solution, both containing the same concentration of pigment. Therefore,  $\beta$  has to be determined from measurements of the absorbance of the sample with and without scattering due to crystallization in order to obtain the value of  $d$ . This can be done by comparison of the absorbance of samples with and without glycerol (see Section 2.3.3).

#### 2.4.3. Time course of fluorescence yield changes.

The charge separation mentioned in the previous paragraph may also cause a change of the fluorescence yield<sup>18</sup>. In order to make the kinetic comparison between light-induced changes of the absorbance and of the fluorescence yield, it is useful to perform both measurements with identical samples, actinic light and optical geometry. In a relatively dense sample (e.g. of absorbance 0.87) one other condition should also be met. Absorbance changes give an average of the changes occurring at the different actinic light intensities throughout the sample (previous section). Fluorescence measurements are more complex. With the geometry of the spectrophotometer described in Section 2.2.1, where the direction of the measured fluorescence and of the excitation light is almost the same, the following has to be taken into account. Strong absorption of the excitation light will cause greater weight to be given to changes occurring in the front part of the cuvette, where actinic intensities are higher than average. On the other hand self absorption of the fluorescence will cause greater weight to be given to changes occurring in the rear of the cuvette, where intensities are less than average. These two effects cancel each other when the absorbance of the sample to the excitation light is equal to the absorbance to the fluorescence pass band (e.g. refs. 35 and 36).

The increment of fluorescence,  $dF$ , emanating from a thin layer of thick-

ness  $dx$  a distance  $x$  from the front layer will be

$$dF = I_x c \epsilon_a \phi \{ \exp [ -c \epsilon_f (d - x) ] \} dx, \quad (2.10)$$

where  $I_x$  is the intensity of the excitation light at  $x$ ;  $c$  is the concentration of the sample content;  $\epsilon_a$  is the extinction coefficient of this content for the exciting pass band;  $\phi$  is the quantum yield of fluorescence;  $\epsilon_f$  is the extinction coefficient for the fluorescence pass band; and  $d$  is the optical path length of the sample,  $0 < x < d$ . Since,  $I_x = I_0 \exp (-c \epsilon_a x)$ , where  $I_0$  is the actinic intensity at the front surface of the sample, (2.10) becomes:

$$dF = I_0 c \epsilon_a \phi [ \exp (-c \epsilon_f d) ] \{ \exp [ c (\epsilon_a - \epsilon_f) x ] \} dx.$$

If  $\epsilon_a = \epsilon_f$ , the dependence on sample depth is eliminated (cf. refs. 35 and 36). Under this condition fluorescence represents a true average of changes occurring through the sample. After the photoreactions have been completed ( $t \rightarrow \infty$ ), each thin layer,  $dx$ , contributes to the same extent to the total amount of measured fluorescence. And, if the fluorescence yield is linearly proportional to the amount of charge separation or of closed reaction centers (see previous section), the time course of the fluorescence change measured at the onset of actinic illumination is dependent on  $I_x$  and therefore on concentration and absorbance of the sample, in the same way as measurements of absorbance changes (eq. 2.9). Fig. 2.8 compares the kinetics of the fluorescence yield increase measured such that  $\epsilon_a = \epsilon_f$  with a concentrated (1 mg chlorophyll/ml) and a dilute (0.05 mg chlorophyll/ml) sample of dark adapted spinach chloroplasts at 77 K. The half time for the fluorescence increase is 4 times smaller with the dilute sample because of the greater average intensity of the actinic light in the dilute sample. For the same reason, due to selfabsorption, the total amount of the measured fluorescence after one minute of illumination ( $t \rightarrow \infty$ ) was about 3 times higher in the dilute than in the concentrated sample. It will be shown later that this time course does not reflect a photoreaction, but presumably a dark reaction following a light-induced reaction.

The theoretical considerations described above also indicate that comparison of the kinetics of light-induced changes of absorbance and of fluorescence yield can only be performed accurately using an optical geometry where the fluorescence is measured which is emitted in the same direction as the excitation light and where the direction of the actinic light makes the same angle to that of the measuring beam for both changes (see also ref. 37). Unless the absorbance of the sample at the wavelength of the excitation light is low, the fluorescence signal measured from another direction originates

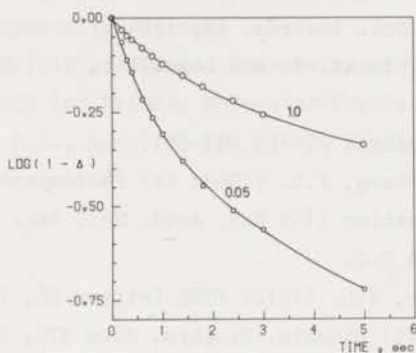


Fig.2.8. Semilogarithmic plots of light-induced fluorescence (692 nm) increase of chloroplasts at 77 K due to irradiation with broad band blue actinic light for a concentrated (1.0 mg chlorophyll/ml) and a dilute (0.05 mg chlorophyll/ml) chloroplast sample (1-mm cuvette).

predominantly from the layers with highest light intensity. Therefore the kinetics will be faster than those of light-induced absorbance changes, which give the average over many or all layers.

#### REFERENCES

1. Hoogenhout, H. and Ames, J. (1965) Arch. Mikrobiol. 50, 10-24
2. Watanabe, A. (1960) J. Gen. Appl. Microbiol. 6, 283-292
3. Cramer, M. and Myers, J. (1952) Arch. Mikrobiol. 17, 384-402
4. Kessler, E., Arthur, W. and Bruggen, J.E. (1957) Arch. Biochem. Biophys. 71, 326-335
5. Ames, J., Duysens, L.N.M. and Brandt, D.C. (1961) J. Theoret. Biol. 1, 59-74
6. Arnon, D.I. (1949) Plant Physiol. 24, 1-15
7. Ames, J. (1964) Thesis, University of Leiden
8. Lundin, A. and Aasa, R. (1972) J. Magn. Res. 8, 70-73

9. Amesz, J., Pulles, M.P.J., Visser, J.W.M. and Sibbing, F.A. (1972) *Biochim. Biophys. Acta* 275, 442-452
10. Millikan, G.A. (1933) *J. Physiol.* 79, 152-157
11. Chance, B. (1942) *Rev. Sci. Instrum.* 13, 158-161
12. Chance, B., Mayer, D., Graham, N. and Legallais, V. (1970) *Rev. Sci. Instrum.* 41, 111-115
13. Butler, W.L. (1972) *Biophys. J.* 12, 851-857
14. Inselberg, E. and Rosenberg, J.L. (1963) in: *Photosynthetic Mechanisms of Green Plants* (Publication 1145 Nat. Acad. Sci. Nat. Res. Council) pp. 717-725, Washington D.C.
15. Lozier, R.H. and Butler, W.L. (1972) *FEBS Letters* 26, 161-164
16. Kouchkovsky, Y. de (1975) *Biochim. Biophys. Acta* 376, 259-267
17. Kitajima, M. and Butler, W.L. (1975) *Biochim. Biophys. Acta* 376, 105-115
18. Duysens, L.N.M. and Sweers, H.E. (1963) in: *Studies on Microalgae and Photosynthetic Bacteria* (Miyachi, S., ed.) pp. 353-372, University of Tokyo Press, Tokyo
19. Pulles, M.P.J., Kerkhof, P.L.M. and Amesz, J. (1974) *FEBS Letters* 47, 143-145
20. Frackowiak, D., Grabowski, J. and Stachowiak-Hans, E. (1969) *Photosynthetica* 3, 39-44
21. Frackowiak, D., Hans, E., Skowron, A. and Froncisz, W. (1974) *Photosynthetica* 8, 279-291
22. Keilin, D. and Hartree, E.F. (1949) *Nature* 164, 254-259
23. Butler, W.L. and Norris, K.H. (1960) *Arch. Biochem. Biophys.* 87, 31-40
24. Mazur, P. (1966) in: *Cryobiology* (Meryman, H.T., ed.) pp. 213-315, Academic Press Inc., London
25. O' Reilly, J.E. (1973) *Biochim. Biophys. Acta* 292, 509-515
26. Kolthoff, I.M. and Tomsicek, W.J. (1935) *J. Phys. Chem.* 39, 945-958
27. Szarvas, P. and Korondan, I. (1971) *Monatshfte Chemie* 102, 1593-1607
28. Spruit, C.J.P. and Kendrick, R.E. (1972) *Planta (Berl.)* 103, 319-326
29. Duysens, L.N.M. (1956) *Biochim. Biophys. Acta* 19, 1-12
30. Borisov, A.Yu., Ivanovskii, R.N. and Samuilov, V.D. (1969) *Biofizika* 14, 676-683
31. Bauman, R.P. (1962) in: *Absorption Spectroscopy*, pp. 376-381, John Wiley and Sons, New York - London
32. *Handbook of Chemistry and Physics* (1957) (Hodgeman, C.D., Weast, R.C. and Selby, S.M., eds.) 39, pp. 282-283, Chemical Rubber Publishing Co, Cleveland



33. Butler, W.L. (1962) *J. Opt. Soc. Am.* 52, 292-299
34. Kubelka, P. (1948) *J. Opt. Soc. Am.* 38, 448-457
35. Förster, Th. (1951) in: *Fluoreszenz organischer Verbindungen*, p. 37, Vandenhoeck Ruprecht, Göttingen
36. Duysens, L.N.M. (1952) *Thesis*, University of Utrecht
37. Amesz, J. (1973) in: *Primary Molecular Events in Photobiology* (Checcucci, A. and Weale, R.A., eds.) 3, pp. 21-43, Elsevier, Amsterdam

CHAPTER III  
PHOTOSYSTEM 1 AT LOW TEMPERATURES

3.1. *Introduction.*

The available data concerning the reversibility of the photoconversion of the primary electron donor of photosystem 1, P700 and of bound ferredoxin (EPR signal at  $g = 2.05, 1.94$  and  $1.86$ ) at low temperatures are contradictory. Some authors<sup>1-4</sup> observed a partial reversibility of the photoconversion of P700, others<sup>5-9</sup> reported a completely or nearly completely irreversible photooxidation at temperatures near 80 K. If P700 is photooxidized reversibly, one would expect a reversible photoreduction of the primary electron acceptor. However, bound ferredoxin, which has been proposed to be the primary electron acceptor of photosystem 1, has been reported to be photoreduced practically irreversibly at 77 K (ref. 10).

The main purpose of the experiments reported in this chapter was a comparative study of the kinetics of P700 and ferredoxin, both by EPR and by optical methods at temperatures between 10 and 200 K. The results are in agreement with the hypothesis that ferredoxin is the primary electron acceptor of photosystem 1. They showed a stoichiometry between  $P^{+}700$  and reduced ferredoxin under various conditions and indicated that the only dark processes that occurred were back reactions between these two compounds. At least three different back reactions were observed with different time constants. Each of these reactions takes place at a different type of reaction center. With decreasing temperature in an increasing fraction of the reaction centers no back reaction occurred at all.

We shall also discuss the results of measurements of the absorbance difference spectrum of P700 oxidation at different temperatures. Analyses of these spectra support the hypothesis that P700 consists of a dimeric chlorophyll molecule, as was also concluded from EPR<sup>11, 12</sup>, ENDOR (ref. 13; Hoff, A.J., personal communication) and CD<sup>14</sup> measurements.

An EPR signal was observed near  $g = 2.05$  in the low temperature spectra of intact cells of green, red and blue-green algae and of spinach chloroplasts. The  $g$ -value and the shape of the signal were similar to that of purified, soluble plastocyanin. Experiments with far-red and red illumination showed that the site of the copper protein *in vivo* is in the electron transport pathway between photosystems 1 and 2. Plastocyanin is not oxidized by illumination at 77 K, indicating that no electron transfer occurs between P700 and plastocyanin at that temperature.

### 3.2. *Materials and methods.*

Suspensions of spinach chloroplasts and algae were prepared as described in Sections 2.1 and 2.3.3. For optical measurements at low temperatures glycerol or glycol (final concentration 55 % v/v) was added to the suspension.

Absorbance changes induced by continuous light were measured with the split-beam spectrophotometer described in Section 2.2.2. The apparatus to measure flash-induced absorbance changes and light-induced fluorescence yield changes is described in Section 2.2.1. The actinic light was filtered by a filter combination, consisting of Schott BG 12 and BG 18 glass filters to give a band with a maximum at 460 nm and bandwidth 80 nm. In some experiments a filter combination consisting of a Schott RG 695 cut-off and AL 718 interference filter was used to provide photosystem 1 light. A Balzers heat reflecting Calfex C filter was added to each filter combination. Appropriate combinations of Schott BG or RG filters and Balzers interference filters (bandwidth 12 nm) were placed in front of the photomultiplier in order to block straylight from the monochromator and to diminish artifacts due to changes in the fluorescence yield of pigment system 2. For the same purpose absorbance measurements in the red spectral region were performed in the presence of dibromothymoquinone (DBMIB), which quenches chlorophyll fluorescence<sup>15</sup>. DBMIB was a kind gift of Dr.A.Trebst, Ruhr-Universität, Bochum.

Measurements of fluorescence were performed with the photomultiplier blocked by a filter combination which consisted of a Corning 4-77 colored glass filter with a Schott AL 692 interference filter or with a combination of a Schott RG 715 and AL 730.

EPR measurements were recorded with the spectrometer at the B.C.P. Jansen Institute, Amsterdam (Section 2.2.3), except for Figs.3.8 and 3.9. Unless otherwise noted no glycerol and DBMIB were added to samples used for EPR experiments.

Soluble oxidized plastocyanin, isolated from spinach<sup>16</sup>, was a gift of Dr.J.S.C.Wessels (Natuurkundig Laboratorium Philips N.V., Eindhoven). The absorbance index,  $A_{278/597}$ , of the sample was 2.3. The concentration was calculated with  $\epsilon_{597} = 9.8 \text{ mM}^{-1} \text{ cm}^{-1}$  (ref. 17).

### 3.3. *Results.*

#### 3.3.1. *Absorbance difference spectra.*

Fig.3.1. shows absorbance difference spectra of spinach chloroplasts, illuminated at low temperature. Fig.3.2 shows the kinetics of the changes at

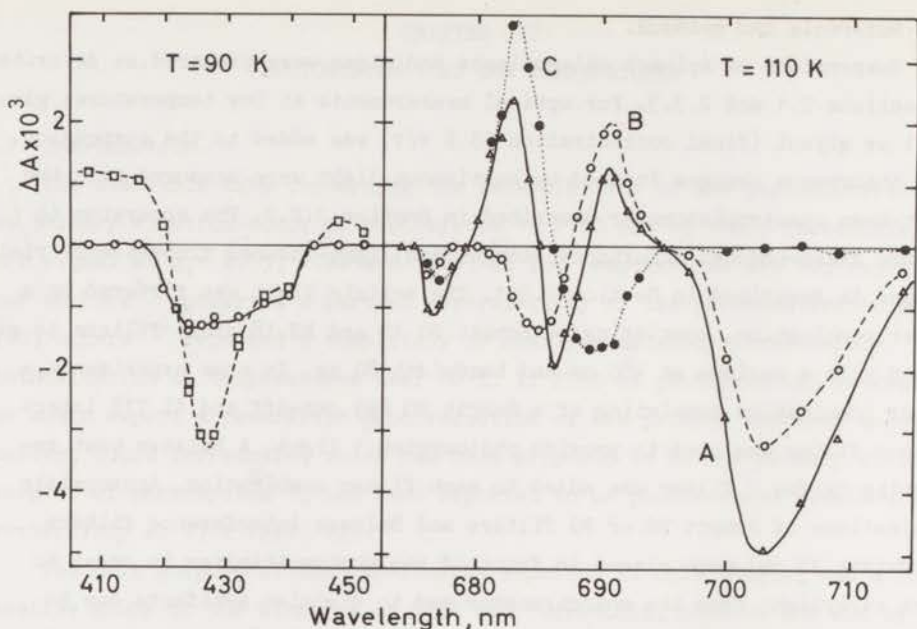


Fig. 3.1. Absorbance difference spectra upon illumination of dark-adapted spinach chloroplasts (0.22 mg chlorophyll/ml) at low temperature. Left hand spectra at 90 K; actinic illumination: circles, 718 nm, 60 nEinstein. $\text{cm}^{-2} \cdot \text{s}^{-1}$ ; squares, absorbance changes induced by 660 nm light (40 nEinstein. $\text{cm}^{-2} \cdot \text{s}^{-1}$ ) with far-red (718 nm) background illumination. Right hand spectra at 110 K and in the presence of DBMIB (50  $\mu\text{M}$ ); actinic illumination: 420 - 500 nm, 10 nEinstein. $\text{cm}^{-2} \cdot \text{s}^{-1}$ . A, spectrum obtained upon the first illumination; B, spectrum of a 5 s light - 1 min dark illumination cycle; C, spectrum of the changes induced by system 2 (see text).

a number of wavelengths. The chloroplasts were kept in the dark at 0 °C for at least 10 min, frozen in the dark, and then illuminated. In the red region the first illumination at 110 K induced absorbance increases at around 683 and 690 nm and decreases near 676, 686 and 702 nm (spectrum A). After several light-dark periods, however, illumination caused a decrease in the region 680 - 687 nm and the band at 702 nm was about 35 % smaller (spectrum B). These results show that at least two different reactions are responsible for the absorbance changes in the spectral region between 670 and 715 nm. Chloroplasts illuminated in the presence of DCMU ( $10^{-5}$  M) and hydroxylamine ( $10^{-2}$  M) shortly before freezing gave a light-induced difference spectrum similar to spectrum B. Since photoreactions of system 2 are blocked by this treatment,

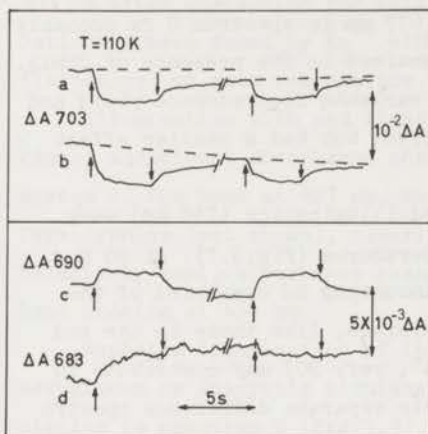


Fig.3.2. Time courses of light-induced absorbance changes at 703, 690 and 683 nm. a, c, d, see Fig.3.1; b, as (a) without DBMIB, but in the presence of  $10^{-5}$  M DCMU and  $10^{-2}$  M  $\text{NH}_2\text{OH}$ , and with blue pre-illumination (5 s) before freezing. Actinic light on at upward, off at downward pointing arrows.

due to accumulation of the reduced electron acceptor<sup>18</sup>, this indicates that spectrum B is caused by system 1 only, and is apparently due to photo-oxidation of P700. The kinetics at 703 nm were the same with and without hydroxylamine and DCMU (Fig.3.2). In both cases the first illumination at 110 K produced an absorbance decrease that was about 35 - 40 % larger than that obtained upon subsequent illumination, even with an intervening dark period as long as 40 min. This indicates that about two-third of the available P700 was reversibly photooxidized; the remaining reaction centers were irreversibly photoconverted.

On basis of these observations the contribution of photosystem-2 driven changes to spectrum A was calculated by subtracting spectrum B, normalized at 703 nm. Spectrum C, thus obtained, could also be recorded directly, if photosystem-1 activity was eliminated by far-red background illumination. Recent measurements of Lozier and Butler<sup>4</sup> at 77 K and of van Gorkom<sup>19</sup> at room temperature in the presence of deoxycholate indicate that absorbance changes in the region 680 - 690 nm are caused by reduction of the primary acceptor of photosystem 2. The shape of the absorbance difference spectrum obtained by Lozier and Butler, however is different from that shown here, and was interpreted as a narrowing and increase of an absorption band at 683 nm. According to our spectrum (C) however, the increase at 683 nm is mainly due to a shift of an absorption band near 686 nm towards shorter wavelength. The

spectrum obtained by van Gorkom can be similarly interpreted as the blue-shift of an absorption band. The small decrease at 677 nm in spectrum C is probably caused by fluorescence yield changes, that remained in the presence of DBMIB. Omission of this quencher enhanced both the variable fluorescence yield and the 677 nm absorbance change by a factor of five, but had a smaller effect upon the changes at 683 and 690 nm.

The absorbance changes induced by far red illumination (718 nm) were rather small in the 430-nm region at low temperatures (Fig.3.1). At 90 K a broad bleaching around 430 nm was observed, amounting to one-third of the 702 nm decrease. The changes were partly reversible, like those in the red region. Since both P700 and ferredoxin ("P430", ref. 20) may contribute to absorbance changes near 430 nm, and since their separate difference spectra at low temperatures are not known, a precise analysis of the spectrum is not possible. It may be noted, however, that the difference spectra of Fig.3.1 are not corrected for particle flattening<sup>21, 22</sup>. With spinach chloroplasts the absorbance changes at 435 and 703 nm are decreased by factors of 3.5 and 1.0, respectively, due to this flattening (ref. 23; Pulles, M.P.J, personal com-

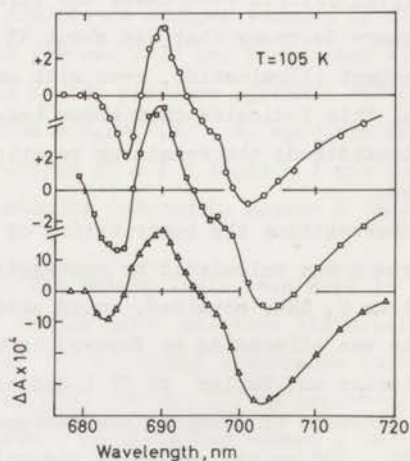


Fig.3.3. Difference spectra (light minus dark) of the reversible absorbance changes at 105 K in the presence of DBMIB (150  $\mu$ M) of intact cells of O, *C. vulgaris*; □, *P. aeruginosum*; Δ, *A. nidulans*. Actinic illumination: 420 - 500 nm, 90 nEinstein. $\text{cm}^{-2}.\text{s}^{-1}$ , in a 5 s light - 1 min dark cycle. Absorbance per mm at 680 nm, corrected for scattering: O, 0.7; □, 0.3; Δ, 1.0.

munication). Therefore, the ratio of the extents of the changes at 435 and 703 nm after correction for this effect is about one (Fig.3.1). A similar ratio has been found by Ke<sup>20</sup> with small photosystem-1 particles (almost no flattening) at room temperature.

Illumination with red light on a background of farred light (Fig.3.1) caused additional absorbance changes apparently due to excitation of photosystem 2. The band at 427 nm, which was not observed in the presence of 3 mM ferricyanide (not shown), clearly reflects oxidation of cytochrome  $b_{559}$  (Ch.IV). Relatively small absorbance changes around 444 nm suggest the red shift of a band peaking at 444 nm.

Repeated illumination of intact cells of *Chlorella vulgaris*, *Porphyridium aeruginosum* or *Anacystis nidulans* at 105 K induced absorbance difference spectra similar to spectrum B (Fig.3.3). Just like with chloroplasts, only part of P700 could be reversibly oxidized. Apparently this phenomenon reflects a basic property of the photosystem-1 reaction center.

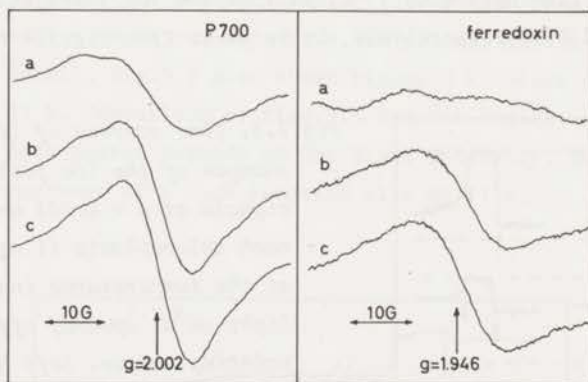


Fig.3.4. EPR spectra at 11 K of spinach chloroplasts (2 mg chlorophyll/ml) near  $g = 2.00$  and  $g = 1.94$ . a, sample frozen in the dark; b, sample frozen in the dark and illuminated for about 30 s with white light at 77 K; c, sample b during subsequent illumination with white light at 11 K. Instrument settings: frequency: 9.080 GHz; power: 2 mW (P700) and 10 mW (ferredoxin); modulation amplitude: 5 G (P700) and 10 G (ferredoxin); time constant: 0.3 s; scan time: 1 G/s. The right hand spectra (ferredoxin) were recorded with four times increased sensitivity. Control experiments showed the same behaviour for the ferredoxin bands at  $g = 2.05$  and 1.86 as at  $g = 1.94$ .

### 3.3.2. EPR spectra of P700 and ferredoxin

The most obvious way to explain the partial irreversibility of P700 oxidation would be by means of a dark reaction that stabilized the charge separation (cf. ref. 4) in an analogous way as proposed for photosystem 2 (ref. 24). For system 2 a secondary electron donor was postulated in order to explain the irreversibility of C550 reduction; for system 1 a secondary electron acceptor might be involved, that oxidizes the reduced acceptor in some of the reaction centers, thus preventing a back reaction with  $P^{+}700$ . As ferredoxin was reported to be reduced practically irreversibly at low temperatures<sup>10</sup> this compound could be the secondary acceptor in such a model. Therefore, we studied the kinetics of the photosystem-1 reactions at low temperature in more detail by means of EPR measurements of Signal I (P700) and of the ferredoxin signal at  $g = 1.86, 1.94$  and  $2.05$ . Fig.3.4 shows spectra, measured with a sample that was illuminated at 77 K and subsequently at 11 K. The spectra of a dark-frozen sample are also given to show the extent of Signal II (ref. 25). If we take the signal height in the spectra which were measured during illumination at 11 K, to indicate 100 % reduction and oxidation of ferredoxin and P700 respectively, it is clear from Fig.3.4 that at 77 K

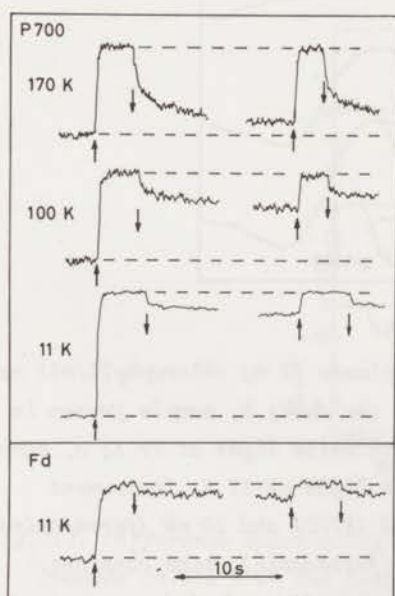


Fig.3.5. Time courses of light-induced changes of the low field maxima of the signals at  $g = 2.002$  and  $1.946$  of spinach chloroplasts (1 mg chlorophyll/ml) at the temperatures indicated. White light on at upward, off at downward pointing arrows. Left hand curves: changes induced by the first illumination; right hand curves: changes after several 5 s light - 1 min dark cycles. Instrument settings: at 170 and 100 K: frequency: 9.084 GHz; power: 2 mW; modulation amplitude: 5 G; time constant: 0.1 s; at 11 K: as in Fig.3.4. Receiver gain: at 170 and 100 K:  $8 \times 10^3$ ; at 11 K for P700:  $5 \times 10^3$ , and for ferredoxin:  $10^4$ .



about 70 % of the total amount of P700 is irreversibly photooxidized and also about 70 % of the ferredoxin photoreduced.

The spectra b of Fig.3.4 were obtained with a dark time of 3 min at 77 K after the illumination. More P700 and ferredoxin were found to be in the oxidized and reduced state, respectively, when samples were cooled to 11 K immediately after the illumination. The relative amount of P<sup>+</sup>700 and reduced ferredoxin were always equal in the same sample.

The reversibility of P700 oxidation and ferredoxin reduction was found to be temperature dependent (Fig.3.5). At 11 K only 20 % of the amount of P700 was photooxidized reversibly. Measurement of the EPR signal at  $g = 1.95$  indicated that similarly 20 % of the amount of ferredoxin was reversibly photo-reduced.

Comparison of the kinetics at much lower intensities showed that also the light-on signals of ferredoxin and P700 were the same (Fig.3.6) with spinach chloroplasts which were frozen in the dark and then illuminated at 11 K with weak ( $2 \text{ mW.cm}^{-2}$ ) actinic illumination. At high intensities ( $100 \text{ mW.cm}^{-2}$ ) the rate of ferredoxin reduction may be slightly slower than that of P700 oxidation; the time resolution of our apparatus was not sufficient to compare these rates into more detail. Fig.3.6 also shows biphasic kinetics at the onset of illumination at 11 K. Comparison of Figs.3.5 and 3.6 indicates that the relative extents of both phases depends on the light intensity. This is in agreement with the occurrence of a back reaction also at 11 K.

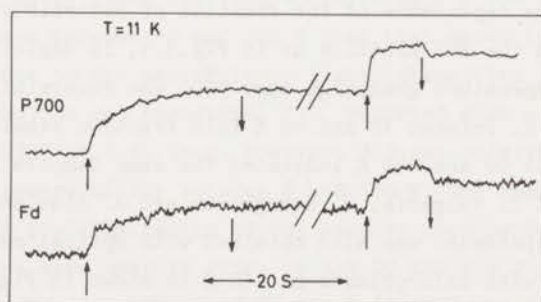


Fig.3.6. Time courses at 11 K of the light-induced changes of P700 and ferredoxin measured as in Fig.3.5. Left hand curves: changes at the first illumination period ( $I = 2 \text{ mW.cm}^{-2}$ ). Right hand curves: changes at the second illumination period ( $I = 100 \text{ mW.cm}^{-2}$ ) after a dark period of 1 min.

If the intensities of the signals of reduced ferredoxin and of  $P^{+}700$  were decreased at 11 K with respect to their extents at slightly higher temperatures (e.g. due to power saturation) a partial reversibility as shown in Figs.3.5 and 3.6 could be caused by heating of the sample in the light. Therefore, we measured the intensities of both signals at temperatures between 8 and 25 K with chloroplasts which had been illuminated with strong continuous light at 8 K. The microwave power was the same as that used for Fig.3.5. The extent of both signals was found to decrease rather than increase upon raising the temperature. This indicates that the partial reversibility of the signals as shown in Figs.3.5 and 3.6 is not due to heating of the sample.

The experiments described above show that both at 77 and 11 K there was always a stoichiometric relation between the amount of  $P^{+}700$  and reduced ferredoxin, both in the light and in the dark. This suggests, in contrast to the above-mentioned model that ferredoxin is the only electron acceptor and that secondary reactions do not occur at these temperatures. Apparently in some reaction centers reduced ferredoxin and  $P^{+}700$  are able to react back with each other, in others they are not. Our data do not exclude the occurrence of a primary electron acceptor which is not identical with ferredoxin if the (secondary) reaction between that acceptor and ferredoxin is very rapid ( $\mu\text{s}$  -  $\text{ms}$ ). Since in part of the reaction centers ferredoxin is reduced reversibly (Figs.3.4 and 3.5), in such a model the charge separation in photosystem 1 in these reaction centers is not stabilized by secondary electron transport.

### 3.3.3. Temperature dependence.

The temperature dependence of the fraction of reversibly photooxidized  $P700$ , measured from the EPR kinetics as in Fig.3.5, is depicted in Fig.3.7. With increasing temperature gradually more  $P700$  was reversibly photooxidized between 40 and 170 K. Between 10 and 40 K this fraction remained constant at 20 %. Experiments at 90 and 180 K indicated the same temperature dependence for intact cells of *C. vulgaris*, *P. aeruginosum* and *A. nidulans* (Fig.3.7). The same temperature dependence was also obtained with optical measurements. A typical experiment with chloroplasts at 110 K is shown in Fig.3.2. These results demonstrate that the phenomenon is not affected by the presence of glycerol. Remarkably, the fraction of irreversibly photoconverted  $P700$  and ferredoxin seemed to be dependent on the temperature only and not on the preceding treatment of the sample. Chloroplasts illuminated at 10 K showed 80 % irreversibly converted  $P700$  and ferredoxin, but after subsequent warming to 77 K, this amount decreased to 70 %, the same number as given in Fig.3.7 for

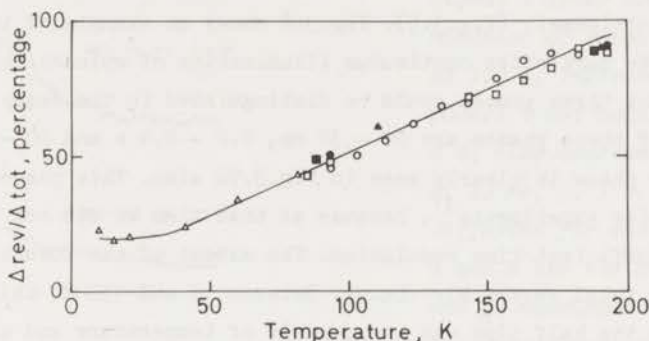


Fig.3.7. Temperature dependence of the fraction of reversibly photooxidized P700, measured as in Fig.3.5.  $\Delta_{tot}$ : extent of the change at first illumination;  $\Delta_{rev}$ : extent of the dark decay. Open symbols refer to different batches of spinach chloroplasts, solid symbols were obtained with *C. vulgaris* ( $\blacktriangle$ ), *A. nidulans* ( $\bullet$ ) and *P. aeruginosum* ( $\blacksquare$ ).

this temperature.

Using the same treatment, Ke et al.<sup>26, 27</sup> recently also reported a temperature dependent irreversibility for photoconversion of P700 and ferredoxin with dark-adapted photosystem-1 particles obtained from spinach chloroplasts. They reported a slightly lower fraction of reversible  $P^+700$  and reduced ferredoxin at temperatures between 10 and 200 K than that shown in Fig.3.7. This difference may be due to the use of lower light intensities in refs. 26 and 27 than for Fig.3.7. Bolton and coworkers<sup>28, 29</sup> reported also a partly reversible photooxidation of P700 at 6 K. They, however, did not observe a temperature dependence of the reversibility between 6 and 170 K. The reason for this discrepancy may be the preillumination of the samples used by Bolton, whereas dark-adapted samples were used in refs. 26 and 27 and for Fig.3.7.

The peak-to-peak width,  $\Delta H_{pp}$ , of Signal I ( $P^+700$ ) was also found to be temperature dependent. At 10, 40, 110 and 200 K  $\Delta H_{pp}$  was 10.5, 9.0, 8.0 and 7.5 G, respectively. This effect was also observed by Feher et al.<sup>30</sup>, who explained this temperature dependence by the assumption of a temperature-dependent electron density on  $CH_3$ -groups of  $P^+700$ .

### 3.3.4. Rate constants of the back reaction.

At temperatures below 150 K the back reaction between  $P^{+700}$  and reduced ferredoxin was multiphasic (Fig.3.5). Fig.3.8 shows an example of the decay of Signal I in the dark after continuous illumination of spinach chloroplasts at 100 K. At least three phases could be distinguished in the decay kinetics; the half times of these phases are 20 - 30 ms, 0.2 - 0.4 s and 20 - 40 s. The 20 - 30 ms decay phase is clearly seen in Fig.3.9A also. This phase was not observed in earlier experiments<sup>31</sup>, because at that time we did not have an apparatus with sufficient time resolution. The extent of the lowest phase was 30 - 50 % of the total reversible change. Between 10 and 150 K, this percentage, as well as the half time was independent of temperature and of the duration of the preceding illumination (up to 20 s). The extents of the 20 - 30 ms and 0.2 - 0.4 s decay components (Fig.3.8) were both about 30 % of the total reversible change. These results show that different types of reaction centers can be distinguished, which are different with respect to the rate of the back reaction. Otherwise reaction centers with a low rate constant would accumulate during prolonged illumination. For *C. vulgaris*, *P. aeruginosum* and *A. nidulans*, measurements of the dark reduction of  $P^{+700}$  at 100 K similarly indicated that 50 - 70 % of the reversibly oxidized fraction decayed within 1 - 3 seconds, and the remaining part more slowly.

A fourth component, which was temperature-dependent, was observed in the decay of the changes at temperatures between 150 and 200 K. The half times of the reaction at 160 and 200 K were 5.5 and 0.3 s, respectively. The activation energy of this back reaction was 4.7 kcal. A calculation shows that the half time of this reaction will be 20 ms at 300 K in reasonable agreement with the rate of back reaction reported by Ke<sup>20</sup> for system-1 particles.

Warden et al.<sup>28</sup> have reported a similar activation energy (6.3 kcal) for a temperature-dependent component in the decay of Signal I, between 150 and 270 K. They, however, observed a monophasic dark decay of the signal at temperatures below 150 K. Ke et al.<sup>26, 27</sup> reported a biphasic decay at temperatures below 150 K similar to that shown in Fig.3.5.

### 3.3.5. Quantum yield.

The extent of Signal I induced by a 7- $\mu$ s, saturating flash at 170 K was about 90 % of that induced by strong, continuous illumination (Fig.3.9). This was also found at 100 K for the first as well as for subsequent illumination periods.

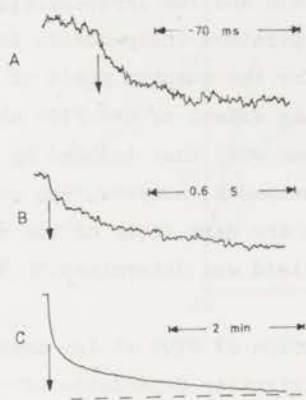


Fig.3.8. Time course of the decay of Signal I after continuous illumination of spinach chloroplasts at 100 K. Instrument settings: power: 2 mW; modulation amplitude: 8 G; time constants: A, 3 ms; B, 10 ms; C, 1 s. Time scales are different for each curve. Curves A and B are the average of 250 and 50 measurements, respectively. All curves were measured with the same sample. Actinic light (white,  $200 \text{ mW.cm}^{-2}$ ) off at downward arrows; A and B, 2 s light - 5 s dark cycles. Relative amplification: A, B, C: 7, 3 and 2 respectively.

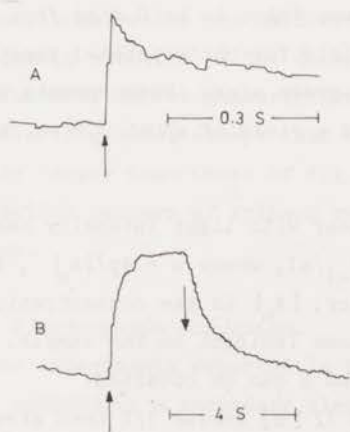


Fig.3.9. Change of Signal I induced by a 7- $\mu\text{s}$ , saturating flash (A) and by continuous light ( $200 \text{ mW.cm}^{-2}$ ) (B) in spinach chloroplasts at 170 K. Continuous light on at upward arrow, off at downward arrow. Instrument settings: power: 4 mW; modulation amplitude 8 G; time constants: A, 3 ms; B, 0.1 s. Curves A and B are the average of 64 and 4 measurements, respectively. Dark time between illumination periods or flashes: 5 s.

If it is assumed that like in system 2 (Chapter IV) "double" (ref. 32) or "multiple" hits do not occur, these data indicate that the quantum yield of the oxidation of P700 is almost unity for reversible and for irreversible charge separation, and also that the yield is temperature-independent. In ref. 31 we have reported a value of 0.65 eg./hv for the quantum yield of the charge separation. This value was obtained from the extent of the P700 absorbance change induced by a short flash in comparison with that induced by continuous light. The time resolution of those measurements, however, was not sufficient to observe the 20 - 30 ms component in the dark decay of the signal (Fig.3.8). Therefore, that value of the quantum yield was determined 30 % too low.

A high quantum efficiency for the photooxidation of P700 at low temperature is also indicated by analysis of the light intensity dependence of the extent of the signal. The intensity dependence of the steady state deflection of the reversible absorbance change at 703 nm upon illumination (10 s dark - 7 s light cycles) of *A. nidulans* with 475-nm light at 105 K is plotted in Fig.3.10. Similar data were obtained with spinach chloroplasts. It can be calculated (see footnote) from Fig.3.10 that 40 % of the centers which are reversible in a dark period of 10 s react back with a first-order rate constant of  $1.5 \text{ s}^{-1}$  and 60 % with  $18 \text{ s}^{-1}$ . Experimentally from EPR kinetics we obtained rate constants of 0.04, 1.7 and  $20 \text{ s}^{-1}$ . Since the data of Fig.3.10 were obtained with a dark time of 10 s between illumination periods, the slowest phase ( $0.04 \text{ s}^{-1}$ ) is not observed in Fig.3.10. For the measurements of Fig.3.10,  $p$  was measured to be 75 % and  $\phi$  was taken to be 0.8 eq./hv. Goedheer<sup>33</sup> has also reported a high quantum yield for photosystem-1 reactions induced by 475-nm actinic irradiation in blue-green algae. Measurements with spinach chloroplasts as for Fig.3.10 indicated a yield of about 0.3 eq./hv

---

\* The reaction system  $A \xrightleftharpoons[k_{-1}]{k_1} B$  where  $k_1$  is linear with light intensity has an equilibrium with:  $[A] / [B] = k_{-1} / k_1 (I) = k_{-1} / \alpha I$ , where  $\alpha = \phi p / [A_0]$ ,  $\phi$  is the quantum efficiency,  $p$  is the absorptancy,  $[A_0]$  is the concentration of A in the dark, and  $I$  is the number of photons incident on the sample. Therefore, the following relation between  $[B]$  and  $I$  can be obtained:  
 $1/[B] = 1/[A_0] + k_{-1} / \alpha [A_0] I$ . A plot of  $1/[B]$  versus  $1/I$  then gives a straight line with slope  $k_{-1} / (\alpha [A_0])$  which intersects the  $1/[B]$  axis at the value of  $1/[A_0]$ . Therefore, if  $\phi$  and  $p$  are known  $k_{-1}$  can be calculated.

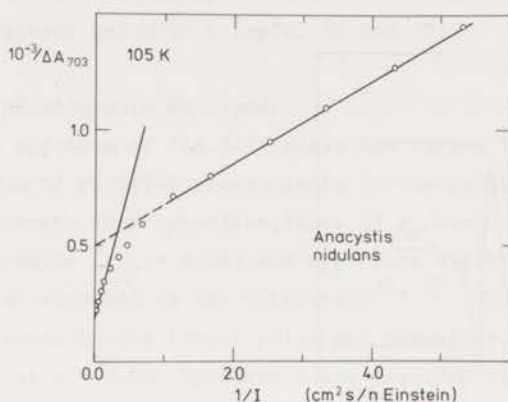


Fig.3.10. Plot of the reciprocal of the steady state extent of the reversible absorbance change at 703 nm versus the reciprocal of the light intensity with *A. nidulans* at 105 K. Actinic light: 475 nm, in a 10 s dark - 7 s light cycle. Absorbance at 680 nm, corrected for scattering:  $1.0 \text{ mm}^{-1}$ .

for 475-nm light. With spinach chloroplasts most of this light is absorbed by chlorophyll b (ref. 34), which transfers the absorbed energy mainly to photosystem 2. It was assumed that no energy transfer between photosynthetic units occurred and that the differential extinction coefficient of P700 oxidation at 703 nm is  $70 \text{ mM}^{-1} \text{ cm}^{-1}$  at 105 K. The latter value gave a ratio of 390 chlorophyll molecules per oxidized P700 in spinach chloroplasts (see Fig.3.1). The biphasic kinetics of the decay as concluded from Fig.3.10 agrees with the results of direct measurements of the EPR kinetics for dark times shorter than 10 s (Fig.3.8), except that the half times calculated from Fig.3.10 are slightly longer than those of Fig.3.8. This may be due to a difference between the reaction centers of spinach chloroplasts and those of intact cells of *A. nidulans*.

### 3.3.6. Plastocyanin oxidation.

The experiments reported in the previous section indicated that  $\text{P}^+700$  is not reduced by a secondary electron donor at low temperatures. This agrees with direct measurements on cytochrome f, which show that cytochrome f is not photooxidized in spinach chloroplasts below about 240 K (ref. 35). Here, we shall describe experiments concerning the reactions of plastocyanin. Oxidized

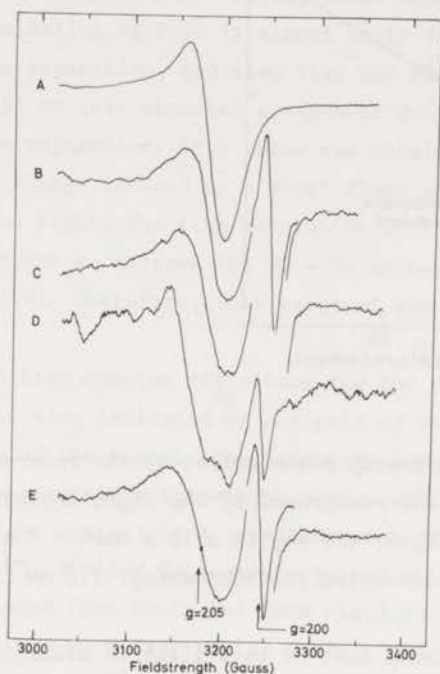


Fig.3.11. EPR spectra taken at 20 K. (A) oxidized plastocyanin ( $36 \mu\text{M}$ ) in phosphate-Tris buffer pH 7.8, (B) spinach chloroplasts ( $1 \text{ mg chlorophyll/ml}$ ), illuminated at room temperature for 10 s with 705-nm light in the presence of  $0.1 \text{ mM}$  methylviologen, then kept in darkness for 10 s and subsequently frozen, (C) *S. obliquus*, illuminated at room temperature and during the initial freezing for about 30 s with 718-nm light, (D) *P. aeruginosum*, illuminated with 705-nm light as for (C), (E) *A. nidulans*, illuminated as for (D). Instrument settings: frequency 9.11 GHz; power 10 mW; modulation amplitude, 10 G; time constant, 1.0 s; scan rate 1 G/s. Receiver gain settings: (A)  $2.0 \times 10^4$ , (B)  $2.0 \times 10^5$ , (C)  $2.5 \times 10^5$ , (D)  $5.0 \times 10^5$  and (E)  $1.5 \times 10^5$ . The signal near  $g = 2.00$  of (B) and (E) was recorded with a modulation amplitude of 5 G. Absorbances per mm at 680 nm, corrected for scattering were: 3.5, 2.2, 1.0 and 4.2 for B, C, D and E, respectively.



plastocyanin can be observed by EPR measurement with sufficient sensitivity only at temperatures below 40 K (refs. 36 and 37).

#### *Occurrence of plastocyanin in algae.*

The upper spectrum of Fig.3.11 shows the larger line ( $g_{\perp} = 2.05$ ) of the EPR spectrum of purified plastocyanin in the oxidized state at 20 K. At a lower field strength four hyperfine lines of  $g_{\parallel}$  were observed (not shown) with similar g-value ( $g_{\parallel} = 2.24$ ) and hyperfine splitting constant ( $A_{\parallel} = 190$  Mcycles/s) as reported in the literature<sup>36, 37</sup>. These four lines are too weak to be detected in the intact cells and therefore we will report only about the line at  $g = 2.05$ . Spectrum B was measured with spinach chloroplasts, illuminated with far-red light at room temperature, then kept in the dark for 10 s and frozen to 20 K. In this spectrum a signal ( $g = 2.05$ ) can be seen at the same position and similar in shape as in the spectrum of purified plastocyanin. The signal is also observed in illuminated cells of *Scenedesmus obliquus* (Fig.3.11C), *P. aeruginosum* (Fig.3.11D), *A. nidulans* (Fig.3.11E) and *C. vulgaris* (see Fig.3.12). Therefore, it is likely that this signal in spinach chloroplasts and in the organisms tested, originates from plastocyanin. As far as we know, this is the first observation of the occurrence of plastocyanin in red algae.

In all spectra, except the one of purified plastocyanin, the signal near  $g = 2.00$  is due to Signal I and/or Signal II.

From the heights (top-bottom) of the copper signal in spectra A and B (Fig.3.11) it was calculated that the concentration of the copper protein, causing the signal at 2.05 in chloroplasts was one mole per 400 moles of chlorophyll, in fair agreement with the results of Malkin and Bearden<sup>37</sup> and with the amount of plastocyanin presents in chloroplasts as determined chemically by Kato et al.<sup>17</sup>.

The concentration of chlorophyll in the suspensions of the algae was difficult to determine by extraction and therefore, the concentration was correlated with that in the chloroplast suspension using the absorbance at 680 nm, corrected for scattering. From this and from the spectra of Figs.3.11 and 3.12 the concentration of plastocyanin relative to that of chlorophyll in the algae was calculated. On this basis the amounts of plastocyanin oxidized by far-red light before and during freezing were found to be the same (within 20 %) in intact cells of *C. vulgaris*, *S. obliquus*, *P. aeruginosum* and *A. nidulans*<sup>38</sup>.

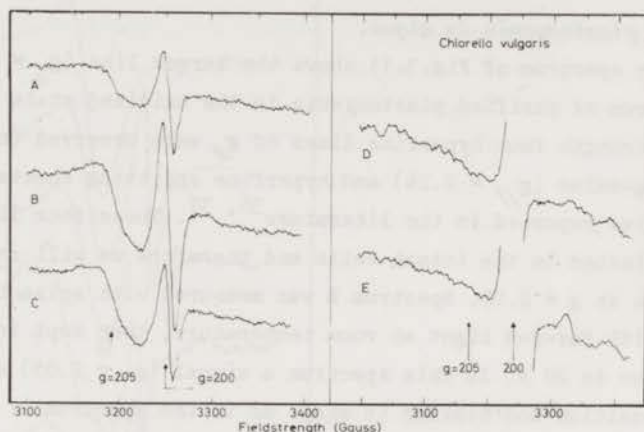


Fig.3.12. *C. vulgaris* (A) sample illuminated with 643-nm light (B) with 705-nm light, (C) with 643-nm light in the presence of 0.1 mM DCMU, (D) sample kept in the dark for about one min before and during the freezing, (E) sample kept in the dark as for (D), and illuminated at 77 K for about 2 min with white light. Conditions and instrument settings as in Fig.3.11, except for (A), (B), (C), receiver gain setting  $2.0 \times 10^5$ , (D) and (E) receiver gain setting  $6.2 \times 10^5$ , temperature 10 K and frequency 9.13 GHz Absorbance at 680 nm, corrected for scattering:  $2.2 \text{ mm}^{-1}$  for (A), (B) and (C); and  $7.0 \text{ mm}^{-1}$  for (D) and (E).

Spectra as for Figs.3.11 and 3.12 obtained with intact cells of *Euglena gracilis* did not show the presence of oxidized plastocyanin. This suggests that the copper protein is absent in *E. gracilis* and that the electron transport chain of this alga is different from that of other algae. This is also supported by optical measurements reported in refs. 39-41.

#### *Site of action of plastocyanin in vivo.*

In Figs.3.11 and 3.12 it is shown that plastocyanin was in the oxidized state when spinach chloroplasts and cells of *S. obliquus*, *P. aeruginosum*, *A. nidulans*, and *C. vulgaris* had been illuminated with photosystem-1 light at

room temperature and during freezing. Plastocyanin was found to be reduced in the dark (Fig.3.12D) as well as after photosystem-2 illumination. The latter reduction was inhibited by DCMU as can be seen in Fig.3.12 for *C. vulgaris*. It is clear that plastocyanin was oxidized after far-red illumination (spectrum B), but that it was partially in the reduced state in the absence of DCMU after 643-nm illumination (spectrum A). In the presence of DCMU, however, plastocyanin was found to be oxidized after red illumination (spectrum C). Similar results were obtained with spinach chloroplasts (see also ref. 37) and with *P. aeruginosa*. These results indicate that plastocyanin is a component of the electron transport chain between photosystems 1 and 2 *in vivo*, and that it is located at the photosystem-1 side of the DCMU block. In order to obtain more definite proof about this site of action of plastocyanin it will be necessary to measure rates of reduction and oxidation, as has been done for other components by optical methods<sup>42</sup>. Measurements of flash-induced absorbance changes<sup>43, 44</sup> at 703, 584 and 553 nm with spinach chloroplasts suggested that at room temperature 85 % of photooxidized P700 is reduced by plastocyanin and only 15 % by cytochrome f.

As is shown in Fig.3.12E plastocyanin is not oxidized upon illumination at 77 K in *C. vulgaris*. P700 is oxidized in these conditions (Sections 3.3.1 and 3.3.2), as is also indicated by the line at  $g = 1.94$  of reduced ferredoxin in the same EPR spectrum. This shows that P700 does not oxidize plastocyanin at 77 K. The same results, but not shown, were obtained with spinach chloroplasts and with *A. nidulans*. This agrees with the conclusion obtained in Sections 3.3.1 - 3.3.4, that P700 is the only reactant of photosystem 1 which is photooxidized at 77 K.

### 3.4. Discussion.

#### 3.4.1. The back reaction.

The results described above support the hypothesis of Malkin and Bearden (refs. 45 and 46) that the primary electron acceptor of photosystem 1 is a ferredoxin with EPR signals at  $g = 2.05$ ,  $1.94$  and  $1.86$ . Below 150 K, the only dark reaction that was observed in our preparation was a back reaction of  $P^+700$  and reduced ferredoxin: even though we observed that the reaction centers of photosystem 1 are heterogeneous with respect to this back reaction, in all types of centers the redox state of ferredoxin was stoichiometrically related to that of P700. Yang and Blumberg<sup>47</sup>, by comparison of

the rate of P<sup>+</sup>700 decay with that reported for ferredoxin by Malkin and Bearden<sup>45</sup> arrived at a different conclusion, and suggested that ferredoxin might not be the primary acceptor of system 1. Our results, however, show a clear stoichiometry for dark times of up to several minutes. Yang and Blumberg<sup>47</sup> arrived at an erroneous conclusion because they assumed that the reversibility of the photoreaction was the same at 10 - 20 K as at 77 K. As was shown in Section 3.3.3 the fraction of reversible reaction center is temperature dependent. Yang and Blumberg<sup>47</sup> observed that the initial decay of P700 at 77 K is not of first order. In Section 3.3.4 it was discussed that there are three different types of reaction centers; in each type a first-order reaction occurs between P<sup>+</sup>700 and reduced ferredoxin, the half times are 20 - 30 ms, 0.2 - 0.4 s and 20 - 40 s.

A possible explanation for these different time constants might be based on the assumption that the distances between ferredoxin and P700 are not the same in all reaction centers. The temperature independence of the rate constants suggests that the back reaction occurs by way of a tunnelling process. The tunnelling rate is known to depend exponentially on the distance between the reacting species (e.g. ref. 48):

$$\frac{1}{\tau} = v_0 \exp \left[ - \frac{4\pi d}{h} (2m \Delta E)^{\frac{1}{2}} \right],$$

where  $\tau$  is the half time of the reaction,  $v_0$  is the frequency of the electron approaching the barrier,  $h$  is Planck's constant,  $d$  and  $\Delta E$  are the width and height of the barrier, respectively, and  $m$  is the mass of an electron. Substituting for  $\Delta E$  the estimated excess energy of the absorbed photon, 0.8 eV and for  $v_0$ ,  $10^{15} \text{ s}^{-1}$  (this number is not very critical as the exponential term dominates the expression), distances of 35, 37 and 41 Å, respectively are obtained for P700 and ferredoxin for  $\tau = 0.03, 0.3$  and  $25 \text{ s}$ , respectively. Because of the assumptions involved in the derivation of the equation used, the distances are only rough approximations. Nevertheless, they are quite compatible with present theories about the structure of the thylakoid membrane. The difference in distance, 2 - 6 Å, is more reliable than the distance itself. On the other hand the different half times might also be due to a difference in height ( $\Delta E$ ) or in both height and width of the barrier. Differences of 0.2 eV or less would account for the differences of the half times for  $d = 40 \text{ Å}$ . Such differences might be due to different surroundings or orientations of the primary reactants.

For spinach chloroplasts it is known that two types of system-1 reaction

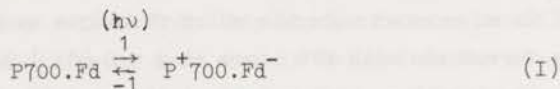
centers can be distinguished, viz. those located in the grana and in the stroma lamellae<sup>49, 50</sup>. However, we observed about the same three half times for the back reactions in spinach chloroplasts and in *A. nidulans*, which have different structures of the thylakoid systems.

Ke et al.<sup>26, 27</sup> have reported biphasic kinetics for the reduction of P<sup>+</sup>700 in the dark at temperatures below 225 K measured with photosystem-1 subchloroplast particles. The extents of both phases were approximately equal, and the half times of the phases were about 3 and 75 s, respectively. The difference between these half times and those given in Section 3.3.4 may be due to structural changes in the ferredoxin-chlorophyll complex caused by the detergent, Triton X-100, which was used by Ke to obtain subchloroplast particles. It will be clear from the calculation above that a slight distortion of the structure may cause large differences in half times. McElroy et al.<sup>51</sup> and Romijn (to be published) similarly showed that the half time of the back reaction in whole cells and reaction centers of the purple bacterium *Rhodospseudomonas spheroides* may be different depending on the detergent treatment used for the isolation of the reaction centers.

Floyd et al.<sup>52</sup> reported that, after a short laser flash, about two-third of P700 decayed very rapidly at liquid nitrogen temperature, with a half time of 30  $\mu$ s. Whatever the cause of this rapid reaction, it seemed to be absent in our conditions, judging from the fact that the total amount of oxidizable P700 we observed was the same as that observed by Floyd et al., relative to that of cytochrome b<sub>559</sub>.

### 3.4.2. The primary acceptor.

The heterogeneity of the reaction centers with respect to the irreversibility of the photoconversion has been discussed above (Section 3.3.2) in terms of a model involving a secondary reaction in part of the centers. It was concluded that such a model does not explain our results, since the redox state of ferredoxin was stoichiometrically related to that of P700. A similar stoichiometry between these redox states at temperatures between 13 and 225 K with photosystem-1 subchloroplast particles has been reported recently by Ke et al.<sup>26, 27</sup>. Our results as well as those of Ke are in agreement with the following model for the reaction centers of photosystem 1 at temperatures below 150 K:

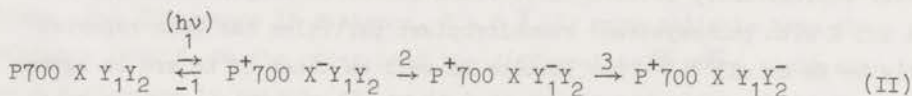


where Fd is "bound" ferredoxin ( $g = 1.94$ ). Our results indicate that at least

four kinds of reaction centers can be distinguished with respect to the half times of the back reaction:  $\tau_{1/2} = 20 - 30$  ms,  $0.2 - 0.4$  s,  $20 - 40$  s and  $> 30$  min (Sections 3.3.4 and 3.4.1). The efficiency of the charge separation (reaction 1) was found to be close to unity (Section 3.3.5).

Contrary to our results McIntosh et al.<sup>53</sup> and Evans and Cammack<sup>54</sup>, very recently reported that Signal I was partially reversible at temperatures below 30 K without a concomitant reversibility of the signal of ferredoxin ( $g = 1.94$ ). McIntosh et al.<sup>53</sup> observed this in photosystem-1 subchloroplast particles which were frozen during illumination. At 6 K they observed two reversible components at  $g$ -values of 1.75 and 2.07 which they attributed to the primary electron acceptor of system 1. Evans and Cammack<sup>54</sup> observed an almost completely reversible Signal I at temperatures below 30 K in photosystem-1 particles which had been exposed to dithionite for 45 - 60 min at pH 10 in order to reduce the ferredoxins chemically prior to freezing. No reversibility of the ferredoxins was observed with these samples. Irreversible photoreduction of a ferredoxin molecule with  $g$ -values of 2.05, 1.92 and 1.89 was observed by Evans and Cammack with subchloroplasts which were poised at -560 mV before freezing. At this redox potential most of the ferredoxin with a  $g$ -value of 1.94 is reduced; the ferredoxin with  $g = 1.92$ , however, is only partially reduced, since its midpoint potential is about -590 mV at pH 10 (refs. 55 and 56). Under similar conditions, however, Ke et al.<sup>27</sup> did not observe photoreduction of the latter ferredoxin ( $g = 1.92$ ).

Although it has to be confirmed by optical measurements of absorbance changes near 700 nm that the reversible signals near  $g = 2.00$  observed by McIntosh et al.<sup>53</sup> and by Evans and Cammack<sup>54</sup> are due to P700 oxidation, these data suggest that the ferredoxin with  $g = 1.94$  may not be the only electron acceptor of system 1 at cryogenic temperatures. The results may also suggest that this ferredoxin is not the primary electron acceptor of photosystem 1. McIntosh et al.<sup>53</sup> proposed the following model for the reaction centers of photosystem 1:



where X is an unknown molecule which functions as primary electron acceptor;  $Y_1$  is a ferredoxin with EPR lines at  $g = 2.05, 1.92$  and  $1.89$ ; and  $Y_2$  is a ferredoxin with lines at  $g = 2.05, 1.94$  and  $1.86$ . The midpoint potentials of

these ferredoxins are -590 and -550 mV, respectively, at pH 10. According to this model the charge separation in photosystem 1 is stabilized by reduction of  $Y_1$  and  $Y_2$ . As shown in Section 3.3.2 this model does not agree with our results and those of Ke et al.<sup>26, 27</sup>; with our preparations the charge separation is not stabilized if the ferredoxin with  $g = 1.94$  is photoreduced.

In support of their model, McIntosh et al.<sup>53</sup> also reported that the quantum yield of P700 oxidation at 6 K is about 2.5 times higher than that of ferredoxin reduction. Again, this observation does not agree with our results and those of Ke<sup>26</sup> obtained at somewhat higher temperatures: the rise of the ferredoxin signal at 11 - 13 K was found to have the same time course as that of Signal I at high and at low intensities. These data indicate that the quantum yield is about the same for photoconversion of P700 and of ferredoxin ( $g = 1.94$ ). This is supported by the observation of Bearden and Malkin (ref. 46) that a short, saturating flash converts equal amounts of P700 and of ferredoxin at 20 K. In analogy with the model of system 2 (Section 4.4.3) the discrepancy between the values of the quantum yield may be explained by a temperature dependence of the rate constants  $k_2$  or  $k_3$ , which may be larger at 11 - 13 K than at 6 K. We did not find evidence for a temperature dependence between 10 and 200 K.

If it is assumed that the primary electron acceptor is not one of the ferredoxins with  $g$ -values of 1.92 and 1.94, respectively, the stoichiometry of the amounts of  $P^+700$  and reduced ferredoxin ( $g = 1.94$ ) at temperatures between 10 and 225 K (Section 3.3.2 and refs. 26, 27 and 46) may be explained by the hypothesis, that firstly,  $k_2$  and  $k_3$  (see model II) are relatively large; secondly, that there are also back reactions -2 and -3, or that there occurs a direct back reaction 4 between  $P^+700$  and reduced ferredoxin ( $Y_2$ ).

In neither of the two models we have a ready explanation for the temperature dependence of the heterogeneity with respect to the rate constants for the back reaction (Fig.3.6), especially in view of the observation that the effect is independent of the preceding treatment. One might speculate that the effect is related to the temperature dependence of the magnetic susceptibility of ferredoxin<sup>57</sup>, which is due to antiferromagnetic coupling between the two (high spin) iron atoms. Since it is known that the EPR signal of ferredoxin ( $g = 1.94$ ) may reflect both iron atoms of the molecule<sup>58</sup>, it might be postulated that a different iron atom is reduced in the reaction centers that are irreversibly photoconverted than in those in which a back

reaction between  $P^{+700}$  and reduced ferredoxin occurs. This may be supported by the conclusion from NMR spectroscopy<sup>59</sup> that the two iron atoms of ferredoxin are not identical with respect to their electron accepting properties.

Furthermore, the existence of two different acceptor sites on the ferredoxin molecule may cause the differences in the rates of the back reaction between  $P^{+700}$  and reduced ferredoxin if the orientation of the latter molecule with respect to P700 is different in different reaction centers. The distance between the iron atoms of the iron-sulfur protein of *Chromatium vinosum* is 3.0 - 3.1 Å (ref. 60). As was discussed in the previous section a similar difference in the distances between P700 and ferredoxin may explain the observed differences of the rate of the back reaction at temperatures below 150 K. The occurrence of a temperature dependent back reaction at higher temperatures then may be due to thermal population of the rotational or vibrational energy levels (Geldof, P.A., personal communication; cf. ref. 61).

Conflicting values have been reported for the fraction of irreversibly photoconverted reaction centers in chloroplasts at low temperature<sup>1-9</sup>. Since most authors did not specify the experimental conditions into sufficient detail, it is impossible to explain these differences with certainty. However, it should be pointed out that the use of low actinic intensities and of strong measuring light will affect the (apparent) fraction of irreversibly converted reaction centers.

#### 3.4.3. *The absorbance difference spectrum of P700.*

A final point discussed here is the shape of the difference spectrum of P700 at low temperature. Negative bands at 700 - 705 nm have been observed repeatedly<sup>1, 2, 5, 7</sup>. More recently, bands at shorter wavelengths were also observed. Our spectrum B is similar to that obtained by Lozier and Butler<sup>4</sup> with a scanning method. This also applies to the spectrum reported by Floyd et al.<sup>52</sup> except that they noted a negative band at 680 - 682 nm instead of 685 nm, which they attributed to P680, the primary electron donor of system 2. Witt<sup>9</sup> recently reported an irreversible increase at 695 nm, instead of 690 nm, and a decrease at 710 instead of 703 nm. The reason for this discrepancy is not clear. He proposed that the increase would reflect the reduction of a chlorophyll molecule. This hypothesis is made unpalatable by at least two observations: firstly that there is a stoichiometry between  $P^{+700}$  and reduced ferredoxin, as measured by EPR, and secondly that the increase in absorption at 690 nm is also present in the difference spectrum of chemically oxidized



P700 (ref. 4).

Two proposals have been put forward to explain the shape of spectra of P700 obtained at room temperature. According to the first one<sup>62, 63</sup> the spectrum is composed of a bleaching centered at about 700 nm and a red shift of a band located at shorter wavelength. In a second proposal of van Gorkom et al.<sup>64</sup> the spectrum was explained by a bleaching near 680 nm and a blue-shift of a pigment absorbing near 693 nm. The bleaching was thought to be due to the conversion of the P700 dimer to its monocation. Analysis of the difference spectrum obtained at 110 K by the first method was found to be impossible, unless the formation of a third band at about 690 nm (broken line) was postulated (Fig.3.13A). The second type of analysis gave the result shown in Fig.3.13B. In this case in addition to a blue shift centered at 698 nm, a two-banded absorbance decrease at 680 - 700 nm (dotted line) was obtained, which could conceivably be explained by the assumption that the absorption band of the dimer cation is narrower and somewhat lower than that of the reduced dimer (as also seems to be true at room temperature<sup>64</sup>), and that both bands are located near 690 nm. According to this analysis the bands of the P700 dimer, the dimer cation and of the species causing the band shift at 698 nm would all be shifted to longer wavelength by lowering the temperature viz. by 24, 26 and by 5 nm, respectively. The same result is obtained from analyses of the difference spectra, shown in Fig.3.3, of P700 in intact cells of *C. vulgaris*, *P. aeruginosum* and *A. nidulans* at 105 K. Red shifts of the

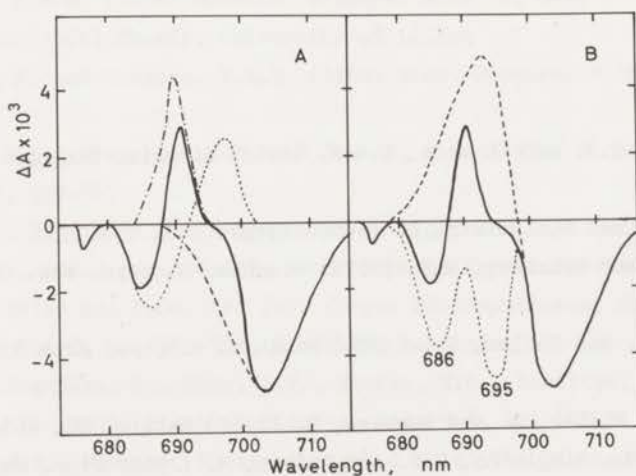


Fig.3.13. Analysis of spectrum B of Fig.3.1 (see text).

absorption bands of bulk<sup>65, 66</sup> and reaction center<sup>65, 67, 68</sup> bacteriochlorophyll, and of chlorophyll in solution<sup>69</sup> upon cooling have been observed earlier. It thus appears that the hypothesis of van Gorkom et al<sup>64</sup> fits not only the data obtained at room temperature but also those obtained at low temperature if allowance is made for the red shifts and narrowing of bands.

If a correction is made for particle flattening<sup>21, 22</sup> the absorbance decreases at 686 and 695 nm (Fig.3.13B) both have the same extent as the bleaching measured at 703 nm. Flattening factors of 2.0, 1.4, and 1.0 (Pulles, M.P.J., personal communication; and ref. 23) were taken for absorbance differences at 684, 690 and 703 nm, respectively.

Various investigators have presented models of chlorophyll complexes which absorb at 700 nm (refs. 11, 70, 71) in an effort to elucidate the structure of P700. Norris et al.<sup>11</sup> proposed a model where P700 consists of two chlorophyll molecules complexed by a water molecule. Tu<sup>70</sup> suggested that P700 is a complex of chlorophyll and flavin. Fong<sup>71</sup> assumed that P700 consist of a chlorophyll dimer containing two water molecules. Our analysis of the absorption difference spectra at 110 K and that of van Gorkom et al<sup>64</sup> at room temperature indicate that the photoreactive chlorophyll absorbs at significantly shorter wavelength than 700 nm, especially at room temperature. This indicates that an absorption band near 700 nm is not a proper criterion for a model of a special P700 dimer.

#### REFERENCES.

1. Vredenberg, W.J. and Duysens, L.N.M. (1965) *Biochim. Biophys. Acta* 94, 355-370
2. Mayne, B.C. and Rubinstein, D. (1966) *Nature* 210, 734-735
3. Yang, C.S. and Blumberg, W.E. (1972) *Biochem. Biophys. Res. Comm.* 46, 422-428
4. Lozier, R.H. and Butler, W.L. (1974) *Biochim. Biophys. Acta* 333, 465-480
5. Witt, H.T., Müller, A. and Rumberg, B. (1961) *Nature* 192, 967-969
6. Androes, G.M., Singleton, M.F. and Calvin, M. (1962) *Proc. Natl. Acad. Sci. U.S.* 48, 1022-1031
7. Chance, B., Kihara, T., DeVault, D., Hildreth, W., Nishimura, M. and

- Hiyama, T. (1969) in: *Progress in Photosynthesis Research* (Metzner, H., ed.) Vol.III, pp. 1321-1346, H. Laupp, Tübingen
8. Cost, K., Bolton, J.R. and Frenkel, A.W. (1969) *Photochem. Photobiol.* 10, 251-258
  9. Witt, K. (1973) *FEBS Letters* 38, 112-115
  10. Malkin, R. and Bearden, A.J. (1971) *Proc. Natl. Acad. Sci. U.S.* 68, 16-19
  11. Norris, J.R., Uphaus, R.A., Crespín, H.L. and Katz, J.J. (1971) *Proc. Natl. Acad. Sci. U.S.* 68, 625-628
  12. Norris, J.R., Uphaus, R.A. and Katz, J.J. (1972) *Biochim. Biophys. Acta* 275, 161-168
  13. Norris, J.R., Scheer, H., Druyan, M.E. and Katz, J.J. (1974) *Proc. Natl. Acad. Sci. U.S.* 71, 4897-4900.
  14. Philipson, K.D., Sato, V.L. and Sauer, K. (1972) *Biochemistry* 11, 4591-4595
  15. Lozier, R.H. and Butler, W.L. (1972) *FEBS Letters* 26, 161-164
  16. Borchert, M.T. and Wessels, J.S.C. (1970) *Biochim. Biophys. Acta* 197, 78-83
  17. Katoh, S., Shiratori, I. and Takamiya, A. (1962) *J. Biochem.* 51, 32-40
  18. Bennoun, P. (1970) *Biochim. Biophys. Acta* 216, 357-363
  19. Van Gorkom, H.J. (1974) *Biochim. Biophys. Acta* 347, 439-442
  20. Ke, B. (1973) *Biochim. Biophys. Acta* 301, 1-33
  21. Duysens, L.N.M. (1956) *Biochim. Biophys. Acta* 19, 1-12
  22. Ames, J. (1964) *Thesis*, University of Leiden
  23. Latimer, P. and Eubanks, C.A.H. (1962) *Arch. Biochem. Biophys.* 98, 274-285
  24. Butler, W.L., Visser, J.W.M. and Simons, H.L. (1973) *Biochim. Biophys. Acta* 325, 539-545
  25. Commoner, B. (1961) in: *A Symposium on Light and Life* (McElroy, W.D. and Glass, B., eds.) pp. 356-377, Johns Hopkins Press, Baltimore
  26. Ke, B. (1974) in: *Proc. 3rd Int. Congr. Photosynthesis, Rehovot* (Avron, M., ed.) Vol.I, pp. 373-382, Elsevier, Amsterdam
  27. Ke, B., Sugahara, K., Shaw, E.R., Hansen, R.E., Hamilton, W.D. and Beinert, H. (1974) *Biochim. Biophys. Acta* 368, 401-408
  28. Warden, J.T., Mohanty, P. and Bolton, J.R. (1974) *Biochem. Biophys. Res. Comm.* 59, 822-838
  29. Bolton, J.R. (1974) in: *Proc. 3rd Int. Congr. Photosynthesis, Rehovot*

- (Avron, M., ed.) Vol.I, pp. 389-399, Elsevier, Amsterdam
30. Feher, G., Hoff, A.J., Isaacson, R.A. and Ackerson, L.C. (1975) Ann. N.Y. Acad. Sci. 244, 239-259
  31. Visser, J.W.M., Rijgersberg, K.P. and Ames, J. (1974) Biochim. Biophys. Acta 368, 235-246
  32. Forbush, B. and Kok, B. (1971) Photochem. Photobiol. 14, 307-321
  33. Goedheer, J.C. (1965) Biochim. Biophys. Acta 102, 73-89
  34. Rabinowitch, E.I. (1951) in: *Photosynthesis and Related Processes*, Vol.II, part 1, pp. 672-736, Interscience Publishers Inc., New York
  35. Ames, J., Pulles, M.P.J., de Grooth, B.G. and Kerkhof, P.L.M. in: *Proc. 3rd Int. Congr. Photosynthesis, Rehovot* (Avron, M., ed.) Vol.I, pp. 307-314, Elsevier, Amsterdam
  36. Blumberg, W.E. and Peisach, J. (1966) Biochim. Biophys. Acta 126, 269-273
  37. Malkin, R. and Bearden, A.J. (1973) Biochim. Biophys. Acta 292, 169-185
  38. Visser, J.W.M., Ames, J. and van Gelder, B.F. (1974) Biochim. Biophys. Acta 333, 279-287
  39. Wildner, G.F. and Hauska, G. (1974) Arch. Biochem. Biophys. 164, 127-135
  40. Wildner, G.F. and Hauska, G. (1974) Arch. Biochem. Biophys. 164, 136-144
  41. Shneyour, A. and Avron, M. (1975) Plant Physiol. 55, 137-141
  42. Ames, J., Visser, J.W.M., van den Engh, G.J. and Dirks, M.P. (1972) Biochim. Biophys. Acta 256, 370-380
  43. Haehnel, W. (1973) Biochim. Biophys. Acta 305, 618-631
  44. Haehnel, W. (1974) in: *Proc. 3rd Int. Congr. Photosynthesis, Stresa* (Avron, M., ed.) Vol.I, pp. 557-567, Elsevier, Amsterdam
  45. Malkin, R. and Bearden, A.J. (1971) Proc. Nat. Acad. Sci. U.S. 68, 16-19
  46. Bearden, A.J. and Malkin, R. (1972) Biochim. Biophys. Acta 283, 456-468
  47. Yang, C.S. and Blumberg, W.E. (1972) Biochem. Biophys. Res. Comm. 46, 422-428
  48. Blochinzew, D.I. (1961) in: *Grundlagen der Quantenmechanik* (Eder, F.X. and Rompe, R., eds.) Vol.4, pp. 371-394, Deutscher Verlag der Wissenschaften, Berlin
  49. Sane, P.V., Goodchild, D.J. and Park, R.B. (1970) Biochim. Biophys. Acta 216, 162-178
  50. Wessels, J.S.C. and Voorn, G. (1971) in: *Proc. 2nd Int. Congr. Photosynth. Res., Stresa* (Forti, G., Avron, M. and Melandri, A., eds.), Vol.I, pp. 833-845, Dr. W. Junk N.V., The Hague

51. McElroy, J.D., Mauzerall, D.C. and Feher, G. (1974) *Biochim. Biophys. Acta* 333, 261-277
52. Floyd, R.A., Chance, B. and DeVault, D. (1971) *Biochim. Biophys. Acta* 226, 103-112
53. McIntosh, A.R., Chu, M. and Bolton, J.R. (1975) *Biochim. Biophys. Acta* 376, 308-314
54. Evans, M.C.W. and Cammack, R. (1975) *Biochem. Biophys. Res. Comm.* 63, 187-193
55. Ke, B., Hansen, R.E. and Beinert, A. (1973) *Proc. Natl. Acad. U.S.* 70, 2941-2945
56. Evans, M.C.W., Reeves, S.G. and Cammack, R. (1974) *FEBS Letters* 49, 111-114
57. Moss, T.H., Petering, D. and Palmer, G. (1969) *J. Biol. Chem.* 244, 2275-2277
58. Dunham, W.R., Palmer, G., Sands, R.H. and Bearden, A.J. (1971) *Biochim. Biophys. Acta* 253, 373-384
59. Poe, M., Phillips, W.D., Glickson, J.D., McDonald, C.C. and San Pietro, A. (1971) *Proc. Natl. Acad. Sci. U.S.* 68, 68-71
60. Carter, C.W., Freer, S.T., Xuong, N.H., Alden, R.A. and Kraut, J. (1971) *Cold Spring Harbor Symposia on Quantitative Biology* 36, 381-385
61. Hopfield, J.J. (1974) *Proc. Natl. Acad. Sci. U.S.* 71, 3640-3644
62. Amesz, J., Fork, D.C. and Nooteboom, W. (1967) *Studia Biophysica Berlin*, 5, 157-181
63. Vernon, L.P., Yamamoto, Y. and Ogawa, T. (1969) *Proc. Natl. Acad. Sci. U.S.* 63, 911-917
64. Van Gorkom, H.J., Tammings, J.J., Haveman, J. and van der Linden, I.K. (1974) *Biochim. Biophys. Acta* 374, 417-438
65. Vredenberg, W.J. and Duysens, L.N.M. (1963) *Nature* 197, 355-357
66. Vredenberg, W.J. and Amesz, J. (1966) *Biochim. Biophys. Acta* 126, 244-253
67. Case, G.D. and Parson, W.W. (1973) *Biochim. Biophys. Acta* 325, 441-453
68. Reed, D.W. and Ke, B. (1973) *J. Biol. Chem.* 248, 3041-3045
69. Brody, S.S. and Broyde, S.B. (1968) *Biophys. J.* 8, 1511-1533
70. Tu, S. and Wang, J.H. (1969) *Biochem. Biophys. Res. Comm.* 36, 79-83
71. Fong, F.K. (1974) *Proc. Natl. Acad. Sci. U.S.* 71, 3692-3695

CHAPTER IV  
PHOTOSYSTEM 2 AT LOW TEMPERATURES

4.1. *Introduction.*

The measurements of light-induced reactions of photosystem 2 at low temperature which had been reported in the literature, concerned mainly the extent of the absorbance, fluorescence and EPR changes caused by the reactants (refs. 1-8). Although several properties of photosystem 2 were elucidated by these measurements (see Ch. I), the first study of the kinetics of several flash-induced absorbance changes at low temperatures by Floyd et al.<sup>9</sup> indicated that measurements of the kinetics may provide useful additional information about the photosystem.

In the present chapter results of kinetic measurements with spinach chloroplasts at 10 - 180 K by optical and EPR methods will be reported. The data indicate that the reaction centers of photosystem 2 are heterogeneous with respect to the ultimate electron donor at low temperature. Furthermore, the quantum yield for the oxidation of these donors was found to be temperature dependent and relatively low at low temperatures. This phenomenon will be explained by the occurrence of a back reaction between the oxidized primary electron donor,  $P^{+680}$ , and the reduced primary acceptor,  $Q^{-}$ . The role of an intermediary electron donor to  $P^{+680}$  will also be discussed.

Under strongly oxidizing conditions irreversible photooxidation of chlorophyll was detected by optical and EPR methods. This reaction was attributed to photooxidation of chlorophyll molecules, which functioned as ultimate electron donors to photosystem 2 under conditions where no other donor was available. New transient EPR signals near  $g = 2$  were observed at 15, 100 and 180 K. These signals are attributed to  $P^{+680}$ , which was photooxidized reversibly.

Finally, a model for the electron transport in and near the reaction center of photosystem 2 will be presented.

4.2. *Materials and methods.*

Chloroplasts were obtained from market spinach as described earlier (Section 2.1). Oxidation-reduction potentials of the suspensions were determined as described in Section 2.3.4. With optical measurements and also with EPR measurements glycerol was added to the suspensions in order to obtain samples which remained clear glasses upon freezing (Section 2.3.3).

Absorbance changes in the red spectral region were measured (see Section 2.3.1) with the split-beam spectrophotometer described in Section 2.2.2. The actinic light was filtered by a blue-green filter combination, consisting of a Corning 4-96 glass filter, a 585-nm short pass interference filter, and a Calflex C heat reflecting filter. For reasons given in Section 3.2 appropriate combinations of Schott RG and Balzers interference filters were placed in front of the photomultiplier. Absorbance changes between 500 and 570 nm were measured with the apparatus described in Section 2.2.1. The continuous actinic light was filtered by a red combination consisting of two 630 -nm interference filters, a 644 -nm short pass interference filter and a Calflex C heat reflecting filter. In some experiments we used another red filter combination, which transmitted a higher light intensity centered near 645 nm: Balzers K6 broad band interference filter, two Schott RG 630 cut-off and a Calflex C filter. The photomultiplier was blocked by a broad band blue-green filter combination (two Corning 4-96 glass filters and a 583 -nm short pass interference filter).

Fluorescence was measured by use of the single beam apparatus (Section 2.2.1) as described in Section 2.3.2. The photomultiplier was provided with a Corning 4-77 colored glass filter and a Schott 692-nm interference filter.

EPR measurements were performed as described in Section 2.2.3. The measurements described in Sections 4.3.6 and 4.3.7 were all performed at the B.C.P. Jansen Institute, Amsterdam; those given in Section 4.3.5 were mainly done at our laboratory.

#### 4.3. Results.

##### 4.3.1. C550, cytochrome $b_{559}$ and fluorescence yield changes at 90 K.

###### *C550 and cytochrome $b_{559}$ .*

The difference spectrum of absorbance changes near 550 nm produced by irradiating a sample of dark-adapted spinach chloroplasts at 90 K is shown in Fig.4.1 (spectrum A). The spectrum obtained in the presence of 0.1 M potassium ferricyanide is also given (spectrum B). We shall first discuss spectrum A. The bleaching at 556 nm is due to the photooxidation of cytochrome  $b_{559}$  (ref. 1) while the bleaching at 547 and the absorbance increase at 543 nm indicate the photoreduction of Q (refs. 2, 10, 11); the substance responsible for the latter changes is generally called C550 (ref. 2). At the short wavelength side of the spectrum rather large absorbance changes occurred upon illumination. These are due to local field effects (near 518 nm) and to absorbance

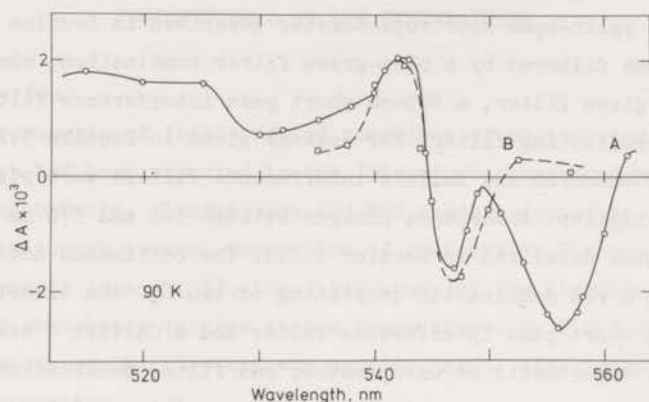


Fig.4.1. Spectra of light-induced absorbance changes of dark-adapted chloroplasts (1 mg chlorophyll/ml) at 90 K. A, control; B, +0.1 M  $K_3Fe(CN)_6$ . Actinic irradiation: A, 630 nm,  $330 \mu W \cdot cm^{-2}$ ; B, broad band red light, 630 - 710,  $3 mW \cdot cm^{-2}$ .

changes, which are caused by photosystem-1 activity (around 530 nm)<sup>12</sup>, probably by photooxidation of P700 (cf. refs. 13, 14). The extent of these changes is relatively small in the 540 - 560 nm region<sup>12</sup>. Since the total change observed at 543 nm is about 20% greater than that at 547 nm (Fig.4.1) we assume that the changes due to P<sup>+</sup>700 enlarged the change at 543 and diminished that at 547 nm by about 10%. With higher intensities of actinic illumination the effect of the changes due to photooxidation of P700 on the spectrum between 540 and 560 nm may be somewhat greater (cf. Section 3.3.4).

In the presence of ferricyanide (Fig.4.1, spectrum B) the bleaching at 556 nm was absent; cytochrome  $b_{559}$  ( $E_m = 365$  mV, ref. 15) was oxidized prior to freezing. The extent of the C550 changes, however, was the same. The ferricyanide kept the redox potential of the chloroplast suspension (in glycerol) at 20 °C at +540 mV. Okayama and Butler<sup>15</sup> have reported that the extent of C550 changes did not depend on the redox potential up to 440 mV. Lozier and Butler<sup>16</sup> have observed a significant decrease of this extent at potentials near 800 mV. Curve B shows that such a decrease does not occur at 540 mV. This indicates that at this potential Q is photoreduced irreversibly to the same extent as without ferricyanide.



From the extent of the changes one may calculate the amounts of Q and cytochrome  $b_{559}$  which are photoconverted by the illumination at 90 K if the specific differential extinction coefficients are known. According to refs. 17-19 the value of this coefficient for cytochrome  $b_{559}$  at room temperature is  $16 \text{ mM}^{-1}\cdot\text{cm}^{-1}$ ; we assume this value increases to  $20 \text{ mM}^{-1}\cdot\text{cm}^{-1}$  due to band sharpening on cooling to 90 K. The extinction coefficient for the difference 540-minus-550 nm of C550 absorbance changes at room temperature was calculated to be  $2.2 \text{ mM}^{-1}\cdot\text{cm}^{-1}$  (ref. 13). At 90 K the C550 changes show a maximum at 543 and a minimum at 547 nm (Fig.4.1); at room temperature the maximum and minimum are located at 540 and 550 nm, respectively<sup>13</sup>. This indicates that the absorbance band which, by a small shift to shorter wavelength, causes the C550 absorbance changes<sup>6</sup>, narrows 2.5 times upon cooling from room temperature to 90 K. If the band shape is Gaussian or Lorentzian, and if the area under the curve of the absorbance band and the band shift are the same at room temperature and at 90 K, this implicates that the extent of the C550 absorbance change increases  $(2.5)^2$  times upon cooling. Thus, the extinction coefficient for the difference 543-minus-547 nm will be  $13 \text{ mM}^{-1}\cdot\text{cm}^{-1}$  at 90 K. Using this value and the data of Fig.4.1 we determined the amount of photoreduced Q at 90 K to be one per 400 chlorophyll molecules. From the same figure we likewise determined the amount of photooxidized cytochrome  $b_{559}$  to be one per 815 chlorophyll molecules. Therefore the molar ratio of photoconverted Q and cytochrome  $b_{559}$  appears to be 2; and, if the concentration of photosystem-2 reaction centers is equal to that of Q, then cytochrome  $b_{559}$  is photooxidized in only half of the total amount of reaction centers. As can be seen in Table 4.1 this ratio may also be calculated from the results of measurements reported by several other investigators, using the extinction coefficients given above.

The values of the ratios chlorophyll per Q and chlorophyll per cytochrome  $b_{559}$  were found to be widely different for data obtained at low temperatures at various laboratories (Table 4.1). This is probably due to different freezing techniques giving different amounts of crystallization of the samples. As has been discussed by Butler<sup>31</sup> the optical pathlength is strongly dependent on the amount of scattering (see also Section 2.4.2). We have measured the absorbance at 550 nm with samples containing spinach chloroplasts with and without glycerol, which were frozen slowly or rapidly. The absorbance was found to vary between 0.1 and 1.5 for the same concentration of chloroplasts ( $0.1 \text{ mg chlorophyll/ml}$ ) in a 1-mm cuvette. The first number was obtained after

Table 4.1. MOLAR RATIO OF Q TO CYTOCHROME  $b_{559}$ \*

Amounts of Q and cytochrome  $b_{559}$  per chlorophyll were calculated from measurements of light-induced absorbance changes between 540 and 560 nm with (spinach) chloroplasts as reported in the literature. Extinction coefficients used were: C550 at room temperature:  $2.2 \text{ mM}^{-1} \cdot \text{cm}^{-1}$  for the difference 540-minus-550 nm; C550 at 77 - 100 K: 7 and  $13 \text{ mM}^{-1} \cdot \text{cm}^{-1}$  for 543 nm and for the difference 543 minus 547 nm, respectively;  $20 \text{ mM}^{-1} \cdot \text{cm}^{-1}$  at 556 nm for cytochrome  $b_{559}$  at 77 - 100 K.

A, room temperature

Chl/Q	remarks*	refs.
100	a	2
400	a	13, 20, 21
200	a	22, 23
200	f	24

B, 77 - 100 K

Chl/Q	Chl/cyt	cyt/Q	remarks*	refs.
400	815	0.49	b	this thesis
400	840	0.48	b	25, 26
100	190	0.52	c	27, 28
180	350	0.51	b, c	16
10	19	0.53	c	15
126	169	0.75	c, e	3
26	33	0.8	c	29
-	-	1.0	c	5
-	-	1.0	c, d	30
475	280	1.7	b	2

- \* a, + ferricyanide  
 b, suspended in glycerol  
 c, with estimated baseline  
 d, intact spinach leaves  
 e, pea chloroplasts  
 f, + DCMU preilluminated

slow cooling in the presence of glycerol, the second one after rapid freezing without glycerol. This indicates that an increase of the optical pathlength by a factor of up to 15 may be obtained by crystallization. As in our samples the pathlength was the same at room temperature and at 77 K (Section 2.3.3), we may assume that our values of the ratios chlorophyll per Q and per cytochrome  $b_{559}$  are not affected by this phenomenon. It has been noted<sup>14</sup> that the presence of glycerol converts about one half of the cytochrome  $b_{559}$  from the high potential ( $E_m = 365$  mV) to a lower-potential form. The presence of glycerol, however, does not influence the ratio of oxidized cytochrome  $b_{559}$  per  $Q^-$ , as can be seen in Table 4.1. From the data given in some reports a ratio of about one can be calculated for the amounts of photoconverted Q and cytochrome  $b_{559}$  at 77 - 100 K. The reason for this is not clear.

Several investigators have reported data, obtained at room temperature, from which a ratio of about 200 chlorophyll molecules per  $Q^-$  can be calculated (with  $\epsilon_{540-550} = 2.2 \text{ mM}^{-1} \text{ cm}^{-1}$ ). For chloroplasts which were not treated with detergent the difference spectra are not as clear as at low temperatures, so the contribution of other components to the absorbance changes cannot be excluded. The spectrum observed by van Gorkom et al.<sup>13</sup> with deoxycholate-treated chloroplasts at room temperature is clearly due to C550 only. Furthermore, they obtained ratios of one to one for the amounts of  $Q^-$  (C550) per reduced plastosemiquinone and per oxidized reaction center chlorophyll with  $\epsilon_{540-550}$  equal to  $2.2 \text{ mM}^{-1} \text{ cm}^{-1}$ . Therefore, this value for the extinction coefficient of C550 at room temperature was taken.

#### *Changes in fluorescence yield; kinetics.*

Time courses of the absorbance changes at 543 and 556 nm and of the fluorescence yield change at 692 nm during irradiation of samples of chloroplasts (without ferricyanide) with (630 nm) actinic light at 90 K are shown in Fig. 4.2. The absorbance decrease of C550 at 547 nm occurred with exactly the same kinetics as the absorbance increase at 543 nm (not shown). The rate of bleaching at 556 nm was appreciably slower than the rate of absorbance increase at 543 nm. The kinetics of the fluorescence yield change were essentially the same as the kinetics of the 556-nm absorbance change. The photoreduction of Q appears to be faster than the photooxidation of cytochrome  $b_{559}$  at 90 K, and the fluorescence yield increase appears to follow the photooxidation of cytochrome  $b_{559}$ , not the photoreduction of Q.

This is in agreement with the observation of Okayama and Butler<sup>15</sup> that the fluorescence yield of spinach chloroplasts at temperatures near 80 K is

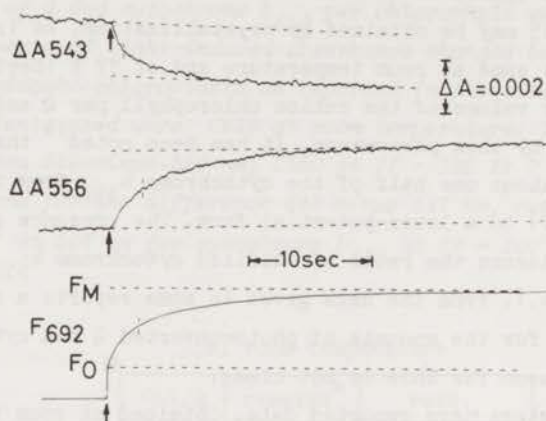


Fig.4.2. Time course of absorbances at 543 and 556 nm and of fluorescence at 692 nm during irradiation of chloroplasts (1 mg chlorophyll/ml) with 630 nm actinic light ( $165 \mu\text{W}\cdot\text{cm}^{-2}$ ) at 90 K. Actinic irradiation on at upward arrows. Vertical lines indicate half times. Downward changes reflect absorbance increases.

not only determined by the redox state of Q, but also by the state of the donor side of photosystem 2.

The measurements of the absorbance and fluorescence presented in Fig.4.2 were all made with identical samples, actinic light and optical geometry so that the rate of change of absorbance and fluorescence could be compared (see Section 2.4.3). In our experiments the 630-nm actinic light was absorbed somewhat more strongly than the 692-nm fluorescence band, so that fluorescence measurements might favour regions of the sample that had a slightly higher than average light intensity (and therefore slightly faster kinetics). Thus, if there is a discrepancy in the comparison of the absorbance and fluorescence kinetics, fluorescence changes will appear faster than the corresponding absorbance changes. Experimental tests comparing the kinetics at different fluorescence wavelengths, however, indicated that this discrepancy is negligible with the actinic and fluorescence passbands used.

The effect of ferricyanide ( $E_h = 540 \text{ mV}$ ) on the kinetics of the changes of the absorbance at 543 nm and of the fluorescence yield upon illumination with continuous 630-nm light at 90 K are shown in Fig.4.3. The upper curves demonstrate that the reduction of Q was not significantly affected by the

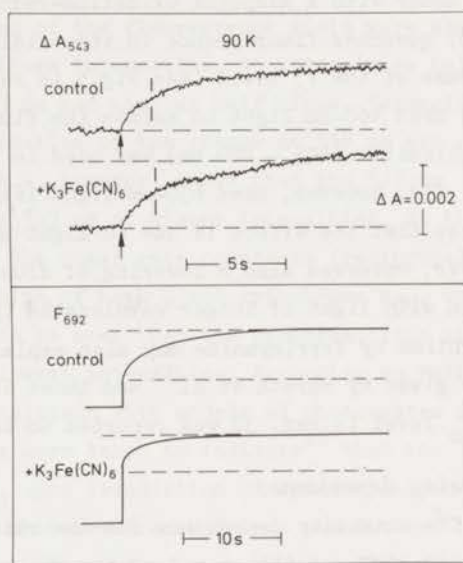


Fig.4.3. Time course of absorbance at 543 nm and of relative fluorescence yield at 692 nm measured at 90 K with samples with and without 80 mM  $K_3Fe(CN)_6$  present. Actinic irradiation: 630 nm,  $150 \mu W \cdot cm^{-2}$ . The amplification for the lower fluorescence curve was twice that of the upper curve. Note also the differences in time scales.

presence of the oxidant. The average of several experiments indicated that, generally, the half time of the absorbance change was slightly longer (20 %) with than without ferricyanide. The fluorescence yield change was smaller and faster with than without ferricyanide (note the different amplification for the two lower curves). The initial fluorescence level,  $F_0$ , however, was not affected. A decrease by a factor of two for the extent of the fluorescence yield change due to the presence of ferricyanide has also been reported by other investigators<sup>15, 30, 32</sup>. Okayama and Butler<sup>15</sup> explained the phenomenon by the assumption that the fluorescence yield may also be determined by the redox state of the donor side of photosystem 2.

The observation of a shorter half time with than without ferricyanide is in contrast with measurements reported by Murata et al.<sup>32</sup>. The absence of an effect of ferricyanide on  $F_0$  is in agreement with measurements of Okayama and Butler<sup>15</sup>. Malkin et al.<sup>33</sup>, however, reported a decrease of the  $F_0$  level in the

presence of ferricyanide, which was explained by the hypothesis that a secondary donor with a midpoint oxidation-reduction potential of 475 mV (refs. 7 and 8) quenches fluorescence in its oxidized state. We have also observed a decrease of the  $F_0$  level (see Fig.5 in ref. 34) upon addition of ferricyanide if we used 460-nm light to excite the fluorescence. About the same wavelength of excitation (475 - 480 nm) was used in refs. 32 and 33; Okayama and Butler (ref. 15), however, used 630-nm light like we did for Fig.4.3. This would suggest that the effect is due to light absorption by ferricyanide. Malkin, however, observed also a lowering of fluorescence by ferricyanide upon excitation with light of longer wavelengths (personal communication). Absorption by ferricyanide may also explain the discrepancy between the half times given by Murata et al.<sup>32</sup> and those in Fig.4.3. In accordance with this, the  $F_0$  level in ref. 32 was reported to be slightly depressed.

#### Intensity dependence.

The intensity dependence for the rate of the changes of the absorbance at 518, 543, 547 and 556 nm and of the fluorescence yield are shown in Fig.4.4. The changes at 543 and 547 nm had the same half times over this range of in-

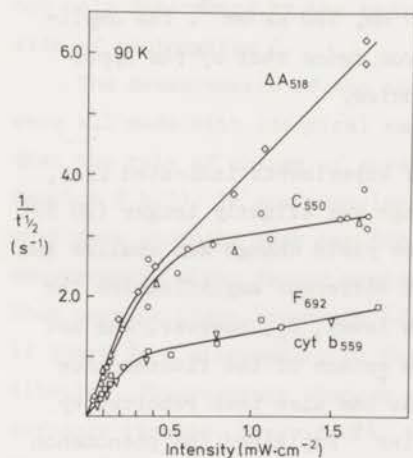


Fig.4.4. Intensity dependence of the rates (reciprocal half times) of the changes of the absorbance at 518 ( $\diamond$ ), 543 ( $\circ$ ), 547 ( $\Delta$ ) and 556 nm ( $\square$ ) and of the fluorescence at 692 nm ( $\nabla$ ). Irradiation with the broad band red actinic source or with 630-nm light.

tensities, which demonstrated that these changes were not significantly influenced by other photoreactions than those of Q (C550). Furthermore, the changes of the absorbance at 556 nm and of the fluorescence yield were also found to have the same half times at these intensities. At intensities below  $0.5 \text{ mW}\cdot\text{cm}^{-2}$  the changes at 518 and 543 nm had similar half times. Vermeiglio and Mathis<sup>12</sup> have reported that the kinetics of the change at 518 nm are nearly identical to those at 542 nm. Fig.4.4, however, shows that the 518 nm change may be twice as fast as that at 543 nm at higher intensities. At the lower intensities, below  $0.2 \text{ mW}\cdot\text{cm}^{-2}$ , the quasi rate constants (reciprocals of the half times) of the photoconversion of both Q and cytochrome  $b_{559}$  were proportional to light intensity. It can be seen that the photoreactions had different rate constants even at the lowest intensities. According to Mathis et al.<sup>28</sup> this type of result is not consistent with models of photosystem 2 with only one light reaction; the data were taken to indicate<sup>28</sup> that the conversion of Q and of cytochrome  $b_{559}$  upon irradiation of spinach chloroplasts at 90 K involves two different photoreactions. Erixon and Butler<sup>5</sup> have demonstrated that the ability to photooxidize cytochrome  $b_{559}$  at 77 K is correlated with the extent of the C550 change in the dark upon chemical reduction of Q prior to freezing. This may indicate that the two light reactions have a common primary electron acceptor. We will show later that the primary electron donor is also the same in all centers. Therefore, in contradistinction to Mathis et al.<sup>28</sup> we conclude that there is one light reaction, but that there are two different types of reaction centers with different secondary electron donors. A model of photosystem 2 to account for these and other results will be discussed in Section 4.4.3.

At intensities above  $0.3 \text{ mW}\cdot\text{cm}^{-2}$  (Fig.4.4) the photoreactions appeared to be less efficient. One would expect that the rate of photoreduction of Q should be linearly proportional to light intensity and that the rate of oxidation of cytochrome  $b_{559}$  should level off at a maximal rate determined by the rate constant of this reaction. The decrease of the slope of the rate-versus-intensity curve of C550 at higher intensities would be explained by a back reaction between the photoproducts which is stimulated at higher light intensities. We have no direct evidence for such a photochemical process. The slope of the rate-versus-intensity curve of the absorbance change at 518 nm decreases less with increasing intensity. This may be explained by a contribution to that change of a photosystem-1 reaction. In agreement with this (see Section 3.3.1), it was observed that the change was partly reversible.

Mathis et al.<sup>28</sup> have also reported measurements of the intensity dependence of the rate of photoconversion of C550 and cytochrome  $b_{559}$  at 100 K. They did not observe a departure from linearity for the reduction of C550 at the higher intensities. Since the average light intensity through a sample is strongly affected by light scattering (Section 2.4.2), this difference may partly be due to the use of crystallized samples by Mathis et al., whereas clear glass samples were used for Fig.4.4. This is supported by a comparison of the half times shown in Fig.4.4 and in ref. 28 at a given light intensity: the half times with the crystallized samples are 3 - 4 times longer than those of the transparent samples.

#### 4.3.2. Secondary electron donors at 170 K.

The effect of temperature on the low temperature photoreactions in the range from 90 - 170 K is indicated in Figs.4.5 and 4.6. The photoreduction of Q (Fig.4.5, C550) showed little temperature dependence over this range. The absorbance change may be somewhat larger at 90 K because the absorption band of C550 is sharper and narrower at the lower temperature. The average of a number of experiments indicated that the rate at 170 K was approximately 30 % faster than the rate at 90 K. The temperature dependence of the photooxidation of cytochrome  $b_{559}$  is also shown in Fig.4.5 (note the different time scales). The maximal absorbance change at 556 nm was generally found at tem-

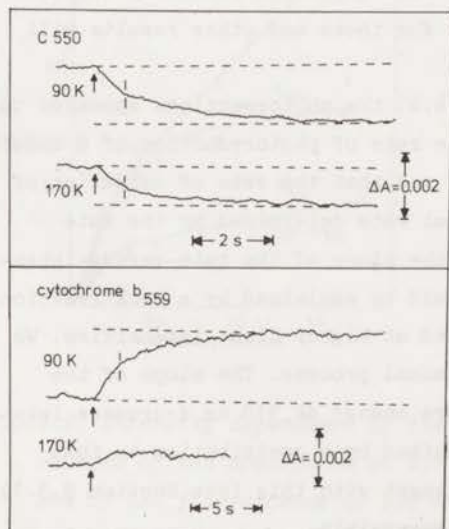


Fig.4.5. Time course of absorbance at 543 and 558 nm during irradiation with 630-nm actinic light at the temperatures indicated. Vertical lines indicate half times. Downward changes reflect absorbance increases.



peratures below 110 K. Less cytochrome  $b_{559}$  was observed above 110 K and little or no oxidation of cytochrome occurred at 170 K. At a given light intensity, the half time of the photooxidation reaction was essentially independent of temperature between 80 and 170 K.

In agreement with results obtained by others at 220 K (refs. 27, 35) we observed photooxidation of the "normal" amount of cytochrome  $b_{559}$  at 170 K with chloroplasts that had been preilluminated with two flashes just before cooling.

The effect of temperature on the light-induced fluorescence yield change is shown in Fig.4.6. The rate of the fluorescence increase showed an appreciable temperature dependence being about 3 - 4 times faster at 170 K than at 90 K. The approach to the final level  $F_m$  was also much slower at the lower temperatures. It has been reported by Joliot and Joliot<sup>36, 37</sup> and by Amesz et al.<sup>35</sup> that the half time of the fluorescence yield changes at 230 K was 3 - 4 times shorter with dark-adapted chloroplasts than with chloroplasts which had been preilluminated with two saturating flashes prior to freezing. Amesz et al.<sup>35</sup> showed that this also occurs at 170 K. Comparison of Fig.4.5 and 4.6 shows that at 170 K with dark-adapted spinach chloroplasts the time course of the fluorescence yield increase is very similar to the time course of the photoreduction of Q.

Fig.4.7 shows the dependence of the fluorescence rise curve on the temperature. A rather large change in the rate of fluorescence increase occurred between 110 and 170 K. A similar temperature dependence of the fluorescence

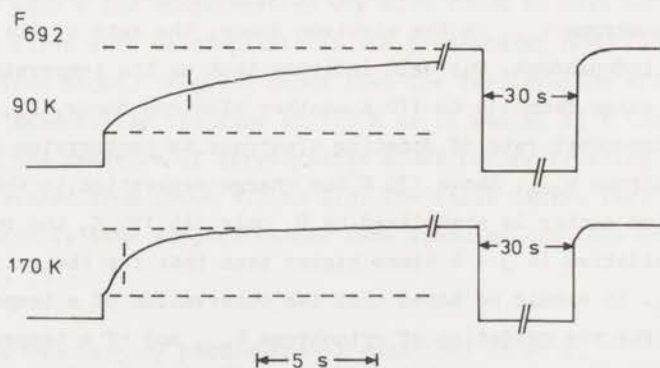


Fig.4.6. Time course of fluorescence of chloroplasts (1.0 mg chlorophyll/ml in 1-mm cuvette) at 692 nm during irradiation with 630-nm actinic light ( $0.1 \text{ mW} \cdot \text{cm}^{-2}$ ) at the temperatures indicated.

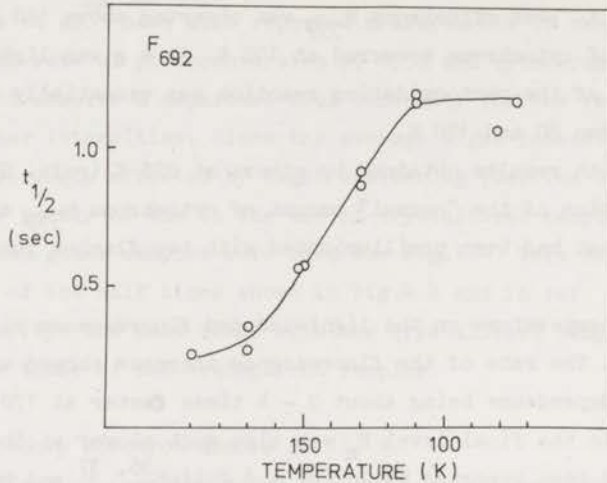


Fig.4.7. Half times of light-induced fluorescence increase as a function of temperature. The fluorescence was measured with dilute (0.05 mg chlorophyll/ml in 1-mm cuvette) samples, therefore the half times are about 4 times faster than those shown in Fig.4.6. Actinic light: 630 nm, 0.1  $\text{mW}\cdot\text{cm}^{-2}$ .

induction curve has been reported previously<sup>38-41</sup>. Our results show that contrary to the earlier hypotheses<sup>38-41</sup> the effect is not related to the efficiency of the primary photoreaction, since the photoreduction of the primary acceptor has no such temperature dependence but, that it is correlated with the oxidation of a secondary electron donor to photosystem 2. At temperatures below 110 K cytochrome  $b_{559}$  is the electron donor, the rate of its donation is temperature independent. Our data indicate that as the temperature is increased in the range from 110 to 170 K another electron donor,  $D_2$ , which has a temperature dependent rate of donating electrons to photosystem 2, takes over from cytochrome  $b_{559}$ . Above 170 K the charge separation in the photosystem 2 reaction center is stabilized by  $D_2$  only. At 170 K, the rate constant for  $D_2$  oxidation is 3 - 4 times higher than that for the oxidation of cytochrome  $b_{559}$ . It should be noted that the observation of a temperature independent rate for the oxidation of cytochrome  $b_{559}$  and of a temperature dependent electron donation to photosystem 2 indicates that  $D_2$  does not react with the same oxidized species as cytochrome  $b_{559}$  does at 90 K. Therefore, one might assume that the photooxidation of cytochrome  $b_{559}$  occurs via an intermediate secondary donor which competes with  $D_2$ . From the data of Fig.4.7 an

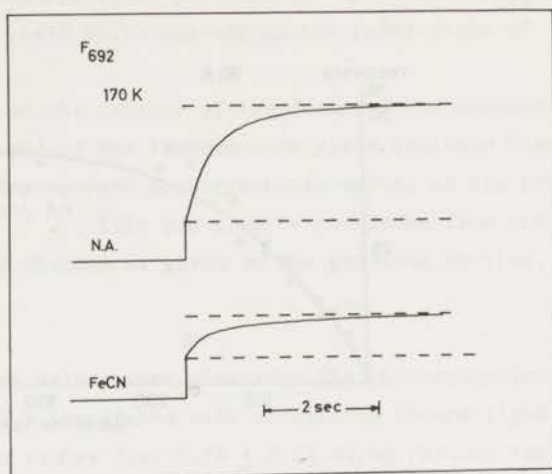


Fig.4.8. Time course of fluorescence increase of chloroplasts (0.05 mg chlorophyll/ml) at 170 K frozen without (N.A.) and with (FeCN) 2 mM potassium ferricyanide.

activation energy of about 1.0 kcal can be calculated for the oxidation of  $D_2$ .

The above results on the temperature dependence of cytochrome  $b_{559}$  photo-oxidation could be taken to suggest that the donor which functions above 170 K is the normal physiological donor to photosystem 2 and that electron donation by cytochrome  $b_{559}$  at lower temperature is an artificial reaction. If so, we would expect ferricyanide (2mM) to have no effect on fluorescence induction at 170 K, as such a low concentration was also found to have no effect on the fluorescence curve with chloroplasts in the presence of DCMU ( $10^{-4}M$ ) at room temperature (not shown). Fig.4.8 shows that the ferricyanide effect on fluorescence is essentially the same at 170 K as it was at 77 K (ref. 15; and Fig.4.3); in the presence of ferricyanide added before freezing the ratio  $F_m/F_o$  is decreased from about 4.0 to 2.0. The basis of the ferricyanide effect on fluorescence is thus subject to the same speculations that were given previously (ref. 15).

#### 4.3.3. A slow recovery of photosystem-2 reactions at 90 K.

A dark decay of the high fluorescence yield condition at low temperatures was shown in Fig.4.6. There was a slow decrease of the fluorescence yield even at 77 K as shown by the effect of a 30-s dark period. A slow dark oxidation of the photoreduced Q, concomitant with the decrease of fluorescence yield

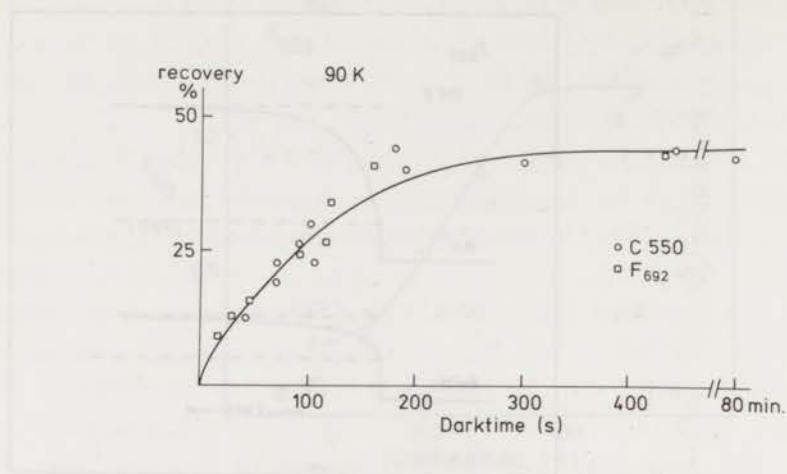


Fig.4.9. Kinetics upon darkening of absorbance at 543 and 547 nm (○, C550) and of the fluorescence yield at 692 nm (□, F692) after illumination (830 nm,  $1 \text{ mW} \cdot \text{cm}^{-2}$ , 30 s) at 90 K with spinach chloroplasts. Extents are given as percentages of the change in signal obtained at the first light period at 90 K.

(Fig.4.9), also occurred under these conditions. The decay seemed to be first-order, the half time was found to be 1.5 min. The extent of the decay was about 50 % of the extent of the total change at the first illumination period at 90 K. Murata et al.<sup>32</sup> have reported a similar time course of dark recovery of fluorescence induction at 77 K. No recovery of cytochrome  $b_{559}$  reactions was observed. The decay was not affected by DCMU or ferricyanide.

The time course of the fluorescence yield upon a second illumination at 90 K (Fig.4.6) was much faster than that upon the first illumination period. The half time of the rise was found to be similar to that of the absorbance changes at 543 and 547 nm. Therefore, at the second light period the fluorescence yield seemed to be quenched by the acceptor side of photosystem 2 only.

The observation that only half of the changes of C550 and of the fluorescence yield recover in the dark at low temperatures, supports the hypothesis that there are two types of photosystem-2 reaction centers at low temperatures, which are present in equal amounts, and which are different with respect to their donor sides only. This is also supported by the absence of a recovery of the photooxidation of cytochrome  $b_{559}$ .

Furthermore, only reaction centers which photooxidize cytochrome  $b_{559}$  at 90 K seem to have a fluorescence yield which depends on the redox state of the donor side.

The close relationship between the extents of the decay of the changes of the absorbance at 543 and 547 nm and of the fluorescence yield indicate that at 90 K there is no energy transfer between photosynthetic units, as has been proposed by Joliot and coworkers<sup>42, 43</sup>. This may also be concluded from the measurements of the flash-induced changes as given in the previous section.

#### 4.3.4. Quantum efficiencies.

In Chapter II, Table 2.1 some values were given for the photoreduction of Q with spinach chloroplasts at 90 K irradiated with continuous 630-nm light. The quantum yield was found to be rather low:  $0.14 \pm 0.02$  el.eq./hv, on basis of a differential extinction coefficient of  $7 \text{ mM}^{-1} \cdot \text{cm}^{-1}$  at 542 nm. As was shown in Fig.4.4, the rates of the photoconversion of Q and cytochrome  $b_{559}$  are not linearly dependent on the intensity of the actinic light. Analysis (according to Section 2.4.2) of the time course of the absorbance changes at 543 and 556 nm induced by continuous 630-nm irradiation of two different intensities gave values for the quantum efficiency of photoconversion of Q at

Table 4.2. QUANTUM EFFICIENCY OF PHOTOCONVERSION OF Q AND CYTOCHROME  $B_{559}$ .

The quantum yield for the photoreduction of Q ( $\gamma_Q$ ) at 90 and 170 K and for the photooxidation of cytochrome  $b_{559}$  ( $\gamma_{\text{cyt}}$ ) at 170 K was calculated by methods described in Chapter II, 2.4.2 from measurements of the time course of the absorbance changes at 543 and 556 nm with spinach chloroplasts (1 mg chlorophyll/ml in 1-mm cuvette) as for Fig.5.2. Extinction coefficients used were 7 and  $20 \text{ mM}^{-1} \cdot \text{cm}^{-1}$  for the changes of Q at 543 and of cytochrome  $b_{559}$  at 556 nm, respectively. The intensity of actinic illumination was  $0.15$  or  $2.0 \text{ mW} \cdot \text{cm}^{-2}$ .

intensity ( $\text{mW} \cdot \text{cm}^{-2}$ )	$\gamma_Q$ (el.eq./hv)	$\gamma_{\text{cyt}}$ (el.eq./hv)	T (K)
0.15	0.34	0.15	90
2.0	0.07	0.03	90
0.15	0.50	—	170
2.0	0.10	—	170

90 and 170 K and of cytochrome  $b_{559}$  at 90 K as given in Table 4.2. The differential extinction coefficient for C550 at 543 nm at 170 K was taken to be  $4.5 \text{ mM}^{-1}\text{cm}^{-1}$ . This value was calculated from measurements as in Fig.4.5, with the assumption that the amount of C550 converted in the light was the same at 90 and at 170 K. It is clear from this table that also at 170 K the rate of the photoreduction of Q is not linearly dependent on the intensity of actinic irradiation.

As shown in Figs.4.5 and 4.6 the kinetics of the light-induced fluorescence yield increase follows closely the kinetics of the photoreduction of Q at 170 K. According to Duysens and Sweers<sup>44</sup> the fluorescence yield at room temperature indicates the redox state of Q. Fig.4.10 shows the kinetics of the fluorescence yield increase measured at room temperature and at 170 K in the presence of DCMU. The half time for the light-induced fluorescence yield increase, which is taken as an index of the quantum requirement for the photoreduction of the primary electron acceptor, is 2.5 times longer at 170 K than at room temperature. If we assume that the quantum yield is unity at room temperature, the quantum yield at 170 K would be 0.40 (from Fig.4.10). This figure is consistent with our measurements (Table 4.2).

The quantum efficiency of the charge separation in the photosystem-2

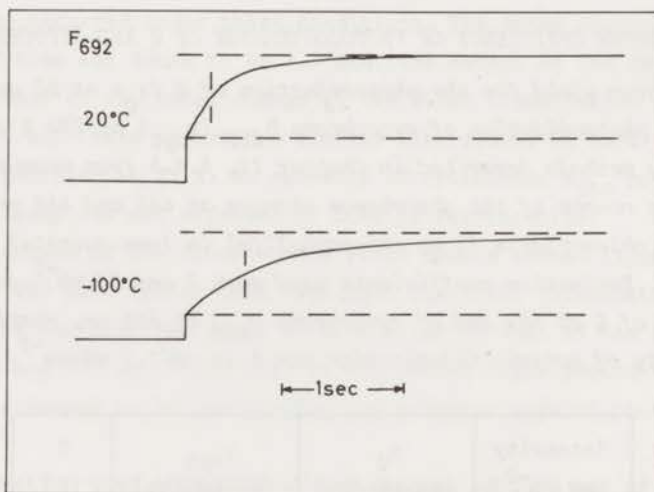


Fig.4.10. Time course of fluorescence at 692 nm of chloroplasts (0.1 mg chlorophyll/ml) in the presence of  $10^{-5} \text{ M}$  DCMU during irradiation with 630-nm actinic light ( $120 \text{ } \mu\text{W}\cdot\text{cm}^{-2}$ ) at the temperatures indicated. Vertical lines on curves indicate half times.

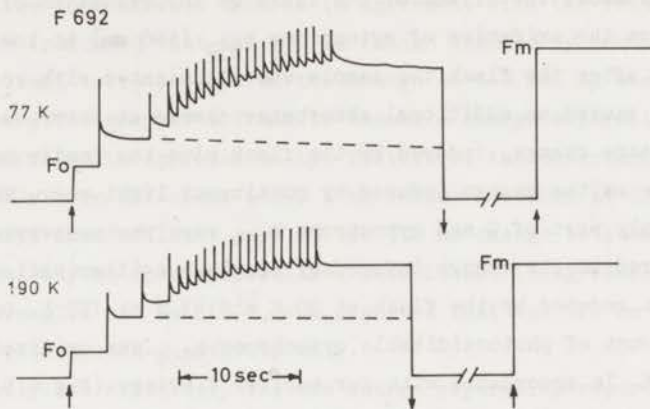


Fig.4.11. Time course of the fluorescence at 77 and 190 K of spinach chloroplasts (0.1 mg chlorophyll/ml) upon illumination with a series of flashes. Fluorescence exciting light (460 nm) on at upward arrows, off at downward arrows. A 7- $\mu$ s flash was given at every upward transient in the curves. At the intersections, the sample was irradiated with strong, actinic, white light for 30 s. Broken lines represent the time course if only one flash was given. Transient spikes are artifacts caused by the fluorescence excited by the flashes.

reaction center may also be studied by measurements of the changes of absorbances of C550 and cytochrome  $b_{559}$  and of the fluorescence yield induced by short, saturating flashes. It has been reported<sup>45</sup> that at low temperature a saturating flash caused an increase in fluorescence yield which was much smaller than that caused by either continuous light at 77 K or by a flash at room temperature. Fig.4.11 shows the effect of saturating flashes on the fluorescence yield at 77 and 190 K. The increase of the fluorescence yield as measured 1 s after the first flash was 27 % of the total variable yield at 77 K, it was 40 % at 170 K. If the intensity of the flash was lowered by a factor of 2 by the use of neutral density filters, these percentages were almost the same (25 and 38 %), which indicates that the flash was closely saturating. The broken lines represent the slow part of the decay of the fluorescence yield after the first flash. At 77 K the half time of the decay was about 1 min, the extent was about half that of the increase brought about by the first flash. At 190 K this decay could not be observed.

Fig.4.12 shows the effect of one flash on the reduction of Q (543 and 547 nm) and on the oxidation of cytochrome  $b_{559}$  (556 nm) at low temperatures. Some seconds after the flash the sample was illuminated with continuous light, which caused an additional absorbance change at these wavelengths. The total absorbance change, induced by the flash plus the continuous light, had the same size as the change induced by continuous light only. The figure shows that only part of Q and cytochrome  $b_{559}$  were photoconverted by one flash. Compared to the change induced by continuous illumination at 90 K 30 % of Q was reduced by the flash at 90 K and 43 % at 170 K. Only 15 % of the total amount of photooxidizable cytochrome  $b_{559}$  was oxidized by the flash at 90 K. In accordance with our earlier findings (Fig.4.5) cytochrome  $b_{559}$  was not photooxidized at 170 K neither by the flash nor by continuous light.

The difference spectrum of the flash-induced absorbance changes at 90 K (not shown) was found to be similar to that of the changes induced by continuous irradiation (Fig.4.1). The only difference between the spectra was the relative extent of the C550 changes in comparison with those of cytochrome  $b_{559}$  and also with those near 520 nm. The extent of the absorbance change at 520 nm induced by the first flash was about 50 % of that induced by con-

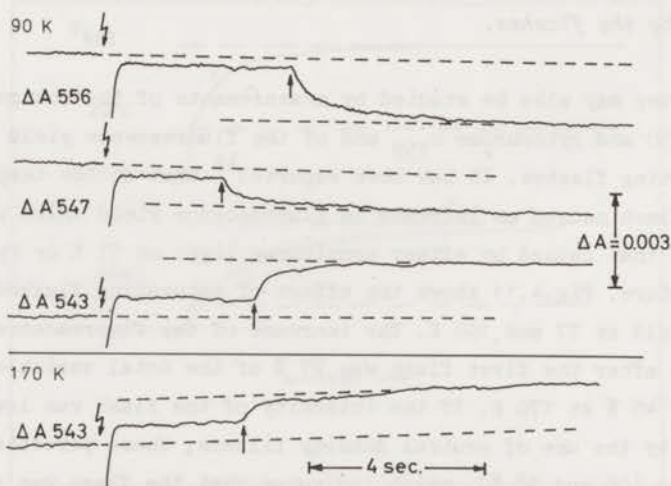


Fig.4.12. Time course of absorbance at 556, 547 and 543 nm at 90 K and at 543 nm at 170 K during irradiation of spinach chloroplasts (1 mg chlorophyll/ml) with a  $7\text{-}\mu\text{s}$ , saturating flash, followed by 645-nm continuous light ( $2.5\text{ mW}\cdot\text{cm}^{-2}$ ). Continuous light on at upward arrows; flash at downward arrows.



tinuous irradiation (not shown). This is in agreement with the results given in Fig.4.4, which indicated that the 520 nm change induced by continuous light may be at least twice as fast as the change at 543 nm. As was shown in Section 3.3.5 the efficiency of a flash to induce a charge separation in photosystem 1 was found to approach unity. Therefore, the observation that a flash is relatively more efficient at 90 K to induce a change at 520 nm than at 543 nm, suggests that at least part of the 520 nm change is caused by photosystem-1 activity at this temperature. This is not in agreement with the hypothesis of Vermeglio and Mathis<sup>12</sup>, who reported that the 520 nm change at 100 K is due to photosystem-2 activity only.

The relatively low efficiency for the charge separation reported here can be explained by the assumption of a back reaction between the photoproducts, which competes with a "stabilizing" reaction with secondary donors mentioned in Section 4.3.2. Direct evidence for such a back reaction will be discussed in the next section.

#### 4.3.5. The back reaction.

#### EPR signal of $P^+680$ .

Fig.4.13 shows kinetic traces of flash-induced EPR signals observed at

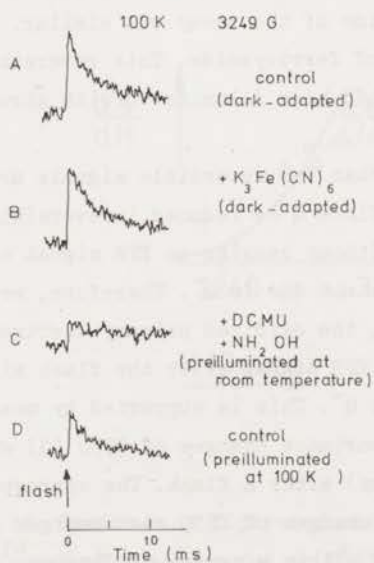


Fig.4.13. Time course of EPR changes at 3249 G upon flash illumination of spinach chloroplasts (0.5 mg chlorophyll/ml) at 100 K. A, control; B, +0.1 M  $K_3Fe(CN)_6$ ; C, + $10^{-5}$  M DCMU +  $10^{-2}$  M hydroxylamine preilluminated for 5 s with white light ( $100 \text{ mW} \cdot \text{cm}^{-2}$ ) before freezing; D, control, preilluminated with 10 flashes at 100 K. Each curve is the average of the changes induced by the first three flashes, except D, which is that of the 11th until the 40th flash. Instrument settings: power: 8 mW; modulation amplitude: 10 G.

the field position (3249 G) of the low-field maximum of the  $P^{+700}$  signal. Each trace (except curve D) is the average of the signals induced by the first three flashes at 100 K. Curve A was measured with dark-adapted chloroplasts. The signal rose within the 100- $\mu$ s time constant of the apparatus. The decay was multiphasic. About 20 % of the signal was irreversible on this time scale and partly reversible at longer times. These 20 % are supposed to be due to  $P^{+700}$ , which is oxidized practically irreversibly on this time scale. The half time of the decay of the reversible part was  $2.0 \pm 0.1$  ms (average of 35 measurements). Curve B was measured with samples containing additionally 0.1 M potassium ferricyanide. In such samples photosystem-1 activity is blocked due to chemical oxidation of P700 before freezing. It can be seen that the kinetics of curves A and B were similar, except that the extent of the irreversible change was smaller in the presence of ferricyanide. In samples of spinach chloroplasts containing DCMU and hydroxylamine, which were preilluminated before freezing, the reversible EPR signal was observed to be abolished (curve C). This treatment with DCMU and hydroxylamine blocks reactions of photosystem 2 (ref. 46). The irreversible change in curve C was the same as that in curve A, which indicates that the irreversible change reflects P700 oxidation. Curve D shows the average of the signals induced by 40 subsequent flashes after the tenth flash in samples of chloroplasts without additions. The extent of the reversible signal was about 30 % of that in curve A; the half time of the decay was similar. The same result was obtained in the presence of ferricyanide. This reversible change was not observed in samples which had been illuminated with strong continuous light (20 s) at 77 K (not shown).

It is clear from these measurements that the reversible signals are due to photosystem-2 reactions at 100 K. Since Q is reduced irreversibly after continuous illumination (Fig.4.1) without causing an EPR signal near  $g = 2$  (cf. Section 3.3.2), the signals are not due to  $Q^{-}$ . Therefore, we assume that the transients are due to  $P^{+680}$ , the oxidized primary electron donor of system 2. The rapid decay of the EPR signal after the flash might be conceivably due to a back reaction with  $Q^{-}$ . This is supported by measurements of Mathis and Vermiglio<sup>47, 48</sup> of absorbance changes of C550 (Q) which indicated a rapid decay (half time 3 - 5 ms) after a flash. The correspondence between the EPR signal and the absorbance changes of C550 also emerges from the observation that the extents decreased within a series of flashes<sup>47</sup> (curve D). Photooxidation of cytochrome  $b_{559}$  with a half time of 4 - 6 ms has

also been reported<sup>9, 47</sup>. The extent of the flash-induced absorbance change at 556 nm was 15 - 25 % of that induced by continuous light. These data support the notion that the cytochrome is oxidized in a secondary reaction with the oxidized primary donor and that the rate of this reaction is 4 - 7 times slower than that of the back reaction.

The kinetics shown in curve B (Fig.4.13) indicate that also in the presence of ferricyanide ( $E_h = 540$  mV) a back reaction occurs at 100 K. This observation, which is not in agreement with models of photosystem 2 proposed by Knaff et al.<sup>49</sup>, will be discussed in the next section.

Fig.4.14 compares the EPR spectrum of the reversible changes measured with samples as used for Fig.4.13 with the light-minus-dark spectrum due to  $P^+700$ . The spectra were found to be slightly different. The g-values were the same;  $\Delta H_{pp}$ , however, was somewhat smaller for the 2.0-ms component (6 G) than for  $P^+700$  (8 G). From the EPR signal height at non-saturating microwave power levels, the extent of the 2.0-ms changes was determined to be larger (1.3 times) than that of the  $P^+700$  signal. The 2.0-ms component saturated at a microwave power of 8 mW, the  $P^+700$  signal at 2 mW at 100 K. From these data the ratio of the number of spins causing the reversible 2.0-ms signal and Signal I, respectively, was calculated to be  $0.7 \pm 0.3$ . This figure is in agreement with the occurrence of a back reaction in only 70 % of the reaction centers and of stabilizing secondary reactions in the other centers.

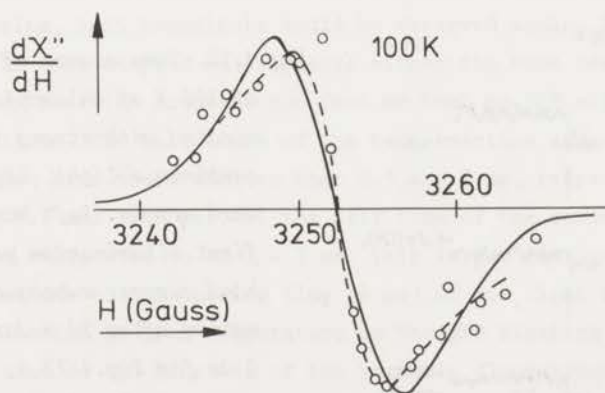


Fig.4.14. Spectrum of light-induced EPR signal shown in Fig.4.13 A, and light-minus-dark spectrum due to  $P^+700$  (solid line). Instrument settings: power: 8 mW; modulation amplitude: 5 G. Spectra are normalized at 3249 G.

From the  $\Delta H_{pp}$ -value of Signal I it has been concluded that P700 is a dimeric chlorophyll molecule<sup>50</sup>. Similarly, the slightly smaller  $\Delta H_{pp}$ -value of the 2.0-ms signal with respect to that of Signal I may be taken to indicate that P680 is a trimeric chlorophyll molecule or a complex of a (dimeric) chlorophyll molecule with another compound. It may be speculated that this other compound is Z, the electron donor to P<sup>+</sup>680 at room temperature, which then functions also at cryogenic temperatures. This will be discussed in Section 4.4.2.

*EPR measurements in continuous light.*

Fig.4.15 shows the EPR kinetics near  $g = 2.00$  upon illumination with strong, continuous light of dark-adapted spinach chloroplasts (as used for Fig.4.13A) at 100 K. A transient signal can be seen which is superimposed on the steady EPR change due to P700 photooxidation. The spectrum of the transient was similar to that of Fig.4.14. The signal decayed in the light with a half time of 30 ms (Fig.4.15). It was observed only at the first illumination period at 100 K. The signal observed in subsequent light periods can be attributed to P700 (Section 3.3.2). Fig.4.15B shows that the transient is absent in spinach chloroplasts in the presence of ferricyanide. This experiment will be discussed in the next section. Fig.4.15C shows that the transient is absent in spinach chloroplasts which were illuminated in

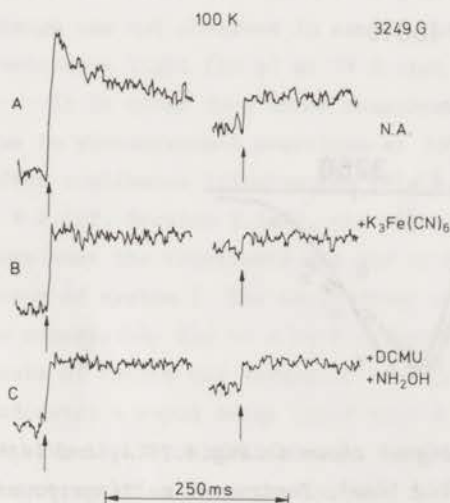


Fig.4.15. Time course of EPR signals at 100 K of chloroplasts illuminated with strong ( $200 \text{ mW}\cdot\text{cm}^{-2}$ ) continuous light. Light on at upward arrows. Left hand curves: first illumination period; right hand curves: subsequent illumination after 20 s dark. A, B and C as for Fig.4.13 A, B and C respectively. Instrument settings as for Fig.4.13, except for amplification.

the presence of DCMU and hydroxylamine prior to freezing in order to block photosystem-2 activity<sup>46</sup>. This indicates that the transient is due to photosystem 2. The change which can be seen in Fig.4.15C is apparently due to photooxidation of P700. In Chapter III, the transient signal was not observed, since the opening time of the light shutter used with those experiments was too slow and the intensity of actinic irradiation was too low to obtain the signal. The extent of the transient signal was found to be strongly dependent on the intensity of actinic irradiation. With the maximal intensity of illumination ( $300 \text{ mW}\cdot\text{cm}^{-2}$ ) in the present experiments the extent of the 30-ms transient was found to be only 30 % of that of the 2.0-ms change. This suggests that also the maximal intensity of continuous light is not saturating.

Reactions of photosystem 2 with a half time of 20 - 40 ms have been attributed previously to secondary electron donation to  $\text{P}^+\text{680}$  at 77 - 110 K (refs. 26, 32). Murata et al.<sup>32</sup> has also observed a 35-ms reaction in measurements of the fluorescence induction at 77 K. Our results provide independent evidence for a secondary reaction which occurs with a half time of  $28 \pm 8$  ms (average of 22 measurements) at 100 K.

#### *Kinetics at 170 K.*

The 2.0 and 30-ms EPR signals shown in Figs.4.13 and 4.15, were not observed in dark-adapted spinach chloroplasts at 180 K (Fig.4.16). With chloroplasts, which were illuminated with two 7- $\mu\text{s}$ , saturating flashes shortly before freezing, both transients could be observed again. This indicates that at 180 K with dark-adapted chloroplasts either the back reaction as well as the secondary reaction occurred too fast or that no EPR signals were generated by the reactions. The half times of the back reaction and of the secondary reactions then have to be shorter than 0.5 and 5 ms, respectively. From the data of Fig.4.7 and from ref. 51 the half time of the secondary reaction at 170 K may be calculated to be 1 - 3 ms. This is too fast to be observed with our apparatus due to the opening time (4 ms) of our light shutter. The effect of preillumination at room temperature on the EPR kinetics (Fig.4.16) is similar to that on the kinetics of the variable fluorescence yield<sup>35-37</sup> at 170 K and on those of the cytochrome  $\text{b}_{559}$  oxidation<sup>27</sup> at about 210 K.

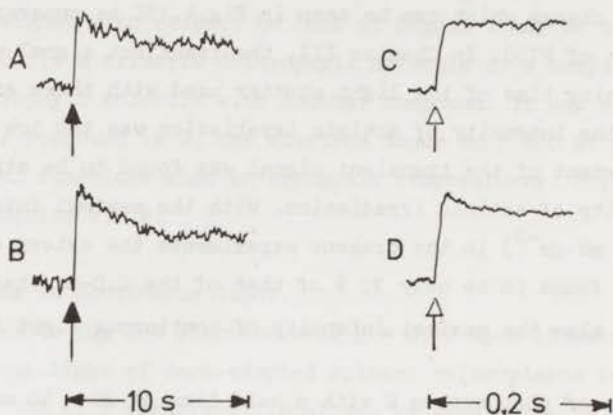


Fig.4.16. Time course of EPR signals at 180 K with samples (curves A and B) as for Fig.4.13A, and with similar samples preilluminated with two flashes 10 s before freezing (curves C and D). Curves A and C were measured as curve A in Fig.4.13; B and D as curve A in Fig.4.15. Amplification for curve A was twice that for curve C. Closed arrows: flashes; open arrows: continuous light.

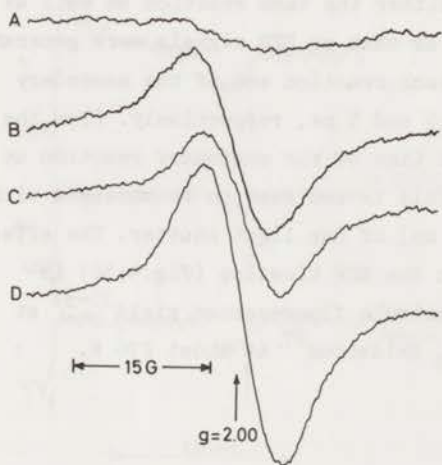


Fig.4.17. EPR spectra at 110 K with spinach chloroplasts (0.5 mg chlorophyll/ml). A, sample frozen in the dark; B, sample A during illumination; C, sample frozen in the dark in the presence of (0.17 M  $K_3Fe(CN)_6$ ); D, sample C after illumination for 7 s with white light ( $100 \text{ mW}\cdot\text{cm}^{-2}$ ). Instrument settings: power: 2 mW; modulation amplitude: 5 G; frequency: 9.080 GHz.

#### 4.3.6. Photooxidation of chlorophyll at 110 K.

##### EPR measurements.

In the previous section it was shown (Figs.4.13B and 4.15B) that also with chloroplasts in the presence of ferricyanide at 100 K, which show no photosystem-1 activity due to chemical oxidation of P700, light-induced EPR signals near  $g = 2$  are present. Fig.4.17 shows EPR spectra near  $g = 2$  of spinach chloroplasts, frozen in the dark and subsequently illuminated at 110 K. Without ferricyanide (A and B) the spectra were similar to those at 11 K (Fig.3.4) of Signal II and  $P^{+}700$ . As discussed in Chapter III (Section 3.3.3) the signal height in spectrum B (minus A) indicates 100 % photooxidation of P700. Comparison of spectra B and C indicates that in the presence of ferricyanide P700 is completely oxidized in the dark. In agreement with this, EPR measurements at 15 K indicated that in the presence of ferricyanide (0.17 M) photoreduction of ferredoxin (at  $g = 2.05, 1.94$  and  $1.86$ ) did not occur (not shown). Spectra C and D show that at 110 K in the presence of ferricyanide continuous illumination caused also an irreversible increase in the extent of the signal near  $g = 2.00$ . The extent of the light-induced signal (spectrum D minus C) was about equal to that of the signal of  $P^{+}700$ . Values of  $g$  and  $\Delta H_{pp}$  were also the same. These results confirm the EPR measurements of Malkin and coworkers<sup>7, 8, 49</sup> and also of Ke et al.<sup>53</sup> concerning the irreversible light-induced signal near  $g = 2.00$  with samples at high redox potentials. These authors, however, attributed the signal to  $P^{+}680$  which was photooxidized irreversibly at 77 K. Knaff et al.<sup>49</sup> have reported that the signal is reversible at temperatures above 170 K. Since Q is known to be photoreduced irreversibly at 90 K (Fig.4.1) also in the presence of ferricyanide, it will be clear, that the occurrence of irreversibly oxidized P680 does not agree with models involving a back reaction between  $P^{+}680$  and  $Q^{-}$ .

The ratio between the number of spins causing this EPR signal and that of  $P^{+}700$  was calculated to be  $1.1 \pm 0.2$ . Since the amount of  $P^{+}700$  was found to be one per 390 chlorophyll molecules in spinach chloroplasts (Section 3.3.5) the amount of oxidized chlorophyll causing the EPR signal in the presence of ferricyanide was about one per 350 chlorophyll molecules.

Fig.4.18 shows the kinetics of the change of the EPR signal upon illumination at 110 K in the presence of ferricyanide, measured with the magnetic field fixed at the maximum of the low field line. At the onset of irradiation

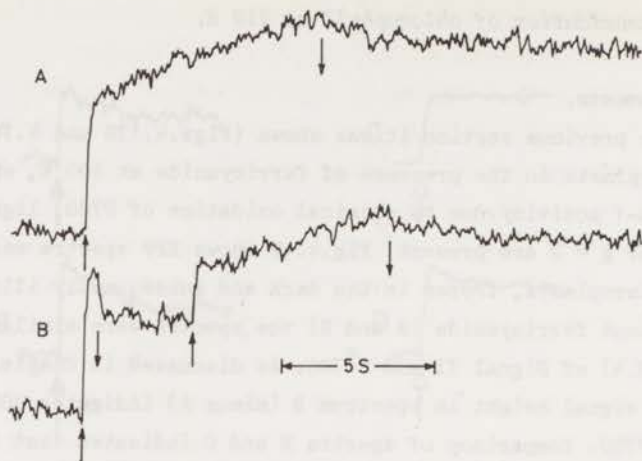


Fig.4.18. Time course of the light-induced EPR signal at  $g = 2.00$  in the presence of potassium ferricyanide (0.17 M) at 110 K. Light on at upward, off at downward pointing arrows. Conditions as for Fig.4.17C.

a fast and a slow rise component can be distinguished. Only part (15 %) of the signal was found to be reversible after prolonged illumination (Fig.4.18A); the halftime of the decay was about three seconds. However, as can be seen in Fig.4.18B, about 30 % of the signal decayed rapidly ( $\tau_{1/2} < 100$  ms) in the dark after a short (0.5 s) illumination period. If the sample was illuminated again after a dark period of three seconds (Fig.4.18B) the signal increased until the level obtained during the first, short illumination period, and subsequently more slowly as in Fig.4.18A. The decay in the dark after a light period of 6.5 s was also equal to that in Fig.4.18. The rapid decay of part of the signal after a short light period (Fig.4.18B) indicates that also at 110 K a back reaction occurs at least in part of the reaction centers in the presence of ferricyanide. This was also concluded from Fig.4.13B.

We interpret the EPR kinetics shown in Fig.4.18 as being due to the formation of two different radicals, which have slightly different EPR spectra (Figs.4.14 and 4.17). At the onset of irradiation the change is due to  $P^{+680}$  which can react back rapidly with  $Q^{-}$ . During prolonged irradiation  $P^{+680}$  is reduced by another chlorophyll molecule in a dark reaction which stabilizes the charge separation.



### *Absorbance changes.*

Spectra between 655 and 705 nm of irreversible absorbance changes induced by continuous illumination at 110 K with chloroplasts in the presence of ferricyanide and DBMIB are shown in Fig.4.19. The spectrum of the band shift due to reduction of Q (spectrum A, without ferricyanide) was taken from Fig.3.1. With ferricyanide present, the shape of the spectrum was found to depend on the intensity and duration of actinic irradiation. Generally, at high light intensities (above  $5 \text{ mW}\cdot\text{cm}^{-2}$ ) a fast and a slow phase could be observed between 668 and 695 nm (Fig.4.20). The shape of the spectrum of the fast phase was different from that of the slow phase (spectra B and C).

The extent of the 676-nm decrease was greater with than without ferricyanide. Therefore, this change was not due to fluorescence yield changes, which were smaller with than without ferricyanide (e.g. Fig.4.3). Lozier and Butler<sup>16</sup> have reported spectra of irreversible light-induced absorbance changes near 680 nm at low temperature measured with a scanning method. These spectra are significantly different from Fig.4.19 (B and C) in the 676-nm region due to an important contribution of the fluorescence excited by the measuring beam. Probably for this reason they did not observe an additional absorbance decrease near 676 nm in the presence of ferricyanide at 77 K.

The extent of the absorbance increase at 683 nm was smaller with ferricyanide present than without. It was shown in Fig.4.1 that the absorbance changes of C550 in the green region are not affected by the presence of the oxidant. Therefore, we assume that the band shift around 686 nm, which is also due to C550 (refs. 13, 16), occurred to the same extent with and without ferricyanide. The difference between spectra measured with and without ferricyanide is shown at the right hand side of Fig.4.19 (B minus A). This difference spectrum resembles that of  $\text{P}^+700$  as obtained by the analysis given in Fig.3.13 at 110 K except for the position and for the absence of the band shift. Therefore, the difference spectrum (B minus A) in Fig.4.19 may be interpreted in a similar way as the spectrum of  $\text{P}^+700$  as being due to the oxidation of a chlorophyll dimer at 110 K (see also ref. 13). Since the absorbance changes were irreversible, they cannot be attributed to  $\text{P}^+680$ , which is supposed to react back with  $\text{Q}^-$  also at 110 K. We interpret this chlorophyll bleaching as being due to secondary electron donation by a chlorophyll dimer to  $\text{P}^+680$ .

EPR measurements indicated that the presence of DBMIB in the samples

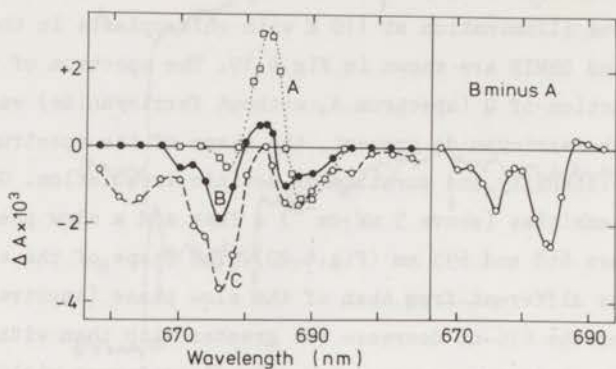


Fig.4.19. Spectra of light-induced absorbance changes at 110 K with chloroplasts (0.2 mg chlorophyll/ml) in the presence of  $10^{-4}$ M DBMIB and with (B and C) or without (A) 85 mM  $K_3Fe(CN)_6$ . Spectrum A was taken from Fig.3.1. Actinic irradiation: 440--570 nm,  $7 \text{ mW}\cdot\text{cm}^{-2}$ . Curves B and C are the spectra of the changes after 1 and 10 s of illumination, respectively.

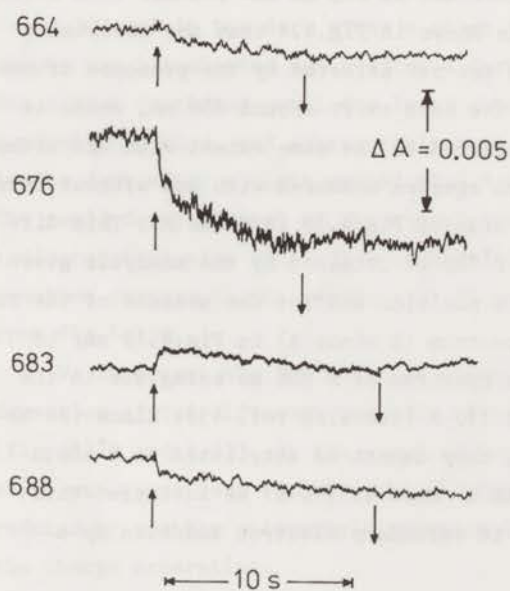


Fig.4.20. Time course of absorbance at 664, 676, 683 and 688 nm at 110 K measured for Fig.4.19.

affects the kinetics of the chlorophyll oxidation. Fig.4.21 shows a biphasic time course for this reaction in the presence of DBMIB. The fast phase occurred to a smaller extent with DBMIB than without. Since the extent of the fast phase was strongly dependent on the light intensity, this may be explained by the assumption<sup>54</sup> that with DBMIB the amount of light available for photosystem-2 reactions is less than without DBMIB. The rate of the slow phase was linearly dependent on the light intensity (not shown). This was also observed for the slow phase of the absorbance changes shown in Fig.4.19. The slow phase also went on for at least several minutes during continuous illumination. The reaction proceeded after closure of all photosystem-2 traps, as indicated by the absorbance changes due to reduction of Q (683-nm increase). This suggests that the reaction occurs directly between (bulk-) chlorophyll and (oxidized) DBMIB molecules. Photoreactions between quinone and chlorophyll molecules *in vitro* at low temperature have been reported in the literature<sup>55</sup>. One might also speculate that oxidized DBMIB is a potent quencher of the fluorescence yield<sup>56</sup> due to its ability to accept electrons from excited chlorophyll molecules. As can be seen in Fig.4.19 a slow bleaching occurred also at the absorbance band of monomeric chlorophyll

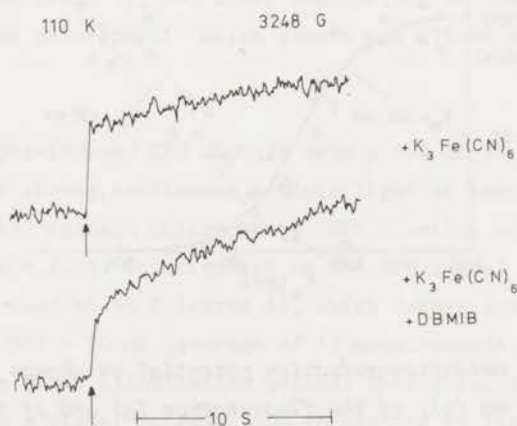


Fig.4.21. Time course of EPR change upon illumination at 110 K with samples as for Fig.4.17C with and without  $10^{-4}$  M DBMIB. The magnetic field was set at the maximum of the signal of  $P^+700$  (3248 G). Light on at upward arrows. Instrument settings as for Fig.4.17.

(664 nm; refs. 57, 58). We interpret this slow change at 664 nm and at other wavelengths as being due to oxidation of chlorophyll by DBMIB. The fast rise phase at 676 nm then is attributed to chlorophyll molecules donating electrons to photosystem 2.

The extent of the fast chlorophyll bleaching in Fig.4.19 (B minus A) is about 40 % of that due to photooxidation of P700 at 703 nm in Fig.3.1. The extents of the fast EPR changes due to chlorophyll oxidation in the presence of ferricyanide and to P700 oxidation without ferricyanide were found to be the same. This indicates that the flattening factor<sup>59, 60</sup> at 676 nm is about 2.5 times greater than at 703 nm. Since the flattening factor is essentially equal to unity at 703 nm, the value of this factor is about 2.5 at 676 nm at 110 K. A similar value has been calculated (Pulles, M.P.J., personal communication; ref. 61) for spinach chloroplasts at room temperature at the maximum of chlorophyll absorption (683 nm). This indicates that the pigmented particles in our suspension did not aggregate or change size upon cooling.

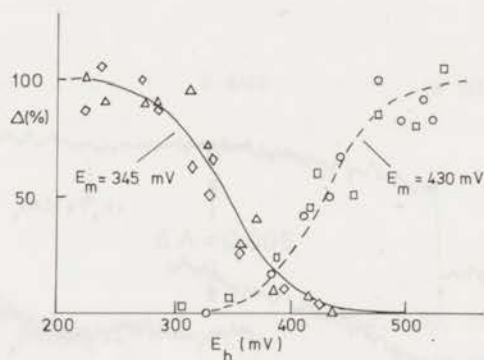


Fig.4.22. Effect of oxidation-reduction potential on change of absorbance at 556 ( $\diamond$ ) and 676 nm ( $\circ$ ), of the fluorescence ( $\Delta$ ) and of the irreversible EPR signal near  $g = 2$  ( $\square$ ) of dark-adapted chloroplasts at 110 K. Contribution of changes due to P700 oxidation are subtracted from the results of EPR measurements and of optical measurements at 676 nm. The fluorescence at  $E_h = 450$  mV was subtracted from the fluorescence yield measured at lower  $E_h$ . The solid and broken lines are one-electron Nernst curves.

#### *Oxidation-reduction titration.*

Fig.4.22 shows redox titration curves for the extents of the light-induced changes at 110 K of the absorbance at 556 and 676 nm, of the fluorescence yield, and of the irreversible photosystem-2 EPR signal near  $g = 2.00$ . The figure shows, firstly, that the extent of the variable fluorescence yield follows closely that of the amount of photooxidizable cytochrome  $b_{559}$ . This is in agreement with measurements of Okayama and Butler<sup>15</sup> who demonstrated that these curves are one-electron Nernst curves with  $E_m = 365$  mV. Our  $E_m$  value is lower due to the presence of glycerol (Section 2.3.4). Furthermore, Fig.4.22 shows that the change of the absorbance at 676 nm and of the EPR signal at  $g = 2.00$  are similar with respect to their extents at various redox potentials ( $n = 1$ ,  $E_m = 430$  mV). This provides strong evidence that these two changes reflect the photoconversion of the same compound. On the basis of the position of the optical bleaching as well as of the shape and  $g$ -value of the EPR signal<sup>50</sup> this compound is probably a dimeric chlorophyll- $a$  molecule, which is photooxidized irreversibly at 77 - 110 K in spinach chloroplasts in the presence of ferricyanide. Recently, Mathis and Vermeglio<sup>48</sup> have observed irreversible light-induced absorbance increases near 820 nm with chloroplasts in the presence of ferricyanide at 100 K. Since chlorophyll cations are known to absorb near 820 nm (ref. 57, 58) these changes may be due to the photooxidation of the same chlorophyll which causes the 676-nm change and the EPR signal.

#### *4.3.7. Transient light-induced EPR signals near $g = 2$ at 10 - 50 K.*

At the onset of strong, continuous actinic light at temperatures below 77 K with dark-adapted spinach chloroplasts EPR kinetics as shown in Fig.4.23 were observed near  $g = 2.00$ . Superimposed on the EPR signal of  $P^{+}700$  a transient signal can be seen at 14 K (curve A), which decays during illumination with a half time of  $500 \pm 30$  ms (average of 13 measurements). The transient occurred only at the first illumination period. Therefore, these kinetics can not be attributed to a signal decrease due to heating by light absorption. Curve B was measured with spinach chloroplasts, which were illuminated in the presence of DCMU and hydroxylamine prior to freezing. The transient signal is abolished by this treatment; the kinetics shown in curve B are due to photooxidation of P700 only (Ch. III). This demonstrates that the transient is due to photosystem-2 activity. Curve C shows the kinetics of the EPR signal upon a short light period (about 0.1 s). As can be seen most of the signal

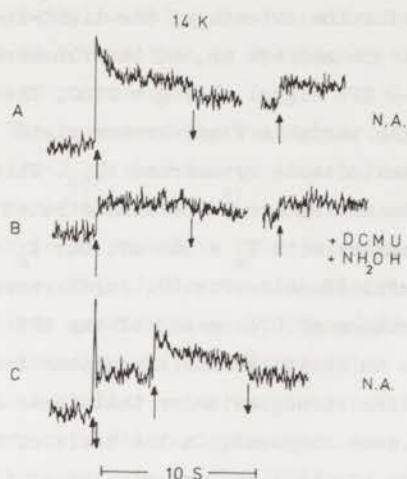


Fig.4.23. Time course of EPR signals at 3230 G of chloroplasts at 14 K. A and C, no additions; with DCMU and hydroxylamine as for curve C of Fig.4.13. Left and right hand curves: first and subsequent light periods, respectively. For recording C the first light period was 0.1 s. Continuous light on at upward arrows, off at downward pointing arrows. Instrument settings: power 2 mW; modulation amplitude: 5 G; frequency: 9.077 GHz.

decays rapidly upon darkening ( $\tau_2 < 0.1$  s). In a subsequent light period the kinetics of the signal are similar to those shown in curve A. This suggests that a back reaction between the primary reactants of photosystem 2 may also occur at 14 K. Furthermore, the rate of the back reaction seems to be high in comparison with that of the secondary dark reaction which stabilizes the charge separation. If it is assumed that the back reaction has the same rate as at 90 K, comparison of Figs.4.15 and 4.23 indicated that the quantum yield for irreversible photoreactions of system 2 at 14 K is about 0.02 eq. per quantum.

The spectrum of the transient and of the  $P^{+700}$  EPR changes are shown in Fig.4.24. The transient signal appeared to be somewhat asymmetrical, but its  $g$ -value was the same as of  $P^{+700}$ . It is not clear which compound caused the transient signal. Since the shape of the spectra was not the same, the method described in ref. 62 was used to calculate the number of spins of the transient signal: a ratio of  $0.8 \pm 0.2$  was found relative to that of  $P^{+700}$ .

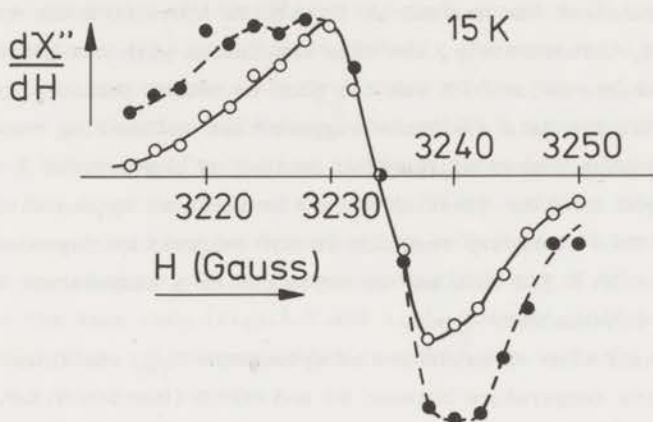


Fig.4.24. Spectrum (closed circles) of the transient EPR signal which decays with a half time of 0.5 s during illumination of dark-adapted chloroplasts at 15 K. The spectrum of  $P^+700$  is also given (open circles, solid line). Instrument settings as for Fig.4.23. Spectra are normalized at 3230 G.

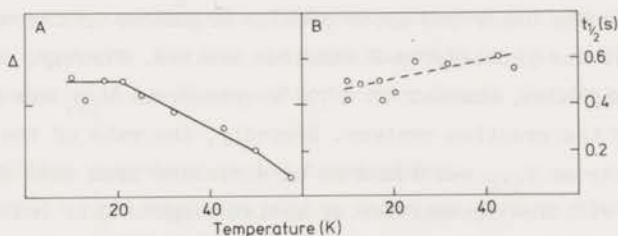


Fig.4.25. Temperature dependence of the transient EPR signal at 3230 G. A, extent (arbitrary units); B, half time of decay. Conditions and instrument settings as for Fig.4.23A.

Since this 500-ms transient was not observed at 100 K (previous section) one may expect a temperature dependent half time for this reaction. The extent of the transient was found to be temperature dependent (Fig.4.25), but the half time of its decay was independent of temperature between 10 and 45 K. The

extent of the transient was maximal at 10 - 20 K. Above 60 K the transient was not observed. Unfortunately, the time resolution with the EPR measurements at temperatures below 80 K was too poor to detect possibly faster decaying transients. The data available suggest that on lowering the temperature in an increasing number of reaction centers of photosystem 2 the 30-ms secondary electron donation (Section 4.3.5) is replaced by one with a half time of 500 ms. This secondary reaction is not temperature dependent. As was discussed in Section 4.3.2 this may be explained by a temperature dependent oxidation of an intermediary donor.

Since the half time of oxidation of cytochrome  $b_{559}$  was found to be independent of the temperature between 90 and 180 K (Section 3.3.2, and ref. 9) our data also suggest that at 14 K cytochrome  $b_{559}$  is not photooxidized. This has not been demonstrated directly so far, but it might explain the failure to observe an EPR spectrum of an oxidized cytochrome at 6 - 20 K in chloroplasts which were illuminated at low temperatures (Visser and Rijgersberg, unpublished observations).

#### 4.4. Discussion

##### 4.4.1. Two different types of reaction centers in photosystem 2 at low temperatures.

Several results described above provide arguments in favour of a heterogeneity of the photosystem-2 reaction centers. Firstly, in Section 4.3.1 it was concluded, that at 77 - 100 K cytochrome  $b_{559}$  was photooxidized in only half of the reaction centers. Secondly, the rate of the photooxidation of cytochrome  $b_{559}$  was found to be different from that of the reduction of Q also with low intensities of actinic light. This indicated that there are two types of reaction centers which differ by the quantum yield for irreversible charge separation. Thirdly, the observation that the extent of the fluorescence yield change decreased by a factor of two and that the rate increased upon addition of ferricyanide prior to freezing may also be explained by the occurrence of two types of reaction centers. In Section 4.3.3 it was concluded that the centers are heterogeneous with respect to a slow back reaction. Half the extent of the changes of fluorescence yield and of the absorbance at 543 nm was found to be slowly reversible at 90 K. The photooxidation of cytochrome  $b_{559}$  was irreversible.

It will be clear from these results that the C550 absorbance changes



indicate the reduction of the primary electron acceptor in both types of centers. Therefore, this acceptor is probably the same in all centers. Cytochrome  $b_{559}$  is the ultimate electron donor of one type of the centers. It has been shown by Bearden and Malkin<sup>8</sup> that at 77 K a compound with a midpoint potential of 465 mV may function as electron donor (see also Section 4.3.6). This may be the donor of the centers which do not oxidize cytochrome  $b_{559}$ . The fluorescence yield may be determined by both types of centers. The observation that the changes of the fluorescence yield and of the absorbance at 556 nm have the same rate (Figs. 4.2 and 4.4), however, indicates that the centers, which show cytochrome oxidation affect the variable fluorescence more strongly than the other centers.

The transient EPR signal, which decayed with a half time of 2.0 ms (Section 4.3.5) at 100 K was observed in about 70 % of the reaction centers. This is in agreement with the observation that about 30 % of all reaction centers are closed by the first flash at 100 K, and that in 70 % of the centers a back reaction occurs after this flash. Therefore, the transient EPR signal seems to be present in both types of reaction centers. And as the signal is due to  $P^{+680}$  this indicates that the primary electron donor is the same in all centers.

The only differences between the two types of reaction centers then seems to be the identity of the ultimate electron donor and the rate of the irreversible charge separation. The difference between the rates may be due to different rate constants for the electron donation by the different secondary donors. This point will be discussed into more detail in the next section.

#### 4.4.2. Intermediate reactions at low temperatures.

Illumination of chloroplasts with a short saturating flash at 90 K caused an oxidation of 15 - 25 % of the total amount of photooxidizable cytochrome  $b_{559}$  (Section 4.3.4, and refs. 9, 16, 47) with a half time of 3 - 5 ms (refs. 9, 47, 48). Since this half time is the same as that of the back reaction (refs. 45, 47, 48) (Section 4.3.5), it is likely that the same oxidized species is reduced either by a back reaction with  $Q^{-}$  or by a secondary reaction with cytochrome  $b_{559}$ . From the data of Section 4.3.5 and of refs. 47 and 48 one would expect this oxidized species to be  $P^{+680}$ . However, den Haan et al.<sup>63</sup> have demonstrated that the fluorescence yield at 77 K increases with a half time of less than 20  $\mu$ s upon flash-illumination of chloroplasts. The fluorescence yield did not change between 40  $\mu$ s and several seconds. The

extent of the change after the first flash was 20 % of the maximum increase attained after a large number of flashes. These data suggest that in 20 % of the reaction centers the reduction of  $P^{+680}$  occurs faster than 20  $\mu$ s at 77 K after the first flash. Since neither  $Q^{-}$  nor cytochrome  $b_{559}$  are (re-)oxidized that fast, this indicates that the reaction centers contain an intermediary donor which, at 77 K, is able to reduce  $P^{+680}$  and to oxidize cytochrome  $b_{559}$ . In the following this intermediate will be denoted by Z.

The occurrence of a reaction  $ZP^{+680} + Z^{+}P680$  with  $\tau_{\frac{1}{2}} < 20 \mu$ s has consequences for the hypothesis of a back reaction (with  $\tau_{\frac{1}{2}} = 2 - 4$  ms) between  $P^{+680}$  and  $Q^{-}$ , which explains the relatively low efficiency of the irreversible charge separation at low temperatures (Section 4.3.4). Since the fluorescence yield did not show a time constant of 2 - 4 ms (ref. 63), it is not likely that  $Z^{+}$  may react back with  $Q^{-}$ . Therefore, it would appear to be fortuitous that the half time of the back reaction and of the oxidation of cytochrome  $b_{559}$  after a flash at 77 K are about the same. However, if it is assumed that the state  $Z^{+}P680$  is in rapid equilibrium with  $ZP^{+680}$  due to a fast ( $\mu$ s) reaction of  $Z^{+}$  with  $P680$ , the similarity of the half times of (re-)oxidation of  $Q^{-}$  and cytochrome  $b_{559}$  as well as the relatively low quantum yield of the irreversible reactions can be explained with the back reaction model. From the extent of the 2.0-ms EPR component (Section 4.3.5) and from the fluorescence yield changes upon flash-illumination<sup>63</sup> at 77 - 100 K it may be concluded that the equilibrium of the reaction  $ZP^{+680}$  with  $Z^{+}P680$  is such that the amount of  $P^{+680}$  is 4 times higher than that of  $Z^{+}$  at the first flash and still more at subsequent flashes. This also explains the ratio of 4 or more between the half times of the back reaction and those of the charge stabilizing secondary reactions, which was proposed to explain the relatively low quantum yield of irreversible charge separation (Section 4.3.4).

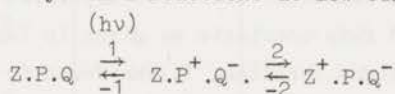
The hypothesis of a rapid equilibrium between  $ZP^{+680}$  and  $Z^{+}P680$  is supported by the observation that the  $\Delta H_{pp}$ -value of the  $P^{+680}$  EPR signal at 100 K is only 6 G (Section 4.3.5).

It may be speculated that the equilibrium is temperature dependent. At room temperature the quantum yield of the irreversible reaction is close to unity, at 10 K this reaction is about 0.02 (Section 4.3.7). As has been discussed by Joliot<sup>51</sup> the half time of charge stabilization is temperature dependent between room temperature and 220 K ( $Q_{10} = 1.3$ ). From Fig.4.7 an activation energy of about 1.0 kcal was calculated for temperatures between 77 and 180 K. Extrapolation of these figures to lower temperature, however,

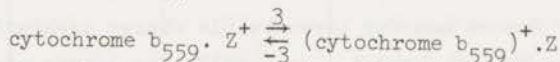
was not consistent with an observed half time of 0.5 s at 15 K (Section 4.3.7). Therefore, we assume that at 14 K  $Z^+$  is reduced by another donor than at 77 K. The displacement of the equilibrium in favour of  $ZP^+680$  upon lowering the temperatures would suggest that the EPR spectrum of the transient signal at 14 K is due to  $P^+680$ . However, the spectrum seems to be different from that of a chlorophyll cation<sup>50</sup>. Clearly, EPR measurements with better time resolution than those of Section 4.3.7 as well as optical measurements at 10 - 40 K will have to be performed before a complete understanding of this transient signal will be possible.

#### 4.4.3. Summary: a model of the photosystem-2 reaction center.

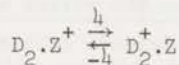
The data and considerations given in this chapter may be summarized in the following model of photosystem-2 reactions at low temperatures.



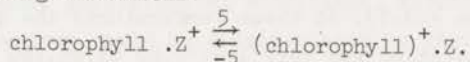
with in half of the centers at 77 - 110 K:



and in the other half:



Under strongly oxidizing conditions:



P and Q are the primary electron donor and acceptor, respectively; Z is an intermediary reactant and  $D_2$  is one of the secondary electron donors. Z, P and Q are the same in all reaction centers. Q is probably a bound plastoquinone molecule<sup>11, 64, 65</sup>. In all centers Q becomes completely reduced in the light, as indicated by the C550 shift (Section 4.3.1, and ref. 5). P is presumably a dimeric chlorophyll molecule (Section 4.3.5), absorbing near 680 nm (refs. 13, 66). Z is an unknown molecule; the midpoint potential of Z is higher than 540 mV (previous section). Z is not chlorophyll, otherwise the 2.0-ms EPR component described in Section 4.3.5 would be larger. At 90 K in half of the centers cytochrome  $b_{559}$  is the ultimate electron donor, in the other half an unknown donor,  $D_2$ , functions as such (Sections 4.3.1 and 4.3.3).  $D_2$  may have a midpoint potential of + 465 mV (Section 4.4.1, and ref. 8). Although Q is photoreduced, at 180 K cytochrome  $b_{559}$  is not photooxidized in dark-adapted chloroplasts. This indicates that then another molecule functions as ultimate

donor. This molecule may be identical with  $D_2$  (ref. 8). In preilluminated chloroplasts at 180 K the secondary donor is cytochrome  $b_{559}$  (refs. 27, 35, 67). The donor system at 10 - 40 K may also be different from that at 77 - 100 K (Sections 4.3.7 and 4.4.2) In spinach chloroplasts at  $E_h = 540$  mV the ultimate donor was found to be chlorophyll at 77 - 110 K (Section 4.3.6 and refs. 8, 48), and also at 180 K and at 10 - 40 K (refs. 8, 49; Visser and Rijgersberg, unpublished results). It seems likely that  $Z/Z^+$  or P680/P<sup>+</sup>680 is so electropositive that also a bulk chlorophyll molecule in the neighbourhood of an oxidized Z may become oxidized if no other electron donor is available. The various donor molecules are assumed to be present in each reaction center, but are oxidized by  $Z^+$  only if they are in the right redox state, and if the center is in the right conformational state.

Assuming that the reactions discussed are first or pseudo-first order reactions, we obtained rate constants as given in Table 4.3. Furthermore, the quantum yield of the light reaction, 1, was found to be unity (Section 4.3.4). Due to the occurrence of the back reaction -1 the quantum yield for oxidation of the secondary donors and for irreversible charge separation was much lower than unity. Since  $k_{-3}$ ,  $k_{-4}$  and  $k_{-5}$  are small, the latter yield depends on the equilibrium  $k_2/k_{-2}$  as well as on the ratios  $k_3/(k_3 + k_{-1})$ ,  $k_4/(k_4 + k_{-1})$  and  $k_5/(k_5 + k_{-1})$ . Thus this yield depends on the identity of the ultimate electron donor. At 10 - 40 K the rate constant of the reduction of  $Z^+$  was found to be  $1.4 \text{ s}^{-1}$  (Section 4.3.7). At these temperatures the quantum yield of irreversible charge separation was very low: 0.02 el.eq./hv (Section 4.4.2). This low efficiency may also be due to the temperature dependence of the equilibrium  $k_2/k_{-2}$ . As photosynthetic energy conversion occurs efficiently under physiological conditions, at room temperature  $k_2$  is greater than  $k_{-2}$  (see e.g. ref. 68). With decreasing temperature, however,  $k_2$  seemed to become smaller than  $k_{-2}$ .

Our results indicate that the electron transport in and near the reaction center of photosystem 2 involves different reactions at 10 - 40 K, at 77 - 110 K and at 170 - 200 K. This may be explained by a temperature dependence of the molecular properties of the reacting compounds. For chlorophyll molecules in vitro important shifts of energy levels upon freezing have been reported<sup>69</sup>. Such changes will also affect electron transport (ref. 70, and P. Geldof, personal communication). Since little is known about the temperature dependence of the molecules, conclusions about the electron transport at room temperature cannot be derived from low-temperature experiments by simple

Table 4.3. RATE CONSTANTS OF PHOTOSYSTEM-2 REACTIONS.

Rate constants (in  $s^{-1}$ ) of the reactions described in Section 4.4.3 at the temperatures indicated. It is assumed that the reactions are first or pseudo-first order reactions. Numbers between parentheses in the right hand column indicate references from the literature.

temperature	77 - 110 K	170 - 190 K	Refs./Sections of Ch. IV
$k_{-1}$ ( $s^{-1}$ )	350	350	4.3.5 (47, 48)
$k_2$	$> 3 \times 10^4$	$> 3 \times 10^4$	4.4.2 (63)
$k_{-2}$	$> 10^5$	$> 6 \times 10^4$	4.4.2 (63)
$k_2/k_{-2}$	$< 3$	$< 2$	4.4.2
$k_3$	20	20	4.3.4 and 4.3.5
$k_{-3}$	$< 10^{-3}$	?	4.3.3
$k_4$	40	160 ?	4.3.1 and 4.4.1
$k_{-4}$	$10^{-2}$	?	4.3.3 (32)
$k_5$	10	?	4.3.6
$k_{-5}$	$< 10^{-2}$	$< 10^{-2}$	4.3.6 (49)

extrapolation. With this restriction our data suggest the following about the electron transport under physiological conditions. Firstly, both at 90 and at 180 K two types of centers could be distinguished by their secondary donors. This suggests that there are similarly two types of centers at room temperature. Secondly, the temperature dependence of  $k_2$  and  $k_{-2}$  (see above) indicates that at room temperature the reduction of  $P^{+680}$  occurs with a half time shorter than 25  $\mu s$ . The available data<sup>71, 72</sup> indicate that in most of the centers  $P^{+680}$  is reduced with a half time of 35  $\mu s$  at room temperature. However, recent results of measurements of fluorescence and luminescence<sup>73, 74</sup> suggest reduction of  $P^{+680}$  within 35  $\mu s$ . Thirdly, also at room temperature  $P680$  is probably a dimeric chlorophyll molecule bound to Z. The primary electron donor of the bacterial reaction center, P870, as well as that of photosystem 1 were also found to be dimers of bacteriochlorophyll and of chlorophyll, respectively<sup>50, 75-78</sup>. Therefore, it may be speculated that the dimeric structure is essential for photosynthetic light reactions.

## REFERENCES

1. Knaff, D.B. and Arnon, D.I. (1969) *Proc. Natl. Acad. Sci. U.S.* 63, 956-962
2. Knaff, D.B. and Arnon, D.I. (1969) *Proc. Natl. Acad. Sci. U.S.* 63, 963-969
3. Bendall, D.S. and Sofrova, D. (1971) *Biochim. Biophys. Acta* 234, 371-380
4. Boardman, N.K., Anderson, J.M. and Hiller, R.G. (1971) *Biochim. Biophys. Acta* 234, 126-136
5. Erixon, K. and Butler, W.L. (1971) *Biochim. Biophys. Acta* 234, 381-389
6. Butler, W.L. and Okayama, S. (1971) *Biochim. Biophys. Acta* 245, 237-239
7. Malkin, R. and Bearden, A.J. (1973) *Proc. Natl. Acad. Sci. U.S.* 70, 294-297
8. Bearden, A.J. and Malkin, R. (1973) *Biochim. Biophys. Acta* 325, 266-274
9. Floyd, R.A., Change, B. and DeVault, D. (1971) *Biochim. Biophys. Acta* 226, 103-112
10. Butler, W.L. (1973) *Accounts Chem. Res.* 6, 177-184
11. Van Gorkom, H.J. (1974) *Biochim. Biophys. Acta* 347, 439-442
12. Vermeglio, A. and Mathis, P. (1974) *Biochim. Biophys. Acta* 368, 9-17
13. Van Gorkom, H.J., Tamminga, J.J., Haveman, J. and van der Linden, I.K. (1974) *Biochim. Biophys. Acta* 347, 417-438
14. Vermeglio, A. and Mathis, P. (1974) in: *Proc. 3rd Int. Congr. Photosynthesis, Rehovot* (Avron, M., ed.) Vol. 1, pp. 323-334, Elsevier, Amsterdam
15. Okayama, S. and Butler, W.L. (1972) *Biochim. Biophys. Acta* 267, 523-529
16. Lozier, R.H. and Butler, W.L. (1974) *Biochim. Biophys. Acta* 333, 465-480
17. Matsuzaki, E. and Kamimura, Y. (1972) *Plant Cell Physiol.* 13, 415-425
18. Garewal, H.S., Singh, J. and Wasserman, A.R. (1971) *Biochem. Biophys. Res. Comm.* 44, 1300-1305
19. Garewal, H.S. and Wasserman, A.R. (1974) *Biochemistry* 13, 4063-4071
20. Vermeglio, A. and Fallot, P. (1972) *C.R. Acad. Sci.* 274, 3461-3464
21. Butler, W.L. (1972) *FEBS Letters* 20, 333-338
22. Knaff, D.B. and Arnon, D.I. (1971) *Biochim. Biophys. Acta* 226, 400-408
23. Kato, S. and Kimimura, M. (1974) *Biochim. Biophys. Acta* 333, 71-84
24. Ben-Hayyim, G. and Malkin, S. (1972) in: *Proc. 2nd Int. Congr. Photosynth. Res., Stresa* (Forti, G., Avron, M. and Melandri, A., eds.) Vol.1,

- pp.61-72, Dr. W. Junk N.V. Publishers, The Hague
25. Butler, W.L., Visser, J.W.M. and Simons, H.L. (1973) *Biochim. Biophys. Acta* 292, 140-151
  26. Butler, W.L., Visser, J.W.M. and Simons, H.L. (1973) *Biochim. Biophys. Acta* 325, 539-545
  27. Vermeglio, A. and Mathis, P. (1973) *Biochim. Biophys. Acta* 314, 57-65
  28. Mathis, P., Michel-Villaz, M. and Vermeglio, A. (1974) *Biochem. Biophys. Res. Comm.* 56, 682-688
  29. Kitajima, M. and Butler, W.L. (1973) *Biochim. Biophys. Acta* 325, 558-564
  30. Boardman, N.K. and Thorne, S.W. (1969) *Biochim. Biophys. Acta* 189, 294-297
  31. Butler, W.L. (1962) *J. Opt. Soc. Am.* 52, 292-299
  32. Murata, N., Itoh, S. and Okada, M (1973) *Biochim. Biophys. Acta* 325, 463-471
  33. Malkin, R., Knaff, D.B. and McSwain, B.D. (1974) *FEBS Letters* 47, 140-142
  34. Visser, J.W.M. and Rijgersberg, C.P. (1974) in: *Proc. 3rd Int. Congr. Photosynthesis, Rehovot* (Avron, M., ed.) Vol.1, pp. 399-408, Elsevier, Amsterdam
  35. Ames, J., Pulles, M.P.J. and Velthuys, B.R. (1973) *Biochim. Biophys. Acta* 325, 472-482
  36. Joliot, P. and Joliot, A. (1972) in: *Proc. 2nd Int. Congr. Photosynth. Res., Stresa* (Forti, G., Avron, M. and Melandri, A., eds.) Vol.1, pp. 26-38, Dr. W. Junk N.V. Publishers, The Hague
  37. Joliot, P. and Joliot, A. (1973) *Biochim. Biophys. Acta* 305, 302-316
  38. Kok, B. (1963) in: *Photosynthetic Mechanisms of Green Plants* (Kok, B. and Jagendorf, A.T., eds.), pp. 45-55, Natl. Acad. Sci., Natl. Res. Council Publ. 1145, Washington D.C.
  39. Murata, N. (1968) *Biochim. Biophys. Acta* 162, 106-121
  40. Thorne, S.W. and Boardman, N.K. (1971) *Biochim. Biophys. Acta* 234, 113-125
  41. Malkin, S. and Michaeli, G. (1972) in: *Proc. 2nd Int. Congr. Photosynth. Res., Stresa* (Forti, G., Avron, M. and Melandri, A., eds.) Vol.1, pp. 149-168, Dr. W. Junk N.V. Publishers, The Hague
  42. Joliot, A. and Joliot, P. (1964) *C.R. Acad. Sci.* 258, 4622-4625
  43. Joliot, P., Joliot, A. and Kok, B. (1968) *Biochim. Biophys. Acta* 153, 635-652
  44. Duysens, L.N.M. and Sweers, H.E. (1963) in: *Studies on Microalgae and*

*Photosynthetic Bacteria* (Miyachi, S., ed.), pp. 353-372, University of Tokyo Press, Tokyo

45. Butler, W.L. (1972) *Proc. Natl. Acad. Sci. U.S.* 69, 3420-3422
46. Bennoun, P. (1970) *Biochim. Biophys. Acta* 216, 357-363
47. Mathis, P. and Vermeglio, A. (1974) *Biochim. Biophys. Acta* 368, 130-134
48. Mathis, P. and Vermeglio, A. (1975) *Biochim. Biophys. Acta*, in the press
49. Kneff, D.B. and Malkin, R. (1974) *Biochim. Biophys. Acta* 347, 395-403
50. Norris, J.R., Uphaus, R.A., Crespín, H.L. and Katz, J.J. (1971) *Proc. Natl. Acad. Sci. U.S.* 68, 625-628
51. Joliot, A. (1974) in: *Proc. 3rd Int. Congr. Photosynthesis, Rehovot* (Avron, M., ed.) Vol.1, 315-322, Elsevier, Amsterdam
52. Pulles, M.P.J., Kerkhof, P.L.M. and Ames, J. (1974) *FEBS Letters* 47, 143-145
53. Ke, B., Sahu, S., Shaw, E. and Beinert, H. (1974) *Biochim. Biophys. Acta* 347, 36-48
54. Kitajima, M. and Butler, W.L. (1975) *Biochim. Biophys. Acta* 376, 105-115
55. Harbour, J.R. and Tollin, G. (1972) *Proc. Natl. Acad. Sci. U.S.* 69, 2066-2068
56. Lozier, R.H. and Butler, W.L. (1972) *FEBS Letters* 26, 161-164
57. Borg, D.C., Fajer, J., Felton, R.H. and Dolphin, D. (1970) *Proc. Natl. Acad. Sci. U.S.* 67, 813-820
58. Fajer, J., Borg, D.C., Forman, A., Felton, R.H., Dolphin, D. and Vegh, L. (1974) *Proc. Natl. Acad. Sci. U.S.* 71, 994-998
59. Duysens, L.N.M. (1956) *Biochim. Biophys. Acta* 19, 1-12
60. Ames, J. (1964) *Thesis*, University of Leiden
61. Latimer, P. and Eubanks, C.A.H. (1962) *Arch. Biochem. Biophys.* 98, 274-285
62. Blankenship, R.E., Babcock, G.T., Warden, J.T. and Sauer, K. (1975) *FEBS Letters* 51, 287-293
63. Den Haan, G.A., Warden, J.T. and Duysens, L.N.M. (1973) *Biochim. Biophys. Acta* 325, 120-125
64. Stiehl, H.H. and Witt, H.T. (1968) *Z. Naturforsch.* 23b, 220-224
65. Stiehl, H.H. and Witt, H.T. (1969) *Z. Naturforsch.* 24b, 1588-1598
66. Döring, G., Renger, G., Vater, J. and Witt, H.T. (1969) *Z. Naturforsch.* 24b, 1139-1143
67. Ames, J. and de Grooth, B.G. (1975) *Biochim. Biophys. Acta* 376, 298-307
68. Van Gorkom, H.J. and Donze, M. (1973) *Photochem. Photobiol.* 17, 333-342



69. Brody, S.S. and Broyde, S.B. (1968) *Biophys. J.* 8, 1511-1533
70. Hopfield, J.J. (1974) *Proc. Natl. Acad. Sci. U.S.* 71, 3640-3644
71. Zankel, K.L. (1971) *Biochim. Biophys. Acta* 245, 373-385
72. Gläser, M., Wolf, Ch., Buchwald, H.E. and Witt, H.T. (1974) *FEBS Letters* 42, 81-85
73. Duysens, L.N.M., den Haan, G.A. and van Best, J.A. (1974) in: *Proc. 3rd Int. Congr. Photosynthesis, Rehovot* (Avron, M., ed.) Vol.1, pp. 1-12, Elsevier, Amsterdam
74. Den Haan, G.A., Duysens, L.N.M. and Egberts, D.J.N. (1974) *Biochim. Biophys. Acta* 368, 409-421
75. Feher, G., Hoff, A.J., Isaacson, R.A. and McElroy, J.D. (1973) *Biophys. Soc. Abstracts*, 61a
76. Norris, J.R., Druyan, M.E. and Katz, J.J. (1973) *J. Amer. Chem. Soc.* 95, 1680-1682
77. Philipson, K.D., Sato, V.L. and Sauer, K (1972) *Biochemistry* 11, 4591-4595
78. Norris, J.R., Scheer, H., Druyan, M.E. and Katz, J.J. (1974) *Proc. Natl. Acad. Sci. U.S.* 71, 4897-4900

1. The first part of the paper is devoted to a general introduction of the subject. It is shown that the problem of the existence of a solution of the differential equation  $y'' + p(x)y' + q(x)y = r(x)$  is equivalent to the problem of the existence of a function  $y(x)$  satisfying the boundary conditions  $y(a) = \alpha$  and  $y(b) = \beta$ .

2. In the second part, the author considers the case where  $p(x)$  and  $q(x)$  are continuous functions on the interval  $[a, b]$ . It is shown that a solution exists if and only if the determinant  $\Delta = \begin{vmatrix} 1 & 0 \\ 0 & 1 \end{vmatrix}$  is non-zero.

3. In the third part, the author considers the case where  $p(x)$  and  $q(x)$  are discontinuous functions. It is shown that a solution exists if and only if the determinant  $\Delta$  is non-zero.

4. In the fourth part, the author considers the case where  $p(x)$  and  $q(x)$  are functions of bounded variation. It is shown that a solution exists if and only if the determinant  $\Delta$  is non-zero.

5. In the fifth part, the author considers the case where  $p(x)$  and  $q(x)$  are functions of bounded variation and  $r(x)$  is a function of bounded variation. It is shown that a solution exists if and only if the determinant  $\Delta$  is non-zero.

6. In the sixth part, the author considers the case where  $p(x)$  and  $q(x)$  are functions of bounded variation and  $r(x)$  is a function of bounded variation. It is shown that a solution exists if and only if the determinant  $\Delta$  is non-zero.

7. In the seventh part, the author considers the case where  $p(x)$  and  $q(x)$  are functions of bounded variation and  $r(x)$  is a function of bounded variation. It is shown that a solution exists if and only if the determinant  $\Delta$  is non-zero.

8. In the eighth part, the author considers the case where  $p(x)$  and  $q(x)$  are functions of bounded variation and  $r(x)$  is a function of bounded variation. It is shown that a solution exists if and only if the determinant  $\Delta$  is non-zero.

9. In the ninth part, the author considers the case where  $p(x)$  and  $q(x)$  are functions of bounded variation and  $r(x)$  is a function of bounded variation. It is shown that a solution exists if and only if the determinant  $\Delta$  is non-zero.

10. In the tenth part, the author considers the case where  $p(x)$  and  $q(x)$  are functions of bounded variation and  $r(x)$  is a function of bounded variation. It is shown that a solution exists if and only if the determinant  $\Delta$  is non-zero.

## SUMMARY.

The studies reported here were performed in order to obtain information about electron transport in and near the photochemically active centers in photosynthetic organisms. A technical difficulty in studying primary and secondary photoreactions at room temperature is that the primary reactions are very rapid. By lowering the temperature part of the reactions became slow enough so that they could be measured by the methods available to us.

Chapter I contains a concise general introduction. Chapter II deals with the experimental methods used. A detailed description of sensitive apparatus for measurements of light-induced changes of fluorescence and absorbance at low temperatures is given. Furthermore a method is described to calculate the quantum yield of photoreactions from measurements of the kinetics of light-induced absorbance changes in suspensions with a high absorbance of the actinic light. Finally, the methodical problems of interpreting kinetic measurements of absorbance and fluorescence have been discussed.

Chapter III deals with the electron transport of photosystem 1 in spinach chloroplasts and in intact, unicellular algae. Analysis of absorbance difference spectra between 670 and 720 nm at 110 K gave independent support for the hypothesis that in the primary reaction a chlorophyll dimer with an absorption maximum at 690 nm is oxidized, and that additionally an absorption band peaking near 700 nm shifts to shorter wavelength. Both phenomena reflect oxidation of the primary electron donor, P700. Furthermore it was found that in a fraction of the reaction centers this photooxidation was completely reversible; this fraction was 0.9 at 200 K and 0.2 at 10 K. In the decay of the reversible part three phases could be distinguished with  $t_{1/2} = 20 - 30$  ms, 0.2-0.4 s and 20-40 s. The extents of these phases were about the same (30-40 % of the total reversible fraction). Between 10 and 150 K the rates of these back reactions were independent of temperature. The photoreduction of an iron-sulphur protein, "bound ferredoxin", with EPR lines at g-values of 2.05, 1.94 and 1.86 was also reversible in part of the centers and the kinetics were identical to those of the photooxidation of P700. These results indicate that different types of photosystem-1 reaction centers occur below 150 K. It is concluded that ferredoxin is the only primary electron acceptor, but that the rates of the back reactions between reduced ferredoxin and  $P^+700$  are different for each type of reaction center. By means of EPR measurements at 20 K it was also shown that the copper-containing protein, plasto-

cyanin, occurs in about equal amounts in various algae and in spinach chloroplasts, and that at room temperature it can be oxidized by system 1 (P700) and reduced by system 2. These reactions did not occur at 77 K.

Measurements of electron transport reactions in and near photosystem 2 are described and a model for the reaction center 2 is discussed in Chapter IV. By a study of light-induced absorbance changes it is found that in about 50 % of the reaction centers cytochrome  $b_{559}$  is oxidized via  $P^{+680}$ , the oxidized primary electron donor of system 2. In the other centers a different, unknown compound acts as secondary donor. At 180 K in none of the centers cytochrome  $b_{559}$  is being oxidized. At this temperature, however, the photo-oxidized P680 is reduced by an unidentified secondary donor,  $D_2$ . This donor may be the same compound that is oxidized at 90 K in those centers which do not oxidize cytochrome  $b_{559}$ . The quantum yield of the photoreduction of the primary electron acceptor (Q) of system 2 appeared to be low. This could be explained by a back reaction between  $P^{+680}$  and  $Q^{-}$ , which is more rapid than the reaction of  $P^{+680}$  with secondary donor(s). From EPR measurements it followed that the half time of this back reaction was 2.0 ms in spinach chloroplasts at 110 K. The dark reaction between  $P^{+680}$  and the secondary donors had half times which depended on the identity of the donor. With cytochrome  $b_{559}$  and  $D_2$   $t_{1/2}$  was equal to 10 - 40 ms. Between 10 and 50 K in a number of reaction centers also a dark reaction with  $t_{1/2}$  equal to 0.5 s was observed. The amount of the centers with the 0.5-s dark reaction was greater at 10 than at 50 K.

The EPR signal of  $P^{+680}$  at 110 K had the same g-value as that of  $P^{+700}$  ( $g = 2.0026$ ), but the peak-to-peak width was only 6 G for  $P^{+680}$  as compared to 8 G for  $P^{+700}$ . At 110 K, with chloroplasts in the presence of the oxidizing agent ferricyanide, EPR and optical spectra were measured which indicated the irreversible photooxidation of a chlorophyll molecule. This chlorophyll molecule was found not to be P680, but it may be oxidized by  $P^{+680}$ , if the other donors are oxidized chemically prior to freezing.

## SAMENVATTING.

Het hier beschreven onderzoek is verricht met het doel gegevens omtrent het electron transport in en nabij de fotochemisch actieve centra in fotosynthetische organismen te verkrijgen. Een technische moeilijkheid bij onderzoek betreffende de primaire en secundaire fotoreacties bij kamertemperatuur vormt de grote snelheid van de primaire reacties. Door temperatuur verlaging werd een deel van de reacties zodanig vertraagd dat ze gemeten konden worden met de ons ter beschikking staande methoden.

Hoofdstuk I bevat een beknopte algemene inleiding. Hoofdstuk II behandelt de gebruikte experimentele methodes. Een gedetailleerde beschrijving wordt gegeven van gevoelige apparatuur voor het meten van licht-geïnduceerde fluorescentie- en absorptieveranderingen bij lage temperaturen. Voorts wordt een methode beschreven om uit metingen van de kinetiek van licht-geïnduceerde absorptieveranderingen in suspensies met een hoge absorptie van het actinisch licht, de quantumopbrengst van fotoreacties te berekenen. Tenslotte volgt een beschouwing over de problemen bij methodes voor het verklaren van kinetische metingen van absorptie- en fluorescentieveranderingen.

Hoofdstuk III gaat over het electron transport van fotosysteem 1 in chloroplasten van spinazie en in intacte, eencellige algen. Analyse van absorptieverschil spectra tussen 670 en 720 nm bij 110 K gaf onafhankelijke steun aan de hypothese dat in de primaire reactie een chlorofyl dimeer met een absorptie maximum bij 690 nm geoxydeerd wordt, en dat bovendien een absorptie band met maximum nabij 700 nm naar korter golflengte verschuift. Beide verschijnselen geven oxydatie van de primaire electron donor, P700, weer. Voorts werd gevonden dat deze fotooxydatie in een deel van de reactie centra geheel reversibel was; dit deel was 90 % van de centra bij 200 K en 20 % bij 10 K. In de terugreactie van het reversibele deel waren drie fasen te onderscheiden met halfwaarde tijden van 20 - 30 ms, 0,2 - 0,4 s en 20 - 40 s. De grootte van deze fasen was ongeveer hetzelfde (30 - 40 % van het totale reversibele deel). Tussen 10 en 150 K waren de snelheden van deze terugreacties onafhankelijk van de temperatuur. De fotoreductie van een ijzer-zwavel eiwit, "gebonden ferredoxine", met EPR lijnen bij g-waarden van 2,05, 1,94 en 1,86 was eveneens reversibel in een deel van de centra en de kinetiek was identiek aan die van de fotooxydatie van P700. Deze resultaten tonen aan dat beneden 150 K verschillende typen reactiecentra van system 1 voorkomen. Geconcludeerd wordt dat ferredoxine de enige primaire electron acceptor is,

maar dat de snelheden van de terugreacties van gereduceerd ferredoxine en geoxydeerd P700 verschillend zijn voor ieder type reactiecentrum. Met behulp van EPR metingen bij 20 K werd voorts aangetoond dat het koper-houdende eiwit, plastocyanine, in verschillende algen en in spinazie chloroplasten in ongeveer dezelfde hoeveelheden voorkomt, en dat het bij kamertemperatuur geoxydeerd kan worden door systeem 1 (P700) en gereduceerd door systeem 2. Deze reacties verliepen niet bij 77 K.

Metingen van electron transport reacties in en nabij fotosysteem 2 en een model voor reactiecentrum 2 worden besproken in hoofdstuk IV. Door onderzoek van licht-geïnduceerde absorptie veranderingen werd gevonden dat bij 90 K in ongeveer 50 % van de reactiecentra cytochroom  $b_{559}$  wordt geoxydeerd via het reactiecentrum chlorofyl  $P^{+680}$ , de geoxydeerde primaire electron donor van systeem 2. In de andere centra fungeert een andere, onbekende stof als secundaire donor. Bij 180 K wordt in geen van de centra cytochroom  $b_{559}$  geoxydeerd. Bij deze temperatuur wordt het door licht geoxydeerde  $P680$  echter door een niet-geïdentificeerde, secundaire donor,  $D_2$ , gereduceerd. Deze donor is misschien dezelfde stof, die ook bij 90 K geoxydeerd wordt door de centra die geen cytochroom  $b_{559}$  oxyderen. De quantumopbrengst voor fotoreductie van de primaire electron acceptor (Q) van systeem 2 bleek laag te zijn. Dit kon verklaart worden door een terugreactie tussen  $P^{+680}$  en  $Q^{-}$ , die sneller is dan de reactie tussen  $P^{+680}$  en de secundaire donor(en). Uit EPR metingen volgde dat de halfwaarde tijd van deze terugreactie in spinazie chloroplasten 2,0 ms was bij 110 K. De (donker-)reactie tussen  $P^{+680}$  en de secundaire donoren had halfwaarde tijden die afhingen van de identiteit van de donor. Met cytochrome  $b_{559}$  en met  $D_2$  was  $t_{\frac{1}{2}}$  gelijk aan 10 - 40 ms. Tussen 10 en 50 K werd in een aantal reactiecentra ook een donkerreactie met  $t_{\frac{1}{2}}$  van 0,5 s waargenomen. Het aantal centra met een 0,5-s donkerreactie was groter bij 10 K dan bij 50 K.

Het EPR signaal van  $P^{+680}$  bij 110 K had dezelfde g-waarde als dat van  $P^{+700}$  ( $g = 2,0026$ ), maar de piek-piek breedte was slechts 6 G voor  $P^{+680}$  terwijl dit 8 G was voor  $P^{+700}$ . Bij 110 K werden met chloroplasten in aanwezigheid van het oxydant kalium-ferricyanide EPR en optische spectra gemeten die duiden op de irreversibele fotooxydatie van een chlorofyl molecule. Dit chlorofyl molecule bleek echter niet  $P680$  te zijn, maar het kan geoxydeerd worden door  $P^{+680}$ , als de andere donoren voor het afkoelen chemisch geoxydeerd zijn.

ABBREVIATIONS AND SYMBOLS.

CD	circular dichroism
C550	compound showing a band-shift near 550 nm upon reduction of the primary acceptor of photosystem 2
DBMIB	2,5-dibromo-3-methyl-6-isopropyl-p-benzoquinone
DCMU	3-(3,4-dichlorophenyl)-1,1-dimethylurea
ENDOR	electron-nuclear double resonance
EPR	electron paramagnetic resonance
NADP	nicotinamide-dinucleotide phosphate;(triphosphopyridine-nucleotide)
P680	reaction center chlorophyll absorbing near 680 nm, primary electron donor of photosystem 2
P700	reaction center chlorophyll absorbing near 700 nm, primary electron donor of photosystem 1
Q	primary electron acceptor of photosystem 2
tricine	N-tris(hydroxymethyl)methylglycine
X	primary electron acceptor of photosystem 1
Z	donor to the primary electron donor of photosystem 2

## CURRICULUM VITAE.

Na het behalen van het eindexamen Gymnasium 3 aan het Triniteits Lyceum te Haarlem in juni 1966 begon ik in september van hetzelfde jaar mijn studie in de natuurkunde met bijvakken wis- en sterrekunde aan de Rijksuniversiteit te Leiden.

In februari 1969 werd het candidaatsexamen afgelegd en daarna werd mijn studie voortgezet in het Biofysisch Laboratorium, geleid door Prof. Dr. L.N.M. Duysens. Daar werd onder leiding van Dr. J. Amesz onderzoek verricht naar het ontstaan van licht-geïnduceerde verschuivingen van absorptiebanden in fotosynthetische organismen, en, later, naar het verloop van het fotosynthetisch electron transport in zuurstof-producerende algen. Studie van het bijvak numerieke wiskunde geschiedde onder leiding van Prof. Dr. G. Zoutendijk. Mijn doctoraal-examen in de experimentele natuurkunde met bijvak wiskunde legde ik af in november 1971.

Hierna werd ik benoemd tot wetenschappelijk medewerker verbonden aan het Biofysisch Laboratorium, en ben ik begonnen met het onderzoek dat tot dit proefschrift heeft geleid.

Sinds augustus 1975 ben ik als wetenschappelijk medewerker in dienst van de Nederlandse Organisatie voor Zuiver Wetenschappelijk Onderzoek (Z.W.O.) verbonden aan het Radiobiologisch Instituut TNO te Rijswijk.



